A Split-GAL4 screen identifies novel sleep-promoting neurons in the Ventral Nerve Cord of *Drosophila*

Joseph Jones[1], Brandon Holder[1], Kiran Eiken[1], Alex Vogt[1], Adriana Velarde[1], Ally Elder[1], Jennifer McEllin[1] and Stephane Dissel[1*]

[1]Department of Genetics, Developmental and Evolutionary Biology, School of Biological and Chemical Sciences, University of Missouri-Kansas City, 5007 Rockhill Rd, Kansas City, MO 64110

[*]Correspondence to: dissels@umkc.edu

Abstract

As in the mammalian system, sleep in *Drosophila* is regulated by multiple brain regions. Among them, neurons projecting to the dorsal Fan-Shaped Body (dFB) have been intensively studied and the data suggest they play a critical role for in sleep regulation. The 23E10-GAL4 driver is the most widely used tool to label and manipulate dFB neurons. Multiple studies have reported that activation of 23E10-GAL4 neurons promotes sleep. However, anatomical analysis revealed that 23E10-GAL4 labels 23-30 dFB neurons in the *Drosophila* brain and many non-dFB neurons in the brain and in the

22 Ventral Nerve Cord (VNC), the fly equivalent of the spinal cord. To better understand
23 the role of individual dFB neurons in sleep regulation, we undertook a Split-GAL4
24 screen to gain access to subsets of 23E10-GAL expressing cells. In this study, we
25 report the discovery of two VNC cholinergic sleep-promoting neurons labeled by the
26 23E10-GAL4 driver.

27

28 **Introduction**

29 Understanding the neural basis of behavior is a major aspect of neurobiology. However,
30 unequivocally assigning a behavior to a specific neuron or group of neurons is not a
31 trivial task. The extreme complexity, diversity and connectivity of the mammalian
32 nervous system renders this task even more daunting. To study the neural basis of a
33 behavior, an investigator must be able to specifically manipulate a distinct group of cells
34 and monitor the behavior of interest. Such approaches require precise genetic tools that
35 allow for the manipulation of discrete neurons or groups of neurons. While such tools
36 exist in mammalian systems (1), they may not be available for all the diverse types of
37 neurons that underlie a specific behavior. It is therefore not surprising that animal
38 models have been extensively used to untangle the neural basis of many different
39 behaviors (2). One such model, the fruit fly *Drosophila melanogaster*, with its simpler
40 nervous system and unparalleled genetic toolbox, has become a workhorse in the study
41 of complex behaviors, such as courtship (3, 4), feeding (5, 6), and sleep (7). Multiple
42 binary systems have been developed to access and manipulate specific groups of
43 neurons in the fly nervous system: GAL4/UAS (8); LexA/LexAop (9) and; QF/QUAS
44 (10). Of these 3 systems, the GAL4/UAS system has been by far the most extensively

45 used. However, the expression patterns of GAL4 drivers are often not restricted enough
46 to clearly link a behavior to specific neurons. Importantly, refinement of GAL4
47 expression pattern can be achieved by employing the intersectional Split-GAL4
48 technology (11).
49
50 Sleep is a behavior that has been described in a variety of species ranging from jellyfish
51 to humans (12). Sleep is regulated by two processes, the circadian clock which gates
52 the occurrence of sleep, and the sleep homeostat which controls the intensity and
53 duration of sleep, in response to prior wakefulness (13). Although the precise function of
54 sleep still remains unknown, there is ample evidence supporting the notion that sleep is
55 required for maintaining optimal physiological and behavioral performance (14). A priori,
56 sleep could appear to be a detrimental activity as it competes with other motivated
57 behaviors such as feeding, mating, or parenting, and renders organisms defenseless
58 against potential predators. However, despite these negative outcomes, sleep has been
59 maintained throughout evolution, emphasizing its essential value (15).
60
61 Over the last 20 years, multiple studies have clearly demonstrated that the mechanisms
62 and regulation of sleep are largely conserved from flies to mammals (16). Like in the
63 mammalian system, sleep-regulating centers are found in many areas in the *Drosophila*
64 brain (16, 17). One such sleep-regulating center that has gathered a lot of attention
65 comprises neurons that project to the dorsal Fan-Shaped body (dFB). The Fan-Shaped
66 Body (FB) is part of the central complex in the *Drosophila* brain, a region organized into
67 multiple layers that plays a role in many functions, including locomotion control (18),

68 courtship behavior (19) and memory (20, 21), nociception (22), visual feature
69 recognition (23) and processing (24), social behaviors (25) and, feeding decision-
70 making (26).
71
72 Previous studies demonstrated that increasing the activity of neurons contained in the
73 C5-GAL4, 104y-GAL4, and C205-GAL4 drivers strongly promotes sleep (27, 28). While
74 the expression patterns of these 3 independent drivers are broad, they show prominent
75 overlap in neurons that project to the dFB (27). Based on these observations, the
76 authors concluded that it is likely that the dFB plays a role in regulating sleep but could
77 not rule out a role for neurons outside the dFB (27). In addition, further studies
78 established that reducing the excitability of 104y-GAL4 neurons reduces sleep (29, 30).
79 Highlighting the strong interaction between sleep and memory, activation of 104y-GAL4
80 neurons consolidates Short-Term Memory (STM) to Long-Term Memory (LTM) (27, 31)
81 and restores STM to the classical memory mutant *rutabaga* and *dunce* (32). Taken
82 together, these data point at dFB neurons as important modulator of sleep.
83
84 Further work supported a role for the dFB in sleep homeostasis by demonstrating that
85 sleep deprivation increases the excitability of 104y-GAL4 dFB neurons (29). A follow up
86 study proposed that increasing sleep pressure switches dFB neurons from an
87 electrically silent to an electrically active state and that this process is regulated by
88 dopaminergic signaling to the dFB (33) and the accumulation of mitochondrial reactive
89 oxygen species in dFB neurons (34). The physiological properties of dFB neurons have

90 led to the suggestion that dFB neurons are functionally analogous to the ventrolateral
91 preoptic nucleus (VLPO), a key sleep-regulating center in the mammalian brain (29, 35).
92
93 Importantly, recent studies have used 23E10-GAL4, a more restrictive driver to
94 manipulate and monitor dFB neurons. (33, 36). Several groups have demonstrated that
95 chronic and acute activation (using thermogenetic or optogenetic methods) of 23E10-
96 GAL4 neurons increases sleep (31, 37-39). Because of its more restricted expression
97 pattern and strong capacity to modulate sleep, 23E10-GAL4 (as it relates to sleep) is
98 seen as a dFB specific driver by most in the scientific community. Remarkably, a recent
99 study described an electron microscopy-based connectome of the central complex
100 including the dFB and demonstrated that the 23E10-GAL4 driver contains 31 neurons in
101 the brain that project to the dFB (40). Whether these 31 dFB neurons can be considered
102 as a functionally homogeneous group is still unclear. Interestingly, Qian *et al*.
103 demonstrated that only a small subset of 23E10-GAL4 neurons express the 5HT2b
104 serotonin receptor and that these cells regulate sleep and sleep homeostasis (37).
105 Unfortunately, this study did not investigate the role of non-5HT2b expressing 23E10-
106 Gal4 neurons in sleep regulation. In addition, whether there are non-dFB 5HT2b
107 expressing 23E10-GAL4 neurons that could potentially play a role in sleep modulation is
108 not clearly addressed in this study either. Taken together, these data suggest that
109 23E10-GAL dFB neurons probably constitute a functionally heterogenous group of cells.
110
111 Surprisingly, activation of 23E10-GAL4 expressing neurons, unlike 104y-GAL4, does
112 not consolidate STM to LTM (31). In this study, the authors demonstrated that in

113 addition to the dFB, 104y-GAL4 expresses in neurons projecting to the ventral FB (vFB)
114 and that these neurons also regulate sleep and are responsible for memory
115 consolidation (31). These data emphasize the need to use genetic tools that are as
116 specific as possible to clearly assign a role in sleep regulation and sleep function to
117 specific neurons/groups of neurons. Often, GAL4 drivers that are extensively used to
118 manipulate a specific neuronal group also express in regions outside the area of
119 interest. This makes it difficult to clearly identify the neural basis of sleep behavior.
120
121 With this in mind, we wanted to know which of the 31 dFB 23E10-GAL4 neurons are
122 important for sleep regulation. To do so, we employed a targeted, intersectional Split-
123 GAL4 strategy (11) focused on 23E10-GAL4 dFB neurons. Surprisingly, our data
124 demonstrates that in the 23E10-GAL driver, there are non-dFB sleep-promoting
125 neurons. Importantly, these cholinergic neurons are located in the Ventral Nerve Cord
126 (VNC), the fly equivalent to the spinal cord. Nevertheless, we confirm that 23E10-GAL4
127 dFB neurons regulate sleep homeostasis while 23E10-GAL4 VNC neurons do not.
128 Thus, our work reveals that there are multiple groups (at least two) of sleep-regulating
129 neurons in an extensively used “dFB-specific” GAL4 driver. These data clearly highlight
130 the need to use extremely specific tools to manipulate limited number of neurons when
131 trying to unequivocally assign a behavior to a group of cells.
132
133 **Results**
134 **The 23E10-GAL4 driver promotes sleep and contains many non dFB neurons in**
135 **the central nervous system**

136 Previous studies have reported that increasing the activity of dFB neurons using the
137 23E10-GAL driver reliably increases sleep (31, 37-39). We first sought to confirm these
138 observations in our laboratory. Thus, we expressed the thermogenetic TrpA1 cation
139 channel, which is activated by transferring flies to 31°C (41), in 23E10-GAL4 expressing
140 neurons. Individual flies were monitored for two days at 22°C (baseline days, no
141 activation), then temperature was raised to 31°C for 24h on day 3 (activation day). A
142 schematic of the experimental setup is provided in Figure 1A. As seen in Figure 1B,C,
143 raising the temperature changes the sleep profile of both parental controls and results in
144 a loss of sleep (Figure 1E). These data are in agreement with previous reports on the
145 effect of high temperature on sleep (42, 43). On the other hand, activating 23E10-GAL4
146 neurons strongly increases sleep (Figure 1D,E). Importantly, activation of 23E10-GAL4
147 neurons does not affect the amount of locomotor activity when the flies are awake
148 (Figure 1F). Thus, we confirmed that activating 23E10-GAL4 neurons promotes sleep
149 and that the increase in sleep is not caused by a general motor defect, in agreement
150 with previous reports using the same GAL4 driver (31, 37-39) .

151

152 23E10-GAL4 has become the driver of choice to manipulate dFB neurons and many in
153 the field see it as a “dFB-specific” tool. However, GAL4 lines often are not that specific
154 and commonly express in neurons outside the region of interest. To clarify the
155 expression pattern of 23E10-GAL4, we expressed GFP and carefully quantified the
156 number of neurons that are GFP positive. As seen in Figure 1G,H, there are many
157 neurons labelled by 23E10-GAL4 in the brain and in the VNC (See also Video 1 and
158 Video 2). Importantly, many of these neurons are not dFB neurons. Our analysis

159 revealed that there are more than 50 neurons in the brain labelled by 23E10-GAL4, only
160 half of which are dFB neurons (Table1). In addition, 23E10-GAL labels about 18
161 neurons in the VNC (Table1). Interestingly, we note that while the electron microscopy
162 study discussed above identified 31 dFB 23E10-GAL4 neurons (40), we do not
163 systematically observe 31 neurons in every brain. This discrepancy is probably due to
164 the different methodologies used in the two studies. We suspect that some 23E10 dFB
165 neurons may be only weakly expressing GAL4 and are therefore not always visible
166 using confocal microscopy. However, based on this expression pattern, we conclude
167 that it is impossible to unequivocally assign a role in sleep promotion to 23E10-GAL4
168 dFB neurons.
169

170 **The 23E10-GAL4 driver contains sleep-promoting neurons that are not dFB**
171 **neurons**

172 To shed light on the role of individual 23E10-GAL4 expressing neurons in sleep
173 regulation, we employed a Split-GAL4 strategy (11) to access a reduced number of
174 23E10-GAL4 expressing cells. In designing this screen, our primary region of interest in
175 the brain was the dFB, a choice dictated by the number of studies supporting a role for
176 this structure in sleep regulation (27-30, 33, 34, 37, 44, 45). Central to the Split-GAL4
177 technology is the fact that the functional GAL4 transcription factor can be separated into
178 two non-functional fragments, a GAL4 DNA-binding domain (DBD) and an activation
179 domain (AD). Different enhancers are used to express these two fragments and the
180 functional GAL4 transcription factor is reconstituted only in the cells in which both
181 enhancers are active (11).

182 We obtained 22 different AD lines based on their associated GAL4 line expressing in
183 the dFB, as observed using the Janelia Flylight website (36, 46). Since the goal of our
184 screen was to identify the contribution of individual 23E10 dFB neurons in sleep
185 regulation, we designed a targeted approach by combining these individual AD lines to
186 a 23E10-DBD line (46, 47), thus creating 22 new Split-GAL4 lines named FBS for Fan-
187 Shaped Body Splits lines (See Table2 for a description of these lines). These newly
188 created lines were screened behaviorally for their ability to modulate sleep and
189 anatomically to identify their expression patterns. To do so, each individual Split-GAL4
190 FBS line was crossed to a line expressing both the thermogenetic TrpA1 cation channel
191 and a mCD8GFP construct. Flies were maintained at 22°C for 2 days before raising the
192 temperature to 31°C at the beginning of day 3 for a duration of 24h. Temperature was
193 brought down to 22°C on day 4 (Figure 2A). For each individual fly, we calculated the
194 percentage of total sleep change between activation day (day3) and baseline day
195 (day2) (Figure 2A). As a control for this screen, we used an enhancerless AD construct
196 (created in the vector used to make all the AD lines) combined with 23E10-DBD, since it
197 is the common element in all the Split-GAL4 lines screened in this experiment. As seen
198 in Figure 2B,D, control female flies show a reduction in sleep upon transferring to 31°C,
199 an effect particularly evident during the night. These data are in agreement with
200 previous studies documenting that changes in temperature modulate sleep architecture
201 and that high temperature disturbs sleep at night (42, 43, 48, 49) . However, acute
202 activation of the neurons contained in 9 of the 22 FBS lines led to significant increases
203 in percentage sleep change in female flies (FBS4, FBS5, FBS42, FBS45, FBS53,
204 FBS68, FBS72, FBS81 and FBS84), when compared with controls. Individual sleep

205 traces for all 22 FBS lines are shown in Figure 2E,F,G,H and Figure 2-figure
206 supplement 1. Importantly, analysis of activity counts during awake time reveals that
207 increases in sleep are not caused by a reduction in locomotor activity (Figure 2C). On
208 the contrary, 3 of the strongly sleep-inducing lines even show an increase in waking
209 activity upon neuronal activation (Figure 2C). This increase is likely explained by the
210 need for a fly to perform tasks that are mutually exclusive to sleep in a reduced amount
211 of waking time. While increases in total sleep are indicative of increase sleep quantity,
212 this measurement does not provide information about sleep quality or sleep depth. To
213 assess whether sleep quality is modulated by FBS lines, we analyzed sleep
214 consolidation during the day and night in these flies. As seen in Figure 2-figure
215 supplement 2A, upon neuronal activation, daytime sleep bout duration is significantly
216 increased in 8 out of the 9 sleep-promoting lines (FBS4, FBS5, FBS42, FBS45, FBS53,
217 FBS68, FBS72 and FBS84), while it is unaffected in FBS81. Notably, increased sleep
218 bout duration is believed to be an indication of increased sleep depth (50). Thus, these
219 data indicate that activating neurons contained in these 8 FBS lines not only increases
220 sleep level but probably also increases sleep depth. Interestingly, one of the lines that
221 did not show an increase in total sleep, has a significant increase in daytime sleep bout
222 duration (FBS28). During the nighttime, the effect of high temperature on sleep is
223 obvious as most lines, including the control, display a significant decrease in sleep bout
224 duration when raising the temperature to 31°C (Figure 2-figure supplement 2B). Only 6
225 of the 9 sleep-promoting lines (FBS4, FBS5, FBS42, FBS45, FBS53 and FBS68)
226 maintain similar nighttime sleep bout durations before and during neuronal activation.
227 Importantly, in these 6 lines nighttime sleep bout duration is significantly increased at

228 31°C when compared to control flies (Figure 2-figure supplement 2B). These data
229 indicate that most sleep-promoting Split-GAL4 lines increase daytime sleep
230 consolidation and suggest that they could also increase nighttime sleep consolidation.
231 However, because of the clear effect of high temperature on nighttime sleep, this claim
232 requires further validation.
233
234 In addition, since sleep in *Drosophila* is sexually dimorphic (51-53), we systematically
235 assessed male flies in our experiments. As seen in Figure 2-figure supplement 3, we
236 obtained almost identical behavioral data when analyzing male flies using our
237 thermogenetic activation approach. Thus, we conclude that we have identified 9 FBS
238 lines that promote sleep when thermogenetically activated in males and females.
239
240 Having identified 9 different Split-GAL4 lines that significantly increased sleep when
241 activated, we sought to identify the neurons that are contained within these lines.
242 Because the goal of our screen was to identify sleep-regulating dFB neurons in the
243 23E10-GAL4 pattern of expression, we expected that most of our FBS lines, sleep-
244 promoting or not, would express in dFB cells. This is indeed the case as 20 out of the
245 22 FBS lines express in some dFB neurons (Figure 2, Figure 2-figure supplement 1,
246 Table 2). The two exceptions to this are FBS25 (expresses in no neurons at all) and
247 FBS5 as discussed below. Regarding sleep-promoting FBS lines, 8 out of 9 have some
248 expression in the dFB. However, and surprisingly, one of the strongly sleep-promoting
249 lines, FBS5, does not express in any dFB neurons at all (Figure 2F, Video 3, Video 4).
250 Rather, FBS5 strongly expresses in two clusters of 4-5 neurons located in the anterior

251 ventrolateral protocerebrum and in 4 VNC cells located in the metathoracic ganglion. A
252 close examination of the anatomy of these 4 VNC neurons indicate that they have
253 processes in the brain. Two of these neurons show a very specific pattern of expression
254 with brain processes located in the superior medial protocerebrum. Because of their
255 characteristic look, we named these processes “bowtie”. These processes are
256 highlighted in the right panel in Figure 2F (see also Video 3). FBS5 additionally labels
257 two neurons in the VNC whose cell bodies are located very close to the “bowtie”
258 neurons. These neurons have characteristic processes in each leg ganglion (yellow
259 arrows in Figure 2F-VNC image). Based on their anatomy, we hypothesize that these
260 cells could be Taste Projection Neurons 1 (TPN1) that receive inputs from sweet
261 gustatory receptor leg neurons (GRNs) and convey this information to the brain in the
262 subesophageal zone (SEZ) (54). We observed these putative TPN1 neurons in 14 out
263 of the 22 FBS lines. Importantly, since all the neurons in FBS5 are part of the 23E10-
264 GAL4 expression pattern, these data indicate that this driver contains non-dFB sleep-
265 promoting cells.
266
267 Most other sleep-promoting line expression patterns are very discrete with only two
268 major areas of expression; dFB neurons, and the metathoracic ganglion region
269 containing the two “bowtie” neurons and TPN1-like cells (FBS42, FBS45, FBS53,
270 FBS68, FBS72, FBS81 and FBS84) (Figure 2G,H; Figure 2-figure supplement 1;
271 Table2). Some of these FBS lines show minimal amount of expression elsewhere in the
272 brain, but there is no consistency in these additionally labeled cells between different
273 lines. Of note, FBS4 expresses in 18-23 dFB neurons (Figure 2E, Table 2) and no other

274 cells in the brain or VNC. Considering that 23E10-GAL4 reliably labels 23-30 dFB
275 neurons in our confocal microscopy experiments (Table1), we conclude that FBS4
276 expresses in 75-80% of 23E10 dFB neurons. Because of its dFB specific expression
277 pattern and its ability to increase sleep when thermogenetically activated, we suspect
278 that FBS4 probably contains neuron(s) that are regulating sleep. However, we also note
279 that the sleep increase triggered by FBS4 thermogenetic activation is not as striking as
280 when activating other strongly sleep-promoting lines like FBS5, FBS53 or FBS68
281 (Figure 2B for females and Figure 2-figure supplement 3A for males).
282
283 One particularly interesting line is FBS45. FBS45 is strongly sleep-promoting and is
284 expressed in 21-32 dFB neurons, indicating that most if not all 23E10 dFB neurons are
285 present in FBS45 (Figure 2G, Table2). However, FBS 45 also expresses in the two
286 “bowtie” neurons. Importantly, FBS45 does not label any other neurons in the brain and
287 VNC.
288
289 When combining behavioral and anatomical data, it appears that the numbers of dFB
290 neurons contained within a specific FBS line cannot be predictive of whether the line
291 can promote sleep upon neuronal activation. For example, FBS68 strongly promotes
292 sleep and expresses in only 3-6 dFB neurons (Figure 2H, Table 2), while FBS60
293 contains 22-27 dFB neurons and does not promote sleep (Figure 2-figure supplement
294 1L, Table 2).
295

296 Remarkably, a careful examination of expression patterns reveals that many FBS lines
297 appear to express in the “bowtie” VNC neurons. Note that the brain processes of these
298 cells are located extremely close to the axonal projections of dFB neurons, making the
299 visualization of these VNC projections sometimes difficult, depending on the strength of
300 dFB projection’s staining. Nevertheless, these VNC “bowtie” neurons are present in 17
301 out of 22 FBS lines (See Figure 2 and Figure 2-figure supplement 1 VNC ”bowtie”
302 processes). Importantly, we can see these neurons and their processes in all sleep-
303 promoting lines with the notable exception of FBS4 (Figure 2, Figure 2-figure
304 supplement 1, Table 2), as discussed above. Upon examination of the literature, we
305 found that neurons with similar projections are frequently seen in many Janelia GAL4
306 lines (55). This study reports that these neurons (referred to as “sparse T” in this work)
307 and their processes are seen in up to 60% of all Janelia GAL4 lines. The fact that these
308 “bowtie” neurons are frequently present in many GAL4 lines probably explains why we
309 see them in the vast majority of our FBS lines (18 out of 22 or 82% of them).
310
311 In conclusion, our thermogenetic screen and anatomical analysis identified 9 sleep-
312 promoting lines with diverse patterns of expression. While the identity of the neurons
313 responsible for sleep promotion in these different lines is not clear at this stage, our
314 analysis indicates that there are multiple groups of sleep-promoting neurons in the
315 23E10-GAL4 pattern of expression; one of which appears to be part of the dFB (FBS4)
316 while the other is non-dFB based (FBS5).
317
318 **Optogenetic confirmation of sleep promoting FBS lines**

319 Because of the strong effect that temperature has on sleep, we sought to confirm our
320 thermogenetic findings using an alternative way to manipulate FBS lines. The logic
321 behind our thinking is that it may be difficult to fully describe and characterize the sleep
322 behaviors of our FBS lines when temperature itself has such a profound effect on sleep.
323 Furthermore, a recent study demonstrated that some of the effects of high temperature
324 on sleep are mediated by GABAergic transmission on dFB neurons (49). Taken
325 together, these data suggest that thermogenetic manipulations may not be optimal to
326 conduct our screen. We thus undertook an optogenetic screen using CsChrimson (56).
327 Our optogenetic experimental setup is described in Figure 3A. Notably, for neurons to
328 be activated when expressing CsChrimson, flies need to be fed all trans-retinal and the
329 neurons must be stimulated with a 627nm LED light source (56). Thus, optogenetic
330 approaches provide a much better control on the timing and parameters of activation.
331 Nonetheless, optogenetic activation gave results that are mostly identical to the
332 thermogenetic approach. That is, most sleep-promoting lines identified using TrpA1 also
333 induce sleep when activated with CsChrimson in retinal-fed flies (FBS5, FBS42, FBS45,
334 FBS53, FBS68 and FBS72) (Figure 3B for female data). Notable differences are FBS4,
335 FBS81 and FBS84 which do not promote sleep when optogenetically activated in
336 female flies. However, activating FBS81 and FBS84 significantly increases sleep in
337 retinal-fed male flies (Figure 3-figure supplement 2A). Importantly, unlike FBS81 and
338 FBS84, activation of FBS4 neurons does not increase sleep in retinal-fed males (Figure
339 3-figure supplement 2A). Thus, there is a clear discrepancy for FBS4 comparing
340 thermogenetic and optogenetic activations. Another difference between the two
341 activation approaches is FBS70 that is sleep-promoting using CsChrimson in retinal-fed

342 female flies while it was not using TrpA1 (Figure 3B). Surprisingly, retinal-fed
343 FBS70>UAS-CsChrimson males do not increase sleep upon LED stimulation,
344 potentially revealing a sexually dimorphic phenomenon (Figure 3-figure supplement 2A).
345 Importantly, assessment of locomotor activity during waking period reveals that
346 optogenetic activation does not decrease waking activity in long sleeping retinal-fed
347 females (Figure 3C) and males (Figure 3-figure supplement 2B), ruling out the
348 possibility that locomotor defects are the underlying cause of the sleep phenotypes
349 observed. Examination of sleep bout duration in retinal-fed flies indicates that most
350 sleep-promoting FBS lines increase sleep consolidation during the day (Figure 3D for
351 females and Figure 3-figure supplement 2C for males) and during the night (Figure 3E
352 for females and Figure 3-figure supplement 2D for males). These data indicate that
353 optogenetic activation increases sleep quantity and probably sleep quality (sleep depth)
354 in many of the FBS lines first identified using our thermogenetic approaches.
355 Interestingly, some FBS lines that did not increase total sleep upon optogenetic
356 activation increased daytime sleep bout duration: FBS57 and FBS60 females (Figure
357 3D) and FBS33, FBS35, FBS64 and FBS87 males (Figure 3-figure supplement 2C).
358 These data suggest that these lines may also express in sleep-regulating neurons.
359
360 Importantly, analysis of sleep parameters in vehicle-fed flies demonstrate that the sleep
361 phenotypes we observed are specific to retinal-fed and LED stimulated flies (Figure 3-
362 figure supplement 1 for females and Figure 3-figure supplement 3 for males).
363

364 In conclusion, our thermogenetic and optogenetic neuronal activation revealed several
365 strongly sleep-promoting lines. When looking at their expression patterns, our data
366 clearly demonstrate that 23E10 GAL4 contains at least two different sleep-promoting
367 regions, one that is part of the dFB and one that is not.
368

369 **The 23E10-GAL4 driver contains sleep-promoting neurons that are not located in**
370 **the brain**

371 To reveal the identity of the non-dFB 23E10 sleep-promoting neurons, we undertook a
372 second screen creating additional Split-GAL4 lines focusing on neurons that are present
373 in FBS5. To facilitate this task, we used Color Depth MIP mask search, a software plug-
374 in for Fiji (57). This approach identified several AD lines (containing neurons of interest)
375 that we combined with our 23E10-DBD stock. An example of such a line is shown in
376 Figure 4A-D. This Split-GAL4 line (VT020742-AD;23E10-DBD) expresses only in 4 VNC
377 neurons (Figure 4C). Projections of 2 of these are clearly “bowtie” like (gray arrows in
378 Figure 4A-B). Projections of the other two appear to be identical to TPN1 neurons that
379 have been previously described (yellow arrows in Figure 4A-D). Remarkably,
380 VT020742-AD;23E10-DBD does not express in any other neurons in the brain and
381 VNC. To confirm the presence of TPN1 neurons in this Split-GAL4 line we expressed
382 GFP using a TPN1 specific driver, 30A08-LexA (54) while simultaneously expressing
383 RFP using VT020742-AD;23E10-DBD. As seen in Figure 4-figure supplement 4A, there
384 is clear GFP and RFP co-expression in two out of the four VT020742-AD;23E10-DBD
385 neurons (yellow arrows). In addition, we also see co-expression of GFP and RFP in the
386 processes that go into each leg ganglion, but only RFP expression in the “bowtie”

387 processes. From these data we conclude that VT020742-AD;23E10-DBD labels 4
388 neurons in the metathoracic ganglion of the VNC: 2 “bowtie” neurons and 2 TPN1 cells.
389 Optogenetic activation of these 4 neurons strongly increases sleep in retinal-fed
390 females (Figure 4K) and males (Figure 4-figure supplement 2A). In addition, daytime
391 and nighttime sleep bout duration are significantly increased in retinal-fed VT020742-
392 AD;23E10-DBD>UAS-CsChrimson flies (Figure 4M-N for females and Figure 4-figure
393 supplement 2C-D for males). Importantly, analysis of waking activity reveals that the
394 sleep increases are not caused by a deficit in locomotor activity (Figure 4L for females
395 and Figure 4-figure supplement 2B for males).
396
397 We then wanted to find out whether TPN1 neurons are the cells involved in sleep
398 promotion in VT020742-AD;23E10-DBD. We thus created a 30A08-AD;23E10-DBD
399 Split-GAL4 line. This line labels only the two TPN1 neurons and no other cells in the
400 brain and VNC (Figure 4E-F). Importantly, optogenetic activation of 30A08-AD;23E10-
401 DBD neurons has no effect on sleep (Figure 4K-N and Figure 4-figure supplement 2A-
402 D), indicating that the sleep-promoting capacity of VT020742-AD;23E10-DBD most
403 likely lies within the two “bowtie” neurons. To further rule out an involvement of TPN1
404 neurons in sleep promotion, we adopted the Split-GAL4 repressor Killer Zipper (KZip+)
405 technology which inhibits an AD and DBD from forming a functional GAL4 (58).
406 Expressing KZip+ with 30A08-LexA while expressing GFP with VT020742-AD;23E10-
407 DBD, reduces the number of GFP positive cells from 4 to 2 (Figure 4-figure supplement
408 4B). Only the two “bowtie” neurons can be seen in this combination. Thus, we can
409 effectively subtract the TPN1 neurons from the VT020742-AD;23E10-DBD pattern of

410 expression. Optogenetic activation of the remaining “bowtie” neurons (in retinal-fed
411 VT020742-AD;23E10-DBD>UAS-CsChrimson, 30A08-LexA>LexAop2-KZip+ flies) still
412 promotes sleep (Figure 4-figure supplement 4C). Taken together these data indicate
413 that the two “bowtie” neurons in VT020742-AD;23E10-DBD (and 23E10-GAL4) increase
414 sleep when activated and that TPN1 neurons are not involved in sleep promotion.
415
416 To further refine our analysis, we constructed an additional Split-GAL4 line (VT013602-
417 AD;23E10-DBD) that only expresses in the two “bowtie” like VNC neurons (gray arrows
418 in Figure 4G-J, Video 5, Video 6). Optogenetic activation of retinal-fed VT013602-
419 AD;23E10-DBD neurons strongly promotes sleep (Figure 4K and Figure 4-figure
420 supplement 2A for male data) and increases daytime (Figure 4M and Figure 4-figure
421 supplement 2C) and nighttime bout duration (Figure 4N and Figure 4-figure supplement
422 2D). Again, increases in sleep are not caused by abnormal locomotor activity (Figure 4L
423 and Figure 4-figure supplement 2B). Importantly, analysis of sleep parameters in
424 vehicle-fed flies reveal sleep phenotypes observed are specific to activation of
425 VT013602-AD; 23E10-DBD neurons (Figure 4-figure supplement 1 and Figure 4-figure
426 supplement 3). Since activating the two ‘bowtie” neurons increases daytime and
427 nighttime sleep bout duration, we hypothesize that this manipulation increases sleep
428 quality, namely sleep depth. To investigate this possibility, we measured arousal
429 thresholds in VT013602-AD;23E10-DBD>UAS-CsChrimson flies. As seen in Figure 4-
430 figure supplement 5, the proportion of retinal-fed flies awakened by mild mechanical
431 perturbations (1 and 2) is significantly reduced in LED stimulated (LED ON, activated)
432 individuals compared with non-activated flies (LED OFF). Thus, these data demonstrate

433 that when activated, the two “bowtie” neurons increase sleep quantity and sleep depth
434 as indicated by an increase in arousal threshold. Importantly, at the highest perturbation
435 level (4), retinal-fed LED activated VT013602-AD;23E10-DBD>UAS-CsChrimson flies
436 respond to the stimulus similarly to controls, indicating that the sleep that is induced by
437 activation of these neurons is reversible.
438
439 To assess whether the “bowtie” neurons seen in VT020742-AD;23E10-DBD and
440 VT013602-AD;23E10-DBD are the same, we constructed a line that carries both
441 VT020742-AD and VT013602-AD as well as 23E10-DBD. Expressing GFP with this line
442 labels only 4 VNC neurons, 2 “bowtie” cells and 2 TPN1 (Figure 4-figure supplement
443 4D). If the “bowtie” neurons were different in VT020742-AD;23E10-DBD and VT013602-
444 AD;23E10-DBD we would expect to see 6 cells. Since this is not the case, we can
445 conclude that the 2 ‘bowtie” neurons observed in VT020742-AD;23E10-DBD and
446 VT013602-AD;23E10-DBD are the same. To provide functional support to this finding,
447 we created an additional Split-GAL4 line, VT013602-AD;VT020742-DBD. This Split-
448 GAL4 line labels 2 “bowtie” cells in the VNC with typical processes in the brain (gray
449 arrows in Figure 4-figure supplement 4E) and promotes sleep when activated
450 thermogenetically (Figure 4-figure supplement 4F-H). Taken together, these data
451 demonstrate that we have unequivocally identified two novel sleep-promoting neurons
452 located in the VNC. Importantly, these cells are part of the 23E10-GAL4 expression
453 pattern. We will from now on refer to these neurons as VNC-SP (for VNC Sleep-
454 Promoting).
455

456 **Silencing VNC-SP neurons reduces sleep**

457 Having demonstrated that activation of VNC-SP neurons increases sleep duration and
458 sleep depth, we wondered whether these cells could modulate sleep bi-directionally.
459 Thus we performed experiments to silence the activity of VNC-SP neurons either
460 chronically, by expressing the inward rectifying potassium channel Kir2.1 (59) or acutely
461 by using the temperature sensitive Shi^{ts1} construct (60). As seen in Figure 5A-B, total
462 sleep is significantly reduced when expressing Kir2.1 in VNC-SP neurons in female
463 flies. This reduction in sleep is accompanied by a reduction of both daytime (Figure 5C)
464 and nighttime sleep bout duration (Figure 5D), suggesting a defect in sleep
465 consolidation. Importantly, analysis of activity counts during waking time reveals that the
466 decrease in sleep is not due to hyperactivity (Figure 5E). We obtained identical
467 behavioral results when expressing Kir2.1 in VNC-SP neurons of male flies (Figure 5F-
468 J). Thus, chronic silencing of VNC-SP neurons decreases sleep and disrupts sleep
469 consolidation.

470

471 To confirm the findings obtained using chronic silencing we decided to employ an acute
472 silencing protocol by expressing Shi^{ts1} (60) in VNC-SP neurons. Notably, this approach
473 relies on increasing temperature to silence neurons. Because of the previously reported
474 effect of temperature on sleep, it is not surprising to see that the shift in temperature
475 reduces sleep in control flies (Figure 5K for females and Figure 5N for males). Acute
476 silencing of VNC-SP neurons also reduces sleep, an effect particularly striking at night
477 (Figure 5L and Figure 5M). Importantly, nighttime sleep is significantly more reduced in
478 VNC-SP> Shi^{ts1} flies than in controls (Figure 5M and Figure 5P).

479 Taken together, our chronic and acute silencing data demonstrate that VNC-SP
480 neurons positively regulate sleep. Importantly, these results further reinforce our
481 findings using optogenetic and thermogenetic activation experiments.
482
483 **VNC-SP neurons express and use acetylcholine to modulate sleep**
484 Having demonstrated that VNC-SP neurons modulate sleep bi-directionally, we sought
485 to identify the neurotransmitter(s) used by these cells. A previous study suggested that
486 most neurons in the VNC use one of three neurotransmitters: GABA, Glutamate or
487 Acetylcholine (61). With this in mind, we expressed GFP in VNC-SP neurons and
488 incubated them with antibodies to GABA, choline acetyltransferase (ChAT), the enzyme
489 necessary to produce Acetylcholine and the vesicular glutamate transporter (VGlut). As
490 seen in Figure 6A, we observed clear co-labelling of GFP and ChAT in VNC-SP
491 neurons. To further confirm that VNC-SP neurons express ChAT, we employed a
492 combinatorial approach expressing RFP in VNC-SP cells and GFP driven by a ChAT-
493 LexA (62) construct that is inserted within the endogenous ChAT locus. This construct
494 ensures that the expression of LexA is controlled by ChAT regulatory sequences and
495 should reflect transcriptional activity at the endogenous ChAT locus. As seen in Figure
496 6-figure supplement 1A, we observe clear co-labelling of GFP and RFP in VNC-SP
497 neurons (gray arrow). In addition, we employed a similar approach using 23E10-GAL to
498 drive expression of RFP. As seen in Figure 6-figure supplement 1B, we observe clear
499 co-labelling of GFP and RFP in two neurons in the metathoracic ganglion of the VNC
500 (gray arrows). The evidence clearly suggests that these two cells are the VNC-SP
501 neurons. Interestingly, in the process of this experiment, we found that 2-3 dFB neurons

502 per brain hemisphere are co-labelled by 23E10-GAL4 and ChAT-LexA construct (Figure
503 6-figure supplement 1B, bottom panels, red arrows). Taken together, these data
504 indicate that VNC-SP neurons and some 23E10-GAL4 dFB neurons are cholinergic.
505
506 Importantly, we did not detect any co-labelling between GFP and VGlut (Figure 6B) or
507 GABA (Figure 6C) in these experiments. To find out whether VNC-SP neurons express
508 any additional neurotransmitters we also performed experiments using antibodies to
509 serotonin (5HT, Figure 6D), tyrosine hydroxylase (TH, Figure 6E), the key enzyme in
510 the synthesis of dopamine, and tyrosine decarboxylase 2 (Tdc2, Figure 6F), an enzyme
511 involved in the synthesis of octopamine. We did not observe any co-labelling with any of
512 these 3 antibodies.
513
514 These data indicate that VNC-SP neurons are cholinergic but they do not provide any
515 information as to whether cholinergic transmission is needed for the sleep modulating
516 role of VNC-SP neurons. To address this question, we sought to disrupt cholinergic
517 transmission in VNC-SP neurons using an RNAi approach. Thus, we obtained two
518 independent RNAi lines for ChAT. We first sought to validate them by crossing them to
519 the pan-neuronal elav-GAL4 driver. One of the lines (60028) led to lethality when
520 crossed to elav-GAL4, indicative of a significative reduction in ChAT levels. The second
521 line (25856) gave rise to progeny suggesting it is not very efficient. Note that a similar
522 approach was used to validate ChAT RNAi constructs in other studies (63). However, to
523 further confirm the efficiency of these ChAT RNAi constructs we performed a qPCR
524 analysis on flies expressing ChAT RNAi (60028) specifically in the eyes using a GMR-

525 GAL4 driver. Figure 6-figure supplement 1C demonstrates that ChAT mRNA levels are
526 significantly reduced (about 20%) in the eyes of GMR-GAL4>ChAT RNAi (60028) flies
527 compared with controls. Notably, ChAT mRNA levels are unaffected in the body of
528 these flies, illustrating the efficiency and specificity of the ChAT RNAi line. Importantly,
529 qPCR analysis of the second ChAT RNAi line (25856) showed no significant reduction
530 in ChAT levels, further demonstrating its inefficiency (data not shown). Based on this
531 data, we decided to only employ one ChAT RNAi (60028) in our behavioral studies.
532
533 As seen in Figure 6-figure supplement 1D-E, ChAT levels as measured by
534 immunocytochemistry are significantly reduced when expressing ChAT RNAi in VNC-
535 SP neurons. Behaviorally, reducing ChAT levels in VNC-SP neurons significantly
536 reduces sleep (Figure 6G-H) and, daytime (Figure 6I) and nighttime (Figure 6J) sleep
537 bout duration in female flies. Importantly, the reduction in sleep is not due to
538 hyperactivity (Figure 6K). We obtained similar behavioral data when looking at males
539 (Figure 6-figure supplement 1F-I). Taken together, our data indicate that cholinergic
540 transmission is involved in regulating the sleep modulating effect of VNC-SP neurons.
541 We also note that the behavioral effects of reducing ChAT levels and silencing VNC-SP
542 neurons are consistent with each other, suggesting that in the absence of ChAT, the
543 ability of VNC-SP neurons to positively regulate sleep is seriously diminished. To further
544 interrogate the necessity of cholinergic transmission for VNC-SP neurons to promote
545 sleep, we activated VNC-SP neurons optogenetically, while simultaneously expressing
546 ChAT RNAi in these cells. As seen in Figure 6L, expression of CsChrimson and a RNAi
547 line targeting GFP (control RNAi) does not prevent sleep increase in retinal-fed flies.

548 However, expressing ChAT RNAi completely abolishes the sleep promotion triggered by
549 activation of VNC-SP neurons. In conclusion, our data clearly demonstrate that VNC-SP
550 neurons are cholinergic and that disruption of cholinergic transmission abolishes the
551 sleep-promoting role of these cells.
552
553 To further confirm that the sleep phenotypes we observe are due to VNC-SP neurons,
554 we optogenetically activated VNC-SP cells while expressing the Split-GAL4 repressor
555 KZip+ (58) under the control of a ChAT-LexA driver. As seen in Figure 6-figure
556 supplement 1J, expressing the KZip+ repressor in ChAT expressing neurons blocks the
557 sleep induction caused by activation of VNC-SP neurons. These data strongly suggest
558 that the KZip+ is expressed in VNC-SP neurons and actively represses the binding of
559 the GAL4-AD and GAL4-DBD constructs. To visually confirm repression of GAL4
560 activity, we expressed GFP in VNC-SP neurons and the KZip+ repressor in ChAT-LexA
561 cells. As seen in Figure 6-figure supplement 1K, expressing the KZip+ repressor in
562 ChAT expressing neurons strongly reduces the amount of GFP staining seen in VNC-
563 SP neurons. Taken together, these data confirm that the sleep phenotypes we observe
564 are due to activation of VNC-SP neurons and further demonstrate that these cells are
565 cholinergic.
566
567 Since VNC-SP neurons are observed in 18 of our 22 FBS lines, and in most sleep-
568 promoting lines (except for FBS4), we wondered whether VNC-SP neurons are the cells
569 responsible for the sleep increase in all our lines. We decided to focus on FBS45, since
570 it expresses in most if not all 23E10-GAL4 dFB neurons (Table 2) and in the two VNC-

571 SP neurons. Importantly, FBS45 is one of the strongest sleep-promoting lines we have
572 studied in this work. Our question was the following: Is the sleep increase caused by
573 activation of FBS45 due to VNC-SP neurons, dFB neurons, or both group of cells? To
574 answer this question, we expressed UAS-CsChrimson in FBS45 neurons while
575 simultaneously driving the expression of the KZip+ repressor in ChAT-LexA cells. We
576 hypothesize that this manipulation should repress GAL4 formation specifically in VNC-
577 SP neurons. However, since we have reported that ChAT-LexA also expresses in some
578 23E10-GAL4 dFB neurons (Figure 6-figure supplement 1B), our manipulation may
579 repress GAL4 in a few dFB neurons. As seen in Figure 6-figure supplement 1L,
580 expressing the KZip+ repressor in ChAT-LexA prevents retinal-fed FBS45>UAS-
581 CsChrimson flies from increasing sleep when activated. These data indicate that the
582 neurons responsible for the sleep increase when activating FBS45 cells are cholinergic
583 and that expressing CsChrimson only in FBS45 neurons that are not targeted by ChAT-
584 LexA (non-cholinergic) cannot promote sleep. We then visually assessed the extent of
585 ChAT-LexA driven KZip+ repression in FBS45 neurons by expressing UAS-GFP. As
586 seen in Figure 6-figure supplement 1M, expressing the KZip+ repressor in ChAT-LexA
587 completely abolishes GFP expression in VNC-SP neurons in *FBS45>UAS-GFP; ChAT-*
588 *LexA>LexAop2-KZip+* flies. However, as we expected based on our previous data,
589 ChAT-LexA>LexAop2-KZip+ consistently removes GFP expression in 4-6 dFB neurons
590 as well. Taken together, these data suggest that the sleep-promoting capacity of FBS45
591 relies on cholinergic neurons. While we strongly believe that the cells responsible are
592 VNC-SP neurons, we cannot completely exclude a role for one of the ChAT expressing

593 23E10-GAL4 dFB neurons. Further work will help clarify the role of cholinergic dFB
594 neurons in sleep regulation.
595 Since the VNC receives and integrates sensory inputs from the periphery and sends
596 this information to the brain (64-66), we wondered whether VNC-SP neurons could
597 similarly send sleep-relevant signals to the brain. The location of VNC-SP neurons in
598 the VNC, and their processes in the brain suggests that this is a likely possibility. To find
599 out, we expressed the dendritic marker DenMark (67) in conjunction with the
600 presynaptic marker synaptotagmin-GFP (syt.eGFP) (68) in VNC-SP neurons. Our data
601 indicate that VNC-SP neurons have mostly postsynaptic sites in the VNC, as expected if
602 these cells receive sensory information from the periphery (Figure 6-figure supplement
603 2, middle panels). However, and surprisingly, the brain processes of these cells are
604 labeled with both the presynaptic and postsynaptic markers (Figure 6-figure supplement
605 2, top panels). This suggests that VNC-SP neurons are well positioned to receive
606 sensory inputs from the periphery in the VNC and that they are sending this information
607 to the brain. However, since the brain processes of VNC-SP neurons are also harboring
608 postsynaptic sites, it is highly likely that they also get inputs in the brain. Nevertheless,
609 our data suggest that VNC-SP neurons send sleep-relevant signals to the brain.
610

611 **Multiple sleep-promoting regions in 23E10-GAL4 with functional specificity**

612 Our data unequivocally demonstrate that VNC-SP neurons, which are part of the
613 23E10-GAL4 pattern of expression, are sleep-promoting. Since 23E10-GAL4 is widely
614 seen as dFB specific driver when it comes to sleep regulation, the identification of VNC-
615 SP neurons is a major finding that impacts our current views about the role of the dFB in

616 sleep regulation. Our data shows that all but one FBS sleep-promoting lines contain
617 VNC-SP neurons. The only sleep-promoting line that is dFB specific (FBS4) only mildly
618 promotes sleep (when compared with other lines) in our thermogenetic screen but does
619 not using optogenetic. These data raise important questions about the role of the dFB in
620 sleep regulation and sleep-promotion.
621
622 To try to address these questions we went back to the 23E10-GAL4 driver and its
623 23E10-LexA counterpart (69). First, we wanted to check whether 23E10-GAL4 and
624 23E10-LexA express in the same number of neurons. This is an important control since
625 it was reported that often for a given enhancer sequence, the LexA expression pattern
626 does not fully recapitulate the GAL4 expression pattern (69). We created a line
627 expressing GFP under the control of 23E10-LexA and RFP under the control of 23E10-
628 GAL4. As seen in Figure 7A-B, the 23E10-LexA driver does not fully recapitulate the
629 23E10-GAL4 pattern of expression in the dFB. Some cells are clearly co-labelled by
630 GFP and RFP (yellow arrows) but some other dFB neurons only express RFP (gray
631 arrow). Importantly, we did not observe any dFB cells (or any other cell in the brain) that
632 are only labeled by 23E10-LexA. These data indicate that, like many other LexA drivers,
633 23E10-LexA only expresses in a subset of the 23E10-GAL4 pattern of expression. We
634 then turned our attention to the metathoracic ganglion of the VNC. As seen in Figure
635 7C, 23E10-LexA labels the two TPN1 neurons (yellow arrows) while 23E10-GAL4 labels
636 the two TPN1 cells as well as the two VNC-SP neurons (gray arrows). The processes of
637 TPN1 neurons are highlighted in Figure 7E and those from VNC-SP in Figure 7D. We
638 see clear co-labelling of TPN1 processes by 23E10-LexA and 23E10-GAL4, but VNC-

639 SP processes are only labeled by 23E10-GAL4. Taken together, we conclude that
640 23E10-LexA only expresses in a subset of 23E10-GAL4 neurons and that 23E10-LexA
641 does not express in VNC-SP neurons.
642
643 We then wondered whether 23E10-LexA could promote sleep when activated
644 optogenetically. As seen in Figure 7F, optogenetic activation of retinal-fed 23E10-
645 GAL4>UAS-CsChrimson strongly increases sleep as expected. Controls show no
646 changes in sleeping levels. However, optogenetic activation of retinal-fed 23E10-
647 LexA>LexAop2-CsChrimson has no effect on sleep (Figure 7G). The stark difference in
648 behavior seen when activating 23E10-GAL4 and 23E10-LexA could be explained by the
649 fact that 23E10-GAL4 expresses in more neurons than 23E10-LexA. In this scenario the
650 absence of VNC-SP neurons in the 23E10-LexA pattern of expression must account for
651 some if not all this difference. However, since 23E10-LexA does not fully recapitulate
652 the expression pattern of 23E10-GAL4 in the dFB, we cannot rule out that some of
653 these missing dFB neurons may be involved in sleep promotion. An alternative
654 explanation is that 23E10-LexA may not be as strong a driver as 23E10-GAL4 and
655 therefore would not express sufficient levels of the CsChrimson construct. In our
656 experience this is very unlikely as we have optogenetically activated other pairs of
657 Gal4/LexA drivers and obtained identical and strong sleep activation with both the LexA
658 and GAL4 counterparts (data not shown).
659
660 Does our data mean that the dFB plays no role at all in sleep regulation? Based on the
661 number of studies supporting a role for this structure in sleep regulation (27-30, 33, 34,

662 37, 44, 45) we think that this is very unlikely. Most of the previous work supports a role
663 for dFB neurons in sleep homeostasis. In particular, sleep deprivation increases the
664 excitability of dFB neurons (29) and augmented sleep pressure switches dFB neurons
665 from an electrically silent to an electrically active state (33). Furthermore, reducing the
666 excitability of dFB neurons by reducing levels of the Rho-GTPase-activating protein
667 encoded by the crossveinless-c (cv-c) gene leads to a defect in sleep homeostasis (29).

668

669 With this in mind, we wanted to assess whether silencing all 23E10-Gal4 neurons, or
670 just 23E10-GAL4 dFB and VNC-SP neurons separately would affect sleep homeostasis
671 (Figure 8A). As seen in Figure 8B, chronic silencing of all 23E10-GAL4 neurons by
672 expression of Kir2.1 effectively blocks homeostatic sleep rebound when compared with
673 both parental controls. Interestingly, chronic silencing of VNC-SP cells does not disrupt
674 homeostatic sleep rebound (Figure 8C) while silencing of most 23E10-GAL4 dFB
675 neurons (contained in the FBS4 line) does (Figure 8D). These data support a role for
676 23E10-GAL4 dFB neurons in sleep homeostasis, in agreement with previous studies.

677

678 Taken together, our data indicate that the 23E10-GAL4 driver contains at least two
679 groups of sleep-regulating neurons, one located in the dFB that is mostly involved in
680 sleep homeostasis and VNC-SP neurons that are dispensable for sleep homeostasis.

681

682

683

684 **Discussion**

685 The strength of the fly model lies in its strong genetic techniques, allowing researchers
686 to selectively manipulate discrete populations of neurons and monitor how specific
687 behaviors are affected. To do so, an impressive collection of binary expression systems
688 have been developed. In particular, the GAL4/UAS system (8) has been the keystone of
689 *Drosophila* neurobiological studies. However, GAL4 drivers are often not specific
690 enough and express in cells outside the region of interest. This can make the task of
691 unequivocally assigning a given behavior to a specific neuron or group of neurons
692 particularly difficult. Importantly, refinement of GAL4 expression pattern can be
693 achieved by employing the intersectional Split-GAL4 technology (11).

694

695 Like mammalian sleep, sleep in *Drosophila* is regulated by multiple areas in the brain
696 (16, 17). Particularly, an expanding amount of evidence supports a role for dFB neurons
697 in sleep regulation (27-30, 33, 34, 37, 44, 45). The most widely used tool to manipulate
698 dFB neurons is the 23E10-GAL4 driver (33, 36), and thermogenetic or optogenetic
699 activation of 23E10-GAL4 neurons results in increased sleep (31, 37-39). However,
700 whether 23E10-GAL4 dFB neurons can be considered as a functionally homogeneous
701 group is still unclear. Also unclear is whether the sleep-promotion caused by activation
702 of 23E10-GAL4 neurons is due to dFB neurons. This concern is reinforced by the fact
703 that 23E10-GAL4 expresses in many neurons outside the dFB in the brain and in the
704 VNC (Figure 1, Table 1). In this study, we sought to identify the role of individual 23E10-
705 GAL4 dFB neurons in sleep regulation.

706

707 To identify sleep-promoting neurons within the 23E10-GAL4 pattern of expression we
708 adopted a targeted Split-GAL4 strategy combining 22 individual AD lines (selected for
709 the strong dFB expression pattern of their GAL4 counterparts) with a 23E10-DBD line.
710 We screened these 22 novel Split-GAL4 FBS lines behaviorally and anatomically. First,
711 we employed a thermogenetic approach to activate the neurons contained in these 22
712 lines. These experiments identified 9 FBS lines that promote sleep when activated in
713 females and males (Figure 2). An anatomical assessment of each line revealed that
714 most sleep-promoting FBS lines express in some dFB neurons, as expected based on
715 our targeted approach. However, they also express in other areas in the brain and
716 especially in the metathoracic ganglion of the VNC. In fact, we identified two very clear
717 and characteristic processes associated with 4 different VNC neurons in many FBS
718 lines, sleep-promoting or not. The first set of two VNC neurons have typical processes
719 in each leg ganglion and send processes in the brain that terminate in the SEZ. Our
720 data demonstrated that these cells are TPN1 neurons (Figure 4) (54). We observed
721 these neurons in 14 out of the 22 FBS lines. However, we demonstrated that TPN1
722 neurons are not promoting sleep when activated (Figure 4). The second set of two VNC
723 neurons send processes to the superior medial protocerebrum. Due to their
724 characteristic anatomical features, we named these processes “bowtie”. Importantly,
725 these processes are seen in 18 out of 22 FBS lines (and in 8 out of the 9 sleep-
726 promoting lines). The high frequency of observation of these processes in our FBS lines
727 suggest that “bowtie” neurons are commonly expressed in many GAL4 lines. In fact, a
728 MultiColor FlpOut (MCFO) study reported that these neurons are observed in more than
729 60% of all Janelia GAL4 lines (55). Only one line, FBS4, promotes sleep when

730 thermogenetically activated and expresses only in dFB cells, containing about 80% of
731 23E10-GAL4 dFB neurons. FBS4 can thus be considered as a dFB specific driver. We
732 note that the amount of sleep induction triggered by thermogenetic activation of FBS4 is
733 lower than in most other sleep-promoting FBS lines. However, the most surprising
734 finding from our anatomical analysis is FBS5, a line that has no expression in the dFB,
735 and still promotes sleep when activated. This clearly demonstrates that 23E10-GAL4
736 contains sleep-promoting neurons that are not dFB cells.
737
738 Because temperature has a strong impact on sleep (42, 43, 48, 49), we confirmed our
739 findings using an optogenetic activation method (Figure 3). Most sleep-promoting FBS
740 lines increased sleep when activated using either methods. The notable exception is the
741 dFB specific FBS4 line, which did not affect sleep at all upon optogenetic activation.
742 What is the source of this discrepancy? We can propose several scenarios. The first
743 possible explanation is that the threshold of activation needed for the neurons contained
744 in FBS4 to fire and promote sleep is high. This would imply that thermogenetic
745 activation, which is constant during the 24h activation day, provides stronger activation
746 than the fragmented optogenetic protocol. Considering that dFB neurons are subject to
747 dopaminergic regulation (33), we hypothesize that under baseline conditions, dFB
748 neurons are under severe dopaminergic inhibition and that our optogenetic activation
749 protocol is not sufficient to bring these cells above firing threshold. A second possibility
750 is that FBS4 expresses in neurons underlying the effect of high temperature on sleep.
751 This hypothesis is supported by a recent study demonstrating that some of the effects of
752 high temperature on sleep are mediated by GABAergic transmission on dFB neurons

753 (49). It is thus conceivable, that activating FBS4 neurons thermogenetically may
754 counteract the effect of increasing temperature on sleep. This would explain why we
755 only see a sleep-promoting effect when activating FBS4 using thermogenetic and not
756 optogenetic.
757
758 A further screen demonstrated that the VNC ‘bowtie” neurons are sleep-promoting
759 (Figure 4). Activating these cells (renamed VNC-SP neurons) increases sleep, sleep
760 consolidation and sleep depth by increasing arousal thresholds. Moreover, chronic, and
761 acute silencing of VNC-SP neurons reduce sleep and sleep consolidation (Figure 5)
762 confirming that VNC-SP neurons positively regulate sleep. We then sought to discover
763 the neurochemical identity of VNC-SP neurons and identified acetylcholine as a key
764 modulator of sleep in VNC-SP neurons (Figure 6). Reducing cholinergic transmission in
765 VNC-SP neurons reduces sleep and sleep consolidation, an effect mirroring the
766 silencing experiments described earlier. Moreover, we demonstrate that VNC-SP
767 neurons use cholinergic transmission to promote sleep when optogenetically activated.
768
769 Since we observed ‘bowtie” processes in most FBS lines, we assume that most of these
770 lines express in VNC-SP neurons. One could therefore wonder why we do not observe
771 total sleep changes when activating these lines? Importantly, our analysis of sleep
772 parameters including day and night sleep bout duration reveals that sleep consolidation
773 is significantly increased using at least one activation protocol with 7 of these “non
774 sleep-promoting” “bowtie” containing lines (FBS28, FBS33, FBS35, FBS57, FBS60,
775 FBS64 and FBS87). Thus, out of the 18 FBS lines that express in VNC-SP neurons, 16

776 of them increase at least one sleep parameter when activated. The only lines that
777 express in VNC-SP neurons and do not affect any sleep parameters when activated are
778 FBS1 and FBS58. Interestingly, we observed that the GFP signal in the VNC-SP
779 “bowtie” processes of these two lines is weak (Figure 2-figure supplement 1), indicating
780 reduced GAL4 expression in these cells. This observation may provide an explanation
781 for the lack of sleep changes when activating these lines. We also suspect that levels of
782 GAL4 expression in VNC-SP neurons could explain why some FBS lines are promoting
783 sleep more strikingly than others.
784
785 Where in the nervous system are these VNC-SP cholinergic signals received? We show
786 that VNC-SP neurons receive synaptic inputs in the VNC and have presynaptic sites in
787 the brain (Figure 6-figure supplement 2). This suggests that VNC-SP neurons are well
788 positioned to receive and integrate sleep-relevant sensory inputs from the periphery in
789 the VNC and that they are sending this information to the brain. The nature of these
790 inputs will require additional investigations that will further uncover the function and role
791 of VNC-SP neurons in sleep regulation. Known modulators of sleep include the immune
792 system and metabolic functions. Based on their location, it is possible that VNC-SP
793 neurons integrate signals relevant to these two sleep-modulating systems.
794
795 Our data raised important questions about the role of dFB neurons in sleep regulation.
796 Importantly, we show that 23E10-GAL4 dFB neurons are involved in sleep homeostasis
797 as silencing them completely abrogates sleep rebound following a night of sleep
798 deprivation (Figure 8). Our data is in agreement with previous work supporting a role for

799 dFB neurons in sleep homeostasis (29, 33). Interestingly, we also demonstrate that
800 VNC-SP neurons are not part of the homeostatic sleep circuit. These findings suggest
801 that dFB neurons and VNC-SP neurons regulate different aspects and functions of
802 sleep. Here again, further work will determine the role of VNC-SP neurons.
803
804 Finally, our data clearly highlight the need to obtain tools that are as specific as possible
805 when attempting to link a given behavior with a specific neuron or group of neurons. In
806 particular, the frequency at which VNC-SP neurons are observed in existing GAL4 lines
807 (in up to 60% of all Janelia GAL4 lines) (55) raises some important methodological
808 questions. For example, are VNC-SP neurons present in the expression pattern of a
809 GAL4 line that is known to modulate sleep and is seen as a tool specific for a given
810 structure in the brain? Future studies using GAL4 lines in sleep studies will need to take
811 account of the potential presence of VNC-SP neurons in their expression pattern.
812 Perhaps more importantly, existing data may need to be reinterpreted in the light of our
813 finding.
814
815 **Conclusions**
816
817 Our work identified a novel group of cholinergic sleep-promoting neurons located in the
818 VNC in *Drosophila*. We show that these cells are perfectly positioned to receive and
819 integrate sensory inputs from the periphery and send this information to the brain. We
820 demonstrate that these cells regulate sleep quantity and sleep quality. We further
821 demonstrate that they are not involved in sleep homeostasis whereas 23E10-GAL4 dFB

822 neurons are. Further work will need to determine the nature of the sleep-relevant

823 information that is relayed by VNC-SP neurons.

824

825 **Materials and Methods**

826

827 **Key Resources Table**

828

Reagent type (species) or resource	**Designation**	**Source or reference**	**Identifiers**	**Additional information**
Genetic reagent (*D. melanogaster*)	P{GMR23E10-GAL4}attP2	Bloomington Drosophila Stock Center	RRID:BDSC_49032	
Genetic reagent (*D. melanogaster*)	w[*]; P{y[+t7.7] w[+mC]=UAS-TrpA1(B).K}attP16	Bloomington Drosophila Stock Center	RRID:BDSC_26263	
Genetic reagent (*D. melanogaster*)	Canton-S	Laboratory of Paul Shaw		
Genetic reagent (*D. melanogaster*)	w[*]; P{y[+t7.7] w[+mC]=10XUAS-IVS-mCD8::GFP}attP40	Bloomington Drosophila Stock Center	RRID:BDSC_32186	
Genetic reagent (*D. melanogaster*)	w[*]; P{y[+t7.7] w[+mC]=10XUAS-IVS-mCD8::GFP}attP2	Bloomington Drosophila Stock Center	RRID:BDSC_32185	
Genetic reagent (*D. melanogaster*)	w[1118]; P{y[+t7.7] w[+mC]=23E10-GAL4.DBD}attP2/TM3	Bloomington Drosophila Stock Center	RRID:BDSC_69269	
Genetic reagent (*D. melanogaster*)	w[1118]; P{y[+t7.7] w[+mC]=p65.AD.Uw}attP40	Bloomington Drosophila Stock Center	RRID:BDSC_71210	Empty-AD
Genetic reagent (*D. melanogaster*)	P{R84C10-p65.AD}attP40	Bloomington Drosophila Stock Center	RRID:BDSC_70833	AD for FBS 4
Genetic reagent (*D. melanogaster*)	P{R23E12-p65.AD}attP40	Bloomington Drosophila Stock Center	RRID:BDSC_70602	AD for FBS 5

Genetic reagent (*D. melanogaster*)	w[1118]; P{y[+t7.7] w[+mC]=VT050238-p65.AD}attP40	Bloomington Drosophila Stock Center	RRID:BDSC_72962	AD for FBS 45
Genetic reagent (*D. melanogaster*)	P{VT023823-p65.AD}attP40	Bloomington Drosophila Stock Center	RRID:BDSC_86629	AD for FBS 68
Genetic reagent (*D. melanogaster*)	P{R12D12-p65.AD}attP40	Bloomington Drosophila Stock Center	RRID:BDSC_70539	AD for FBS 1
Genetic reagent (*D. melanogaster*)	P{R42H01-p65.AD}attP40	Bloomington Drosophila Stock Center	RRID:BDSC_70687	AD for FBS 6
Genetic reagent (*D. melanogaster*)	P{R22A12-p65.AD}attP40	Bloomington Drosophila Stock Center	RRID:BDSC_70120	AD for FBS 25
Genetic reagent (*D. melanogaster*)	P{R54G07-p65.AD}attP40	Bloomington Drosophila Stock Center	RRID:BDSC_70737	AD for FBS 28
Genetic reagent (*D. melanogaster*)	P{R49C04-p65.AD}attP40	Bloomington Drosophila Stock Center	RRID:BDSC_71075	AD for FBS 33
Genetic reagent (*D. melanogaster*)	P{R65C03-p65.AD}attP40	Bloomington Drosophila Stock Center	RRID:BDSC_71005	AD for FBS 35
Genetic reagent (*D. melanogaster*)	P{VT058545-p65.AD}attP40	Bloomington Drosophila Stock Center	RRID:BDSC_74090	AD for FBS 41
Genetic reagent (*D. melanogaster*)	P{R12G09-p65.AD}attP40	Bloomington Drosophila Stock Center	RRID:BDSC_68826	AD for FBS 42
Genetic reagent (*D. melanogaster*)	P{VT043400-p65.AD}attP40	Bloomington Drosophila Stock Center	RRID:BDSC_75874	AD for FBS 53
Genetic reagent (*D. melanogaster*)	P{VT025720-p65.AD}attP40	Bloomington Drosophila Stock Center	RRID:BDSC_73432	AD for FBS 57
Genetic reagent (*D. melanogaster*)	P{VT064566-p65.AD}attP40	Bloomington Drosophila Stock Center	RRID:BDSC_71451	AD for FBS 58
Genetic reagent (*D. melanogaster*)	P{VT023818-p65.AD}attP40	Bloomington Drosophila Stock Center	RRID:BDSC_73262	AD for FBS 60
Genetic reagent (*D. melanogaster*)	P{VT027956-p65.AD}attP40	Bloomington Drosophila Stock Center	RRID:BDSC_73061	AD for FBS 64

Genetic reagent (*D. melanogaster*)	P{VT034811-p65.AD}attP40	Bloomington Drosophila Stock Center	RRID:BDSC_71337	AD for FBS 70
Genetic reagent (*D. melanogaster*)	P{VT026953-p65.AD}attP40	Bloomington Drosophila Stock Center	RRID:BDSC_74413	AD for FBS 72
Genetic reagent (*D. melanogaster*)	P{R74G10-p65.AD}attP40	Bloomington Drosophila Stock Center	RRID:BDSC_71131	AD for FBS 81
Genetic reagent (*D. melanogaster*)	P{VT007754-p65.AD}attP40	Bloomington Drosophila Stock Center	RRID:BDSC_74138	AD for FBS 84
Genetic reagent (*D. melanogaster*)	P{VT045793-p65.AD}attP40	Bloomington Drosophila Stock Center	RRID:BDSC_71441	AD for FBS 87
Genetic reagent (*D. melanogaster*)	w[1118]; P{y[+t7.7] w[+mC]=20XUAS-IVS-CsChrimson.mVenus}attP40	Bloomington Drosophila Stock Center	RRID:BDSC_55135	
Genetic reagent (*D. melanogaster*)	P{VT020742-p65.AD}attP40	Bloomington Drosophila Stock Center	RRID:BDSC_73460	
Genetic reagent (*D. melanogaster*)	P{R30A08-p65.AD}attP40	Bloomington Drosophila Stock Center	RRID:BDSC_71007	
Genetic reagent (*D. melanogaster*)	P{VT013602-p65.AD}attP40	Bloomington Drosophila Stock Center	RRID:BDSC_74209	
Genetic reagent (*D. melanogaster*)	P{GMR30A08-lexA}attP40	Bloomington Drosophila Stock Center	RRID:BDSC_54756	
Genetic reagent (*D. melanogaster*)	y[1] w[*]; P{y[+t7.7] w[+mC]=10XUAS-IVS-mCD8::RFP}attP18 P{y[+t7.7] w[+mC]=13XLexAop2-mCD8::GFP}attP8	Bloomington Drosophila Stock Center	RRID:BDSC_32229	
Genetic reagent (*D. melanogaster*)	w[*]; P{y[+t7.7] w[+mC]=13XLexAop2-KZip+.3XHA}su(Hw)attP5/CyO; TM6B, Tb[1]/MKRS	Bloomington Drosophila Stock Center	RRID:BDSC_76253	
Genetic reagent (*D. melanogaster*)	w[*]; P{y[+t7.7] w[+mC]=13XLexAop2-KZip+.3XHA}attP2	Bloomington Drosophila Stock Center	RRID:BDSC_76254	
Genetic reagent (*D. melanogaster*)	P{VT020742-GAL4.DBD}attP2	Bloomington Drosophila Stock Center	RRID:BDSC_72912	

Genetic reagent (*D. melanogaster*)	w[1118]; P{y[+t7.7] w[+mC]=GAL4.DBD.Uw}attP2	Bloomington Drosophila Stock Center	RRID:BDSC_71209	Empty-DBD
Genetic reagent (*D. melanogaster*)	w[*]; P{w[+mC]=UAS-Hsap\KCNJ2.EGFP}7	Bloomington Drosophila Stock Center	RRID:BDSC_6595	UAS-Kir2.1
Genetic reagent (*D. melanogaster*)	pJFRC100-20XUAS-TTS-Shibire-ts1-p10 in VK00005	Laboratory of Gerry Rubin	(70)	UAS-Shi^{ts1}
Genetic reagent (*D. melanogaster*)	GMR-GAL4	Laboratory of Jeff Price	(71)	
Genetic reagent (*D. melanogaster*)	P{GawB}elav[C155]	Bloomington Drosophila Stock Center	RRID:BDSC_458	elav-GAL4
Genetic reagent (*D. melanogaster*)	P{TRiP.HMC05021}attP40	Bloomington Drosophila Stock Center	RRID:BDSC_60028	Expresses dsRNA for RNAi of ChAT under UAS control
Genetic reagent (*D. melanogaster*)	y[1] v[1]; P{y[+t7.7] v[+t1.8]=UAS-GFP.VALIUM10}attP2	Bloomington Drosophila Stock Center	RRID:BDSC_35786	Control RNAi line
Genetic reagent (*D. melanogaster*)	w[1118]; P{w[+mC]=UAS-Dcr-2.D}2	Bloomington Drosophila Stock Center	RRID:BDSC_24650	UAS-Dicer2 on chromosome 2
Genetic reagent (*D. melanogaster*)	w[1118]; P{w[+mC]=UAS-Dcr-2.D}10	Bloomington Drosophila Stock Center	RRID:BDSC_24651	UAS-Dicer2 on chromosome 3
Genetic reagent (*D. melanogaster*)	w[1118]; P{y[+t7.7] w[+mC]=20XUAS-IVS-CsChrimson.mVenus}attP2	Bloomington Drosophila Stock Center	RRID:BDSC_55136	
Genetic reagent (*D. melanogaster*)	w[1118]; P{y[+t7.7] w[+mC]=20XUAS-IVS-CsChrimson.mVenus}attP18	Bloomington Drosophila Stock Center	RRID:BDSC_55134	
Genetic reagent (*D. melanogaster*)	w[*]; Mi{Trojan-lexA:QFAD.0}ChAT[MI04508-TlexA:QFAD.0] CG7715[MI04508-TlexA:QFAD.0-X]/TM6B, Tb[1]	Bloomington Drosophila Stock Center	RRID:BDSC_60319	ChAT-LexA
Genetic reagent (*D. melanogaster*)	P{GMR23E10-lexA}attP40	Bloomington Drosophila Stock Center	RRID:BDSC_52693	

Genetic reagent (*D. melanogaster*)	w[1118]; P{y[+t7.7] w[+mC]=13XLexAop2-IVS-CsChrimson.mVenus}attP18	Bloomington Drosophila Stock Center	RRID:BDSC_55137	
Genetic reagent (*D. melanogaster*)	w[1118]; P{w[+mC]=UAS-syt.eGFP}3	Bloomington Drosophila Stock Center	RRID:BDSC_62138	
Genetic reagent (*D. melanogaster*)	w[*]; P{y[+t7.7] w[+mC]=5XUAS-DenMark::smGdP-V5}su(Hw)attP5	Bloomington Drosophila Stock Center	RRID:BDSC_6926	
Genetic reagent (*D. melanogaster*)	P{TRiP.JF01877}attP2 (RNAi against ChAT)	Bloomington Drosophila Stock Center	RRID:BDSC_25856	Expresses dsRNA for RNAi of ChAT under UAS control
Antibody	Anti-GFP (Chicken polyclonal)	Aves Labs, Inc	GFP-1020	dilution 1:1000
Antibody	anti-bruchpilot (mouse monoclonal)	Developmental Studies Hybridoma Bank	nc82-s	dilution 1:50
Antibody	Anti-DsRed (rabbit polyclonal)	Takara	632496	dilution 1:250
Antibody	Anti-ChAT (mouse monoclonal)	Developmental Studies Hybridoma Bank	Chat4B1-c	dilution 1:100
Antibody	Anti-VGlut (rabbit)	Aaron DiAntonio (Washington University)	(72)	dilution 1:500
Antibody	Anti-GABA (rabbit polyclonal)	Sigma-Aldrich	A2052	dilution 1:1000
Antibody	Anti-5-HT (rabbit polyclonal)	Sigma-Aldrich	S5545	dilution 1:500
Antibody	Anti-TH (mouse monoclonal)	Immunostar	22941	dilution 1:100
Antibody	Anti-Tdc2 (rabbit polyclonal)	Covalab	pab0822-P	dilution 1:200
Antibody	Anti-V5 (mouse monoclonal)	Sigma-Aldrich	V8012	dilution 1:400
Antibody	Goat anti-chicken Alexafluor 488	Invitrogen	A32931	dilution 1:800
Antibody	Goat anti-mouse Alexafluor 555	Invitrogen	A32727	dilution 1:400

Antibody	Goat anti-rabbit Alexafluor 555	Invitrogen	A32732	dilution 1:400
Antibody	Goat anti-mouse Alexafluor 633	Invitrogen	A21052	dilution 1:400
Antibody	Goat anti-rabbit Alexafluor 633	Invitrogen	A21071	dilution 1:400
Chemical compound, drug	retinal	Sigma	R2500	400μM
Chemical compound, drug	Vectashield	Vector Laboratories	H-1000	
Chemical compound, drug	20% paraformaldehyde	Electron Microscopy Sciences	15713	4% dilution
Media	Drosophila Schneider's Medium	Gibco	21720024	
Media	Normal Goat Serum	MP Biomedicals	191356	5% dilution

829

830 **Flies**

831 Flies were cultured at 25˚C with 50% humidity under a 12-hour light: 12-hour dark cycle.
832 Flies were kept on a standard yeast and molasses diet (per 1L: 50g yeast, 15g sucrose,
833 28g corn syrup, 33.3mL molasses, 9g agar).

834

835 **Sleep**

836 Sleep was assessed as previously described (32, 73). 4-10 day old virgin females or
837 males were used as described in figure legends. Briefly, flies were placed into individual
838 65 mm tubes and all activity was continuously measured through the Trikinetics
839 Drosophila Activity Monitoring System (www.Trikinetics.com, Waltham, Ma). Locomotor
840 activity was measured in 1-minute bins and sleep was defined as periods of quiescence
841 lasting at least 5 minutes.

842 **Optogenetic activation**

843 For optogenetic activation, flies expressing CsChrimson were loaded into individual
844 65mm tubes with food supplemented with 400μM all-trans retinal (Sigma, #R2500) and
845 kept in the dark for 48 hours. Sleep was then monitored under low-light conditions for 48
846 hours of baseline measurements. To activate CSChrimson, flies were put under 627nm
847 LEDs (LuxeonStar LXM2-PD01-0040) set to a pulse cycle of (5ms on, 95ms off) x 20
848 with a 4 second delay between pulse cycles. The light intensity of this protocol is
849 0.024mW/mm^2

850

851 **Sleep deprivation**

852 Sleep deprivation was performed as previously described (32, 74). Briefly, flies were
853 placed into individual 65 mm tubes and the sleep-nullifying apparatus (SNAP) was used
854 to sleep deprive flies for 12 hours during the dark phase. Sleep homeostasis was
855 calculated for each individual fly as the ratio of the minutes of sleep gained above
856 baseline during 24h of recovery sleep divided by the total min of sleep lost during 12 h
857 of sleep deprivation.

858

859 **Arousal threshold**

860 Retinal or vehicle-fed VNC-SP>UAS-CsChrimson flies were placed into individual 65
861 mm tubes in Trikinetics monitors. These were then loaded in the SNAP sleep
862 deprivation apparatus. The SNAP tilts asymmetrically from −60° to +60°, such that
863 sleeping flies are disturbed during each downward movement (75). Each individual

864 SNAP movement takes 15 seconds to complete. To assess arousal threshold, we
865 modified the SNAP parameters so that flies were subjected to only 1, 2, or 4 downward
866 movements in the SNAP every hour for 24h and their locomotor responses were
867 analyzed. We then averaged each individual hour response to obtain the percentage of
868 flies awakened by a given strength of perturbation.
869

870 **QPCR**

871 QPCR were performed as previously described (32, 76). Briefly, total RNA was isolated
872 from the bodies and eyes of ~10 flies per replicate with Trizol (Invitrogen, Carlsbad, CA)
873 and DNAse I digested. cDNA synthesis was performed using Superscript IV VILO
874 (Invitrogen) according to manufacturer protocol. cDNA samples were loaded in
875 duplicate and quantitatively analyzed using SYBR Green Master Mix (Applied
876 Biosystems) and gene specific primers using the Applied Biosystems 7500 system.
877 Expression values for RP49 were used to normalize results between groups. The
878 following primer sets were used: rp49: fw aagaagcgcaccaagcacttcatc, rev
879 tctgttgtcgatacccttgggctt and ChAT: fw caccgagcgatacaggatgg, rev
880 ggcaccttgggtagagtgtc.

881

882 **Immunocytochemistry**

883 Flies were cold anesthetized, brains and VNC were dissected in ice cold Schneider's
884 Drosophila Medium (Gibco, 21720024) and blocked in 5% normal goat serum.
885 Following blocking flies were incubated overnight at 4˚C in primary antibody, washed in

886 PBST and incubated overnight at 4˚C in secondary antibody. Description of antibodies
887 used can be found in the resources table. Brains and VNCs were mounted on polylysine
888 treated slides in Vectashield H-1000 mounting medium. Imaging was performed on a
889 Zeiss 510 meta confocal microscope using a Plan-Apochromat 20x or Plan-Neofluar
890 40x objective. Z-series images were acquired with a 1 uM slice size using the same
891 settings (laser power, gain, offset) to allow for comparison across genotypes. Images
892 were processed and analyzed using ImageJ.

893

894 **Statistics**

895 Statistical analyses were performed with Prism9 software (GraphPad). Normal
896 distribution was assessed with the D'Agostino-Pearson test. Normally distributed data
897 were analyzed with parametric statistics: t-test, one-way analysis of variance or two-way
898 ANOVA followed by the planned pairwise multiple comparisons as described in the
899 legends. For data that significantly differed from the normal distribution, non-parametric
900 statistics were applied, Mann-Whitney U test or Kruskal–Wallis test followed by Dunn's
901 multiple test. Some non-normally distributed data were subjected to log transformation
902 or Box-Cox transformation before two-way ANOVA followed by planned pairwise
903 multiple comparisons as described in the legends. All statistically different groups are
904 defined as *P < 0.05, **P<0.01, ***P<0.001 and ****P<0.0001.

905

906 **Author Contributions**

907 S.D., J.J. and J.M.E. designed the experiments and wrote the paper. J.J., B.H., K.E.,
908 A.V., A.V., A.E., J.M.E and S.D. performed the experiments. J.J., J.M.E and S.D.
909 analyzed the data.

910

911 **Acknowledgments**

912 We thank Aaron DiAntonio, Gerry Rubin, Paul Shaw and Jeff Price for sharing reagents.

913

914 **Competing Interests**

915 The authors have no competing interests.

916

917 **References**

918 1. Park HG, Carmel JB. Selective Manipulation of Neural Circuits. Neurotherapeutics.
919 2016;13(2):311-24.
920 2. Moulin TC, Covill LE, Itskov PM, Williams MJ, Schioth HB. Rodent and fly models in behavioral
921 neuroscience: An evaluation of methodological advances, comparative research, and future
922 perspectives. Neurosci Biobehav Rev. 2021;120:1-12.
923 3. Yamamoto D, Koganezawa M. Genes and circuits of courtship behaviour in Drosophila males.
924 Nat Rev Neurosci. 2013;14(10):681-92.
925 4. Anderson DJ. Circuit modules linking internal states and social behaviour in flies and mice. Nat
926 Rev Neurosci. 2016;17(11):692-704.
927 5. Bhumika, Singh AK. Regulation of feeding behavior in Drosophila through the interplay of
928 gustation, physiology and neuromodulation. Front Biosci (Landmark Ed). 2018;23:2016-27.
929 6. Scott K. Gustatory Processing in Drosophila melanogaster. Annu Rev Entomol. 2018;63:15-30.
930 7. Ly S, Pack AI, Naidoo N. The neurobiological basis of sleep: Insights from Drosophila. Neurosci
931 Biobehav Rev. 2018;87:67-86.
932 8. Brand AH, Perrimon N. Targeted gene expression as a means of altering cell fates and generating
933 dominant phenotypes. Development. 1993;118(2):401-15.
934 9. Lai SL, Lee T. Genetic mosaic with dual binary transcriptional systems in Drosophila. Nat
935 Neurosci. 2006;9(5):703-9.
936 10. Potter CJ, Tasic B, Russler EV, Liang L, Luo L. The Q system: a repressible binary system for
937 transgene expression, lineage tracing, and mosaic analysis. Cell. 2010;141(3):536-48.
938 11. Luan H, Peabody NC, Vinson CR, White BH. Refined spatial manipulation of neuronal function by
939 combinatorial restriction of transgene expression. Neuron. 2006;52(3):425-36.

940 12. Keene AC, Duboue ER. The origins and evolution of sleep. J Exp Biol. 2018;221(Pt 11).
941 13. Borbely AA. A two process model of sleep regulation. Hum Neurobiol. 1982;1(3):195-204.
942 14. Krause AJ, Simon EB, Mander BA, Greer SM, Saletin JM, Goldstein-Piekarski AN, et al. The sleep-
943 deprived human brain. Nat Rev Neurosci. 2017;18(7):404-18.
944 15. Miyazaki S, Liu CY, Hayashi Y. Sleep in vertebrate and invertebrate animals, and insights into the
945 function and evolution of sleep. Neurosci Res. 2017;118:3-12.
946 16. Shafer OT, Keene AC. The Regulation of Drosophila Sleep. Curr Biol. 2021;31(1):R38-R49.
947 17. Dissel S. Drosophila as a Model to Study the Relationship Between Sleep, Plasticity, and
948 Memory. Front Physiol. 2020;11:533.
949 18. Strauss R. The central complex and the genetic dissection of locomotor behaviour. Curr Opin
950 Neurobiol. 2002;12(6):633-8.
951 19. Sakai T, Kitamoto T. Differential roles of two major brain structures, mushroom bodies and
952 central complex, for Drosophila male courtship behavior. J Neurobiol. 2006;66(8):821-34.
953 20. Joiner MA, Griffith LC. Mapping of the anatomical circuit of CaM kinase-dependent courtship
954 conditioning in Drosophila. Learn Mem. 1999;6(2):177-92.
955 21. Sakai T, Inami S, Sato S, Kitamoto T. Fan-shaped body neurons are involved in period-dependent
956 regulation of long-term courtship memory in Drosophila. Learn Mem. 2012;19(12):571-4.
957 22. Hu W, Peng Y, Sun J, Zhang F, Zhang X, Wang L, et al. Fan-Shaped Body Neurons in the
958 Drosophila Brain Regulate Both Innate and Conditioned Nociceptive Avoidance. Cell Rep.
959 2018;24(6):1573-84.
960 23. Liu G, Seiler H, Wen A, Zars T, Ito K, Wolf R, et al. Distinct memory traces for two visual features
961 in the Drosophila brain. Nature. 2006;439(7076):551-6.
962 24. Weir PT, Dickinson MH. Functional divisions for visual processing in the central brain of flying
963 Drosophila. Proc Natl Acad Sci U S A. 2015;112(40):E5523-32.
964 25. Kacsoh BZ, Bozler J, Hodge S, Bosco G. Neural circuitry of social learning in Drosophila requires
965 multiple inputs to facilitate inter-species communication. Commun Biol. 2019;2:309.
966 26. Sareen PF, McCurdy LY, Nitabach MN. A neuronal ensemble encoding adaptive choice during
967 sensory conflict in Drosophila. Nat Commun. 2021;12(1):4131.
968 27. Donlea JM, Thimgan MS, Suzuki Y, Gottschalk L, Shaw PJ. Inducing sleep by remote control
969 facilitates memory consolidation in Drosophila. Science. 2011;332(6037):1571-6.
970 28. Ueno T, Tomita J, Tanimoto H, Endo K, Ito K, Kume S, et al. Identification of a dopamine pathway
971 that regulates sleep and arousal in Drosophila. Nat Neurosci. 2012;15(11):1516-23.
972 29. Donlea JM, Pimentel D, Miesenbock G. Neuronal Machinery of Sleep Homeostasis in Drosophila.
973 Neuron. 2014;81(6):1442.
974 30. Liu Q, Liu S, Kodama L, Driscoll MR, Wu MN. Two dopaminergic neurons signal to the dorsal fan-
975 shaped body to promote wakefulness in Drosophila. Curr Biol. 2012;22(22):2114-23.
976 31. Dag U, Lei Z, Le JQ, Wong A, Bushey D, Keleman K. Neuronal reactivation during post-learning
977 sleep consolidates long-term memory in Drosophila. Elife. 2019;8.
978 32. Dissel S, Angadi V, Kirszenblat L, Suzuki Y, Donlea J, Klose M, et al. Sleep restores behavioral
979 plasticity to Drosophila mutants. Curr Biol. 2015;25(10):1270-81.
980 33. Pimentel D, Donlea JM, Talbot CB, Song SM, Thurston AJF, Miesenbock G. Operation of a
981 homeostatic sleep switch. Nature. 2016;536(7616):333-7.
982 34. Kempf A, Song SM, Talbot CB, Miesenbock G. A potassium channel beta-subunit couples
983 mitochondrial electron transport to sleep. Nature. 2019;568(7751):230-4.
984 35. Alam MA, Kumar S, McGinty D, Alam MN, Szymusiak R. Neuronal activity in the preoptic
985 hypothalamus during sleep deprivation and recovery sleep. J Neurophysiol. 2014;111(2):287-99.
986 36. Jenett A, Rubin GM, Ngo TT, Shepherd D, Murphy C, Dionne H, et al. A GAL4-driver line resource
987 for Drosophila neurobiology. Cell Rep. 2012;2(4):991-1001.

988 37. Qian Y, Cao Y, Deng B, Yang G, Li J, Xu R, et al. Sleep homeostasis regulated by 5HT2b receptor in
989 a small subset of neurons in the dorsal fan-shaped body of drosophila. Elife. 2017;6.
990 38. Yap MHW, Grabowska MJ, Rohrscheib C, Jeans R, Troup M, Paulk AC, et al. Oscillatory brain
991 activity in spontaneous and induced sleep stages in flies. Nat Commun. 2017;8(1):1815.
992 39. Berry JA, Cervantes-Sandoval I, Chakraborty M, Davis RL. Sleep Facilitates Memory by Blocking
993 Dopamine Neuron-Mediated Forgetting. Cell. 2015;161(7):1656-67.
994 40. Hulse BK, Haberkern H, Franconville R, Turner-Evans DB, Takemura SY, Wolff T, et al. A
995 connectome of the Drosophila central complex reveals network motifs suitable for flexible navigation
996 and context-dependent action selection. Elife. 2021;10.
997 41. Hamada FN, Rosenzweig M, Kang K, Pulver SR, Ghezzi A, Jegla TJ, et al. An internal thermal
998 sensor controlling temperature preference in Drosophila. Nature. 2008;454(7201):217-20.
999 42. Ishimoto H, Lark A, Kitamoto T. Factors that Differentially Affect Daytime and Nighttime Sleep in
1000 Drosophila melanogaster. Front Neurol. 2012;3:24.
1001 43. Lamaze A, Ozturk-Colak A, Fischer R, Peschel N, Koh K, Jepson JE. Regulation of sleep plasticity
1002 by a thermo-sensitive circuit in Drosophila. Sci Rep. 2017;7:40304.
1003 44. Donlea JM, Pimentel D, Talbot CB, Kempf A, Omoto JJ, Hartenstein V, et al. Recurrent Circuitry
1004 for Balancing Sleep Need and Sleep. Neuron. 2018;97(2):378-89 e4.
1005 45. Tainton-Heap LAL, Kirszenblat LC, Notaras ET, Grabowska MJ, Jeans R, Feng K, et al. A
1006 Paradoxical Kind of Sleep in Drosophila melanogaster. Curr Biol. 2021;31(3):578-90 e6.
1007 46. Tirian L, Dickson BJ. The VT GAL4, LexA, and split-GAL4 driver line collections for targeted
1008 expression in the *Drosophila* nervous system. BioRxiv 198648 [Preprint] October 5, 2017 Available from:
1009 https://doiorg/101101/198648. 2017.
1010 47. Dionne H, Hibbard KL, Cavallaro A, Kao JC, Rubin GM. Genetic Reagents for Making Split-GAL4
1011 Lines in Drosophila. Genetics. 2018;209(1):31-5.
1012 48. Parisky KM, Agosto Rivera JL, Donelson NC, Kotecha S, Griffith LC. Reorganization of Sleep by
1013 Temperature in Drosophila Requires Light, the Homeostat, and the Circadian Clock. Curr Biol.
1014 2016;26(7):882-92.
1015 49. Kim JH, Ki Y, Lee H, Hur MS, Baik B, Hur JH, et al. The voltage-gated potassium channel Shaker
1016 promotes sleep via thermosensitive GABA transmission. Commun Biol. 2020;3(1):174.
1017 50. van Alphen B, Yap MH, Kirszenblat L, Kottler B, van Swinderen B. A dynamic deep sleep stage in
1018 Drosophila. J Neurosci. 2013;33(16):6917-27.
1019 51. Isaac RE, Li C, Leedale AE, Shirras AD. Drosophila male sex peptide inhibits siesta sleep and
1020 promotes locomotor activity in the post-mated female. Proc Biol Sci. 2010;277(1678):65-70.
1021 52. Khericha M, Kolenchery JB, Tauber E. Neural and non-neural contributions to sexual dimorphism
1022 of mid-day sleep in Drosophila melanogaster: a pilot study. Physiol Entomol. 2016;41(4):327-34.
1023 53. Wu B, Ma L, Zhang E, Du J, Liu S, Price J, et al. Sexual dimorphism of sleep regulated by juvenile
1024 hormone signaling in Drosophila. PLoS Genet. 2018;14(4):e1007318.
1025 54. Kim H, Kirkhart C, Scott K. Long-range projection neurons in the taste circuit of Drosophila. Elife.
1026 2017;6.
1027 55. Meissner GW, Dorman Z, Nern A, Forster K, Gibney T, Jeter J, et al. An image resource of
1028 subdivided Drosophila GAL4-driver expression patterns for neuron-level searches. bioRxiv.
1029 2020:2020.05.29.080473.
1030 56. Klapoetke NC, Murata Y, Kim SS, Pulver SR, Birdsey-Benson A, Cho YK, et al. Independent optical
1031 excitation of distinct neural populations. Nat Methods. 2014;11(3):338-46.
1032 57. Otsuna H, Ito M, Kawase T. Color depth MIP mask search: a new tool to expedite Split-GAL4
1033 creation. BioRxiv 318006 [Preprint] May 9, 2018 Available from: https://doiorg/101101/318006v1.
1034 2018.

1035 58. Dolan MJ, Luan H, Shropshire WC, Sutcliffe B, Cocanougher B, Scott RL, et al. Facilitating Neuron-
1036 Specific Genetic Manipulations in Drosophila melanogaster Using a Split GAL4 Repressor. Genetics.
1037 2017;206(2):775-84.
1038 59. Baines RA, Uhler JP, Thompson A, Sweeney ST, Bate M. Altered electrical properties in
1039 Drosophila neurons developing without synaptic transmission. J Neurosci. 2001;21(5):1523-31.
1040 60. Kitamoto T. Conditional modification of behavior in Drosophila by targeted expression of a
1041 temperature-sensitive shibire allele in defined neurons. J Neurobiol. 2001;47(2):81-92.
1042 61. Lacin H, Chen HM, Long X, Singer RH, Lee T, Truman JW. Neurotransmitter identity is acquired in
1043 a lineage-restricted manner in the Drosophila CNS. Elife. 2019;8.
1044 62. Diao F, Ironfield H, Luan H, Diao F, Shropshire WC, Ewer J, et al. Plug-and-play genetic access to
1045 drosophila cell types using exchangeable exon cassettes. Cell Rep. 2015;10(8):1410-21.
1046 63. Ni JD, Gurav AS, Liu W, Ogunmowo TH, Hackbart H, Elsheikh A, et al. Differential regulation of
1047 the Drosophila sleep homeostat by circadian and arousal inputs. Elife. 2019;8.
1048 64. Allen AM, Neville MC, Birtles S, Croset V, Treiber CD, Waddell S, et al. A single-cell transcriptomic
1049 atlas of the adult Drosophila ventral nerve cord. Elife. 2020;9.
1050 65. Court R, Namiki S, Armstrong JD, Borner J, Card G, Costa M, et al. A Systematic Nomenclature for
1051 the Drosophila Ventral Nerve Cord. Neuron. 2020;107(6):1071-9 e2.
1052 66. Tsubouchi A, Yano T, Yokoyama TK, Murtin C, Otsuna H, Ito K. Topological and modality-specific
1053 representation of somatosensory information in the fly brain. Science. 2017;358(6363):615-23.
1054 67. Nicolai LJ, Ramaekers A, Raemaekers T, Drozdzecki A, Mauss AS, Yan J, et al. Genetically encoded
1055 dendritic marker sheds light on neuronal connectivity in Drosophila. Proc Natl Acad Sci U S A.
1056 2010;107(47):20553-8.
1057 68. Zhang YQ, Rodesch CK, Broadie K. Living synaptic vesicle marker: synaptotagmin-GFP. Genesis.
1058 2002;34(1-2):142-5.
1059 69. Pfeiffer BD, Ngo TT, Hibbard KL, Murphy C, Jenett A, Truman JW, et al. Refinement of tools for
1060 targeted gene expression in Drosophila. Genetics. 2010;186(2):735-55.
1061 70. Pfeiffer BD, Truman JW, Rubin GM. Using translational enhancers to increase transgene
1062 expression in Drosophila. Proc Natl Acad Sci U S A. 2012;109(17):6626-31.
1063 71. Takahashi Y, Hirose F, Matsukage A, Yamaguchi M. Identification of three conserved regions in
1064 the DREF transcription factors from Drosophila melanogaster and Drosophila virilis. Nucleic Acids Res.
1065 1999;27(2):510-6.
1066 72. Daniels RW, Collins CA, Chen K, Gelfand MV, Featherstone DE, DiAntonio A. A single vesicular
1067 glutamate transporter is sufficient to fill a synaptic vesicle. Neuron. 2006;49(1):11-6.
1068 73. Shaw PJ, Cirelli C, Greenspan RJ, Tononi G. Correlates of sleep and waking in Drosophila
1069 melanogaster. Science. 2000;287(5459):1834-7.
1070 74. Seugnet L, Suzuki Y, Vine L, Gottschalk L, Shaw PJ. D1 receptor activation in the mushroom
1071 bodies rescues sleep-loss-induced learning impairments in Drosophila. Curr Biol. 2008;18(15):1110-7.
1072 75. Shaw PJ, Tononi G, Greenspan RJ, Robinson DF. Stress response genes protect against lethal
1073 effects of sleep deprivation in Drosophila. Nature. 2002;417(6886):287-91.
1074 76. Dissel S, Seugnet L, Thimgan MS, Silverman N, Angadi V, Thacher PV, et al. Differential activation
1075 of immune factors in neurons and glia contribute to individual differences in resilience/vulnerability to
1076 sleep disruption. Brain Behav Immun. 2015;47:75-85.

1077

1078

1079 **Figure Legends**

1080 **Figure 1. The 23E10-GAL4 driver contains many neurons outside the dFB.**

1081 **A)** Diagram of the experimental assay. Sleep was measured at 22°C for 2 days to
1082 establish baseline sleep profile. Flies were then shifted to 31°C for 24h at the start of
1083 day3 to increase activity of the targeted cells by activating the TrpA1 channel, and then
1084 returned to 22°C. White bars (L) represent the 12h of light and black bars (D) represent
1085 the 12h of dark that are oscillating daily.

1086 **B-C)** Sleep profile in minutes of sleep per hour for day 2 (22°C, blue line) and day 3
1087 (31°C, red line) for parental control female flies: *23E10-Gal4/+* (B) and *UAS-TrpA1/+*
1088 (C).

1089 **D)** Sleep profile in minutes of sleep per hour for day 2 (22°C, blue line) and day 3 (31°C,
1090 red line) for *23E10-GAL4>UAS-TrpA1* female flies.

1091 **E)** Box plots of total sleep change in % ((total sleep on day3-total sleep on day2/total
1092 sleep on day2) X 100) for data presented in B-D. The bottom and top of each box
1093 represents the first and third quartile, and the horizontal line dividing the box is the
1094 median. The whiskers represent the 10th and 90th percentiles. Flies expressing UAS-
1095 TrpA1 in 23E10-GAL4 significantly increase sleep when switched to 31°C compared
1096 with parental controls, Kruskal-Wallis ANOVA followed by Dunn's multiple comparisons.
1097 ****P<0.0001, n=25-31 flies per genotype.

1098 **F)** Box plots of locomotor activity counts per minute awake for flies presented in B-D.
1099 The bottom and top of each box represents the first and third quartile, and the horizontal
1100 line dividing the box is the median. The whiskers represent the 10th and 90th percentiles.
1101 Two-way repeated measures ANOVA followed by Sidak's multiple comparisons test
1102 found no differences in locomotor activity between 22°C and 31°C. n.s.= not significant.
1103 n=25-31 flies per genotype.

1104 **G-H)** Representative confocal stacks of a female *23E10-GAL4>UAS-mCD8GFP* brain
1105 (G) and ventral nerve cord (VNC, H). Green, anti-GFP; magenta, anti-nc82 (neuropile
1106 marker).

1107 **Figure 2: Thermogenetic screen of FBS lines.**

1108 **A)** Diagram of the experimental assay. Sleep was measured at 22°C for 2 days to
1109 establish baseline sleep profile. Flies were then shifted to 31°C for 24h at the start of
1110 day3 to increase activity of the targeted cells by activating the TrpA1 channel, and then
1111 returned to 22°C. White bars (L) represent the 12h of light and black bars (D) represent
1112 the 12h of dark that are oscillating daily.

1113 **B)** Box plots of total sleep change in % ((total sleep on day3-total sleep on day2/total
1114 sleep on day2) X 100) for female control (Empty-AD; 23E10-DBD) and 22 FBS lines
1115 expressing UAS-TrpA1; UAS-GFP. The bottom and top of each box represents the first
1116 and third quartile, and the horizontal line dividing the box is the median. The whiskers
1117 represent the 10th and 90th percentiles. The gray rectangle spanning the horizontal axis
1118 indicates the interquartile range of the control. Kruskal-Wallis ANOVA followed by
1119 Dunn's multiple comparisons revealed that 9 FBS lines increase sleep significantly more
1120 than control flies when transferred to 31°C. **P<0.01, ***P<0.001, ****P<0.0001, n=30-
1121 51 flies per genotype.

1122 **C)** Box plots of locomotor activity counts per minute awake for flies presented in B. The
1123 bottom and top of each box represents the first and third quartile, and the horizontal line
1124 dividing the box is the median. The whiskers represent the 10th and 90th percentiles.
1125 Two-way repeated measures ANOVA followed by Sidak's multiple comparisons test
1126 found that for 3 sleep-promoting FBS lines (FBS5, FBS45 and FBS53) locomotor
1127 activity per awake time is increased while no differences are seen for the other 6 sleep-
1128 promoting lines between 22°C and 31°C. **P<0.01, ***P<0.001, ****P<0.0001, n=30-51
1129 flies per genotype.

1130 **D-H)** Left, sleep profile in minutes of sleep per hour for day 2 (22°C, blue line) and day 3
1131 (31°C, red line) for empty control (Empty-AD; 23E10-DBD, D), FBS4 (E), FBS5 (F),
1132 FBS45 (G) and FBS68 (H) female flies expressing TrpA1 and GFP. Right,
1133 Representative confocal stacks for each *FBS>UAS-TrpA1; UAS-mCD8GFP* line of a
1134 female brain (left panel), VNC (middle panel) as well as a magnified view of VNC
1135 "bowtie" processes as indicated by the gray rectangle in F. Yellow arrows in F indicate
1136 TPN1-like processes in FBS5. Green, anti-GFP; magenta, anti-nc82 (neuropile marker).

1137 **Figure 3: Optogenetic screen of FBS lines.**

1138 **A)** Diagram of the experimental assay. Sleep was measured in retinal-fed and vehicle-
1139 fed flies for 2 days without 627nm LED stimulation to establish baseline sleep profile.
1140 LEDs were were then turned on for 24h at the start of day3 to increase activity of the
1141 targeted cells by activating the CsChrimson channel, and then turned off on day4. White
1142 bars (L) represent the 12h of light and black bars (D) represent the 12h of dark that are
1143 oscillating daily.

1144 **B)** Box plots of total sleep change in % ((total sleep on day3-total sleep on day2/total
1145 sleep on day2) X 100) for control (Empty) and 22 experimental vehicle-fed and retinal-
1146 fed female flies expressing CsChrimson upon 627nm LED stimulation. The bottom and
1147 top of each box represents the first and third quartile, and the horizontal line dividing the
1148 box is the median. The whiskers represent the 10th and 90th percentiles. Two-way
1149 ANOVA followed by Sidak's multiple comparisons revealed that 7 retinal-fed FBS lines
1150 increase sleep significantly when stimulated with 627nm LEDs when compared with
1151 vehicle-fed flies. **P<0.01, ***P<0.001, ****P<0.0001, n=21-39 flies per genotype and
1152 condition.

1153 **C)** Box plots of locomotor activity counts per minute awake for retinal-fed flies presented
1154 in B. The bottom and top of each box represents the first and third quartile, and the
1155 horizontal line dividing the box is the median. The whiskers represent the 10th and
1156 90th percentiles. Two-way repeated measures ANOVA followed by Sidak's multiple
1157 comparisons test found that for most sleep-promoting FBS lines, locomotor activity per
1158 awake time is not affected when the flies are stimulated with 627nm LEDs while it is
1159 increased in *FBS45>UAS-CsChrimson* flies. ****P<0.0001, n=21-38 flies per genotype.

1160 **D)** Box plots of daytime sleep bout duration (in minutes) for retinal-fed flies presented in
1161 B. The bottom and top of each box represents the first and third quartile, and the
1162 horizontal line dividing the box is the median. The whiskers represent the 10th and
1163 90th percentiles. Two-way repeated measures ANOVA followed by Sidak's multiple
1164 comparisons indicate that daytime sleep bout duration is increased in 10 FBS lines
1165 expressing CsChrimson when stimulated with 627nm LEDs. *P<0.05, **P<0.01,
1166 ****P<0.0001, n=21-38 flies per genotype.

1167 **E)** Box plots of nighttime sleep bout duration (in minutes) for retinal-fed flies presented
1168 in B. The bottom and top of each box represents the first and third quartile, and the
1169 horizontal line dividing the box is the median. The whiskers represent the 10th and
1170 90th percentiles. Two-way repeated measures ANOVA followed by Sidak's multiple
1171 comparisons indicate that nighttime sleep bout duration is increased in 6 FBS lines
1172 expressing CsChrimson when stimulated with 627nm LEDs. ****P<0.0001, n=21-38 flies
1173 per genotype.

1174

1175 **Figure 4: The 23E10-GAL driver contains sleep-promoting neurons that are**
1176 **located in the VNC.**

1177 **A-D)** Representative confocal stacks of a female *VT020742-AD; 23E10-DBD>UAS-GFP*
1178 brain (A), brain sagittal view (B), VNC (C) and VNC sagittal view (D). The cell bodies
1179 panel in C is a magnified view of the metathoracic area of the VNC. Yellow arrows
1180 indicate TPN1 like processes and gray arrows "bowtie" processes. Green, anti-GFP;
1181 magenta, anti-nc82 (neuropile marker). A= anterior, P= posterior, V= ventral and D=
1182 dorsal.

1183 **E-F)** Representative confocal stacks of a female *30A08-AD; 23E10-DBD>UAS-GFP*
1184 brain (E) and VNC (F). The cell bodies panel in F is a magnified view of the
1185 metathoracic area of the VNC. Yellow arrows indicate TPN1 processes in the brain and
1186 VNC. Green, anti-GFP.

1187 **G-J)** Representative confocal stacks of a female *VT013602-AD; 23E10-DBD>UAS-GFP*
1188 brain (G), brain sagittal view (H), VNC (I) and VNC sagittal view (J). The cell bodies
1189 panel in I is a magnified view of the metathoracic area of the VNC. Gray arrows indicate
1190 "bowtie" processes and cell bodies in I and J. Green, anti-GFP; magenta, anti-nc82
1191 (neuropile marker). A= anterior, P= posterior, V= ventral and D= dorsal.

1192 **K)** Box plots of total sleep change in % for control (*Empty-AD; 23E10-DBD>UAS-*
1193 *CsChrimson*), *VT020742-AD; 23E10-DBD>UAS-CsChrimson*, *30A08-AD; 23E10-*
1194 *DBD>UAS-CsChrimson* and *VT013602-AD; 23E10-DBD>UAS-CsChrimson* vehicle-fed
1195 and retinal-fed female flies upon 627nm LED stimulation. The bottom and top of each

1196 box represents the first and third quartile, and the horizontal line dividing the box is the
1197 median. The whiskers represent the 10th and 90th percentiles. Two-way ANOVA
1198 followed by Sidak's multiple comparisons revealed that retinal-fed *VT020742-AD;*
1199 *23E10-DBD>UAS-CsChrimson* and *VT013602-AD; 23E10-DBD>UAS-CsChrimson* flies
1200 increase sleep significantly when stimulated with 627nm LEDs when compared with
1201 vehicle-fed flies. **P<0.01, ****P<0.0001, n.s.= not significant. n=13-34 flies per
1202 genotype and condition.

1203 **L)** Box plots of locomotor activity counts per minute awake for retinal-fed flies presented
1204 in K. The bottom and top of each box represents the first and third quartile, and the
1205 horizontal line dividing the box is the median. The whiskers represent the 10th and
1206 90th percentiles. Two-way repeated measures ANOVA followed by Sidak's multiple
1207 comparisons test shows that locomotor activity per awake time is not affected when the
1208 flies are stimulated with 627nm LEDs. n.s.= not significant. n=15-34 flies per genotype.

1209 **M)** Box plots of daytime sleep bout duration (in minutes) for retinal-fed flies presented in
1210 K. The bottom and top of each box represents the first and third quartile, and the
1211 horizontal line dividing the box is the median. The whiskers represent the 10th and
1212 90th percentiles. Two-way repeated measures ANOVA followed by Sidak's multiple
1213 comparisons indicates that daytime sleep bout duration is increased in retinal-fed
1214 *VT020742-AD; 23E10-DBD>UAS-CsChrimson* and *VT013602-AD; 23E10-DBD>UAS-*
1215 *CsChrimson* flies when stimulated with 627nm LEDs. **P<0.01, ****P<0.0001, n.s.= not
1216 significant. n=15-34 flies per genotype.

1217 **N)** Box plots of nighttime sleep bout duration (in minutes) for retinal-fed flies presented
1218 in K. The bottom and top of each box represents the first and third quartile, and the
1219 horizontal line dividing the box is the median. The whiskers represent the 10th and
1220 90th percentiles. Two-way repeated measures ANOVA followed by Sidak's multiple
1221 comparisons indicates that nighttime sleep bout duration is increased in retinal-fed
1222 *VT020742-AD; 23E10-DBD>UAS-CsChrimson* and *VT013602-AD; 23E10-DBD>UAS-*
1223 *CsChrimson* flies when stimulated with 627nm LEDs. ***P<0.001, ****P<0.0001, n.s.=
1224 not significant. n=15-34 flies per genotype.

1225

1226 **Figure 5: Silencing VNC-SP neurons reduces sleep.**

1227 **A)** and **F)** Sleep profile in minutes of sleep per hour for control (*Empty-AD; 23E10-*
1228 *DBD>UAS-Kir2.1,* blue line) and *VNC-SP>Kir2.1* (*VT013602-AD; 23E10-DBD>UAS-*
1229 *Kir2.1,* red line) female (A) and male (F) flies.

1230 **B)** and **G)** Box plots of total sleep time (in minutes) for flies presented in A and F,
1231 respectively. The bottom and top of each box represents the first and third quartile, and
1232 the horizontal line dividing the box is the median. The whiskers represent the 10th and
1233 90th percentiles. A two-tailed unpaired t test revealed that total sleep is significantly
1234 reduced in *VNC-SP>Kir2.1* female flies compared to controls (B). A two-tailed Mann-
1235 Whitney U test revealed that total sleep is significantly reduced in *VNC-SP>Kir2.1* male
1236 flies compared to controls (G). ****P<0.0001. n=58-60 flies per genotype for females
1237 and n=48 flies per genotype for males.

1238 **C)** and **H)** Box plots of daytime sleep bout duration (in minutes) for flies presented in A
1239 and F, respectively. The bottom and top of each box represents the first and third
1240 quartile, and the horizontal line dividing the box is the median. The whiskers represent
1241 the 10th and 90th percentiles. Two-tailed Mann-Whitney U tests revealed that daytime
1242 sleep bout duration is significantly reduced in *VNC-SP>Kir2.1* female (C) and male (H)
1243 flies compared to controls. *P<0.05, ***P<0.0001. n=58-60 flies per genotype for
1244 females and n=48 flies per genotype for males.

1245 **D)** and **I)** Box plots of nighttime sleep bout duration (in minutes) for flies presented in A
1246 and F, respectively. The bottom and top of each box represents the first and third
1247 quartile, and the horizontal line dividing the box is the median. The whiskers represent
1248 the 10th and 90th percentiles. Two-tailed Mann-Whitney U tests revealed that nighttime
1249 sleep bout duration is significantly reduced in *VNC-SP>Kir2.1* female (D) and male (I)
1250 flies compared to controls. ***P<0.001. n=58-60 flies per genotype for females and n=48
1251 flies per genotype for males.

1252 **E)** and **J)** Box plots of locomotor activity counts per minute awake for flies presented in
1253 A and F, respectively. The bottom and top of each box represents the first and third
1254 quartile, and the horizontal line dividing the box is the median. The whiskers represent

1255 the 10th and 90th percentiles. Two-tailed Mann-Whitney U tests revealed that activity per
1256 minute awake is significantly reduced in *VNC-SP>Kir2.1* female (E) while it is
1257 unchanged in male (J) flies compared to controls. **P<0.001, n.s.= not significant. n=58-
1258 60 flies per genotype for females and n=48 flies per genotype for males.

1259 **K)** and **N)** Sleep profile in minutes of sleep per hour for control (*Empty-AD; 23E10-*
1260 *DBD>UAS-Shi^{ts1}*) female (K) and male (N) flies at 22°C (blue line) and 32°C (red line).

1261 **L)** and **O)** Sleep profile in minutes of sleep per hour for *VNC-SP>UAS-Shi^{ts1}* female (L)
1262 and male (O) flies at 22°C (blue line) and 32°C (red line).

1263 **M)** and **P)** Box plots of nighttime sleep change in % for female flies presented in K and L
1264 (M) and male flies presented in N and O. The bottom and top of each box represents
1265 the first and third quartile, and the horizontal line dividing the box is the median. The
1266 whiskers represent the 10th and 90th percentiles. Two-tailed unpaired t tests revealed
1267 that *VNC-SP>Shi^{ts1}* flies lose significantly more sleep when transferred to 32°C
1268 compared with controls in both males and females. *P<0.05. n=27-31 flies per
1269 genotype for females and n=31 flies per genotype for males.

1270

1271 **Figure 6: VNC-SP neurons are cholinergic.**

1272 **A-F)** Representative confocal stacks focusing on the metathoracic ganglion of the VNC
1273 of female *VT013602-AD; 23E10-DBD>UAS-GFP* flies stained with antibodies to ChAT
1274 (A), VGlut (B), GABA (C), 5HT (D), TH (E) and Tdc2 (F). Gray arrows in A indicate
1275 colocalization of GFP and ChAT staining in VNC-SP neurons. Green, anti-GFP;
1276 magenta, anti-ChAT (A), anti-VGlut (B), anti-GABA (C), anti-5HT (D), anti-TH (E) and
1277 anti-Tdc2 (F).

1278 **G)** Sleep profile in minutes of sleep per hour for control (*Empty-AD; 23E10-DBD>UAS-*
1279 *ChAT$^{RNAi\ 60028}$*, blue line) and *VNC-SP>ChAT^{RNAi}* (*VT013602-AD; 23E10-DBD> UAS-*
1280 *ChAT$^{RNAi\ 60028}$*, red line) female flies.

1281 **H)** Box plots of total sleep time (in minutes) for flies presented in G. The bottom and top
1282 of each box represents the first and third quartile, and the horizontal line dividing the

1283 box is the median. The whiskers represent the 10th and 90th percentiles. A two-tailed
1284 unpaired t test revealed that *VNC-SP> ChAT*^{RNAi} flies sleep significantly less than
1285 controls. ****P<0.0001. n=22-30 flies per genotype.

1286 **I)** Box plots of daytime sleep bout duration (in minutes) for flies presented in G. The
1287 bottom and top of each box represents the first and third quartile, and the horizontal line
1288 dividing the box is the median. The whiskers represent the 10th and 90th percentiles. A
1289 two-tailed Mann-Whitney U test revealed that *VNC-SP> ChAT*^{RNAi} flies daytime sleep
1290 bout duration is significantly reduced compared with controls. ****P<0.0001. n=22-30
1291 flies per genotype.

1292 **J)** Box plots of nighttime sleep bout duration (in minutes) for flies presented in G. The
1293 bottom and top of each box represents the first and third quartile, and the horizontal line
1294 dividing the box is the median. The whiskers represent the 10th and 90th percentiles. A
1295 two-tailed Mann-Whitney U test revealed that *VNC-SP> ChAT*^{RNAi} flies nighttime sleep
1296 bout duration is significantly reduced compared with controls. ****P<0.0001. n=22-30
1297 flies per genotype.

1298 **K)** Box plots of locomotor activity counts per minute awake for flies presented in G. The
1299 bottom and top of each box represents the first and third quartile, and the horizontal line
1300 dividing the box is the median. The whiskers represent the 10th and 90th percentiles. A
1301 two-tailed Mann-Whitney U test revealed that there is no difference in waking activity
1302 between *VNC-SP> ChAT*^{RNAi} flies and controls. n.s= not significant. n=22-30 flies per
1303 genotype.

1304 **L)** Box plots of total sleep change in % for vehicle-fed and retinal-fed *VT013602-AD;*
1305 *23E10-DBD>UAS-Cs Chrimson; UAS-GFP.VALIUM10* (control) and *VT013602-AD;*
1306 *23E10-DBD>UAS-Cs Chrimson; UAS-ChAT*$^{RNAi\ 60028}$ flies stimulated by 627nm LEDs.
1307 The bottom and top of each box represents the first and third quartile, and the horizontal
1308 line dividing the box is the median. The whiskers represent the 10th and 90th percentiles.
1309 A two-way ANOVA followed by Sidak's multiple comparisons shows that sleep is
1310 significantly increased in control flies and that expressing ChAT RNAi in VNC-SP
1311 neurons completely abolishes the sleep-promoting effect of VNC-SP neurons activated

1312 by 627nm LEDs. ****P<0.0001, n.s= not significant. n=31-36 flies per genotype and
1313 condition.

1314

1315 **Figure 7: The 23E10-LexA driver does not express in VNC-SP neurons.**

1316 **A-E)** Representative confocal stacks of a female *23E10-LexA>LexAop2-GFP; 23E10-*
1317 *GAL4>UAS-RFP* fly showing the brain (A), a magnified view of dFB neurons (B), the
1318 VNC (C), VNC-SP neurons projections in the brain (D) and TPN1 neurons processes in
1319 the VNC (E). Yellow arrows in B show dFB neurons that are labeled by both the 23E10-
1320 LexA and 23E10-GAL4 drivers, while the gray arrow shows a neuron that is only labeled
1321 by 23E10-GAL4. Our analysis revealed that in these co-labelling experiments, 23E10-
1322 LexA expresses in 13-20 dFB neurons while 23E10-GAL4 labels 19-26 dFB cells per
1323 brain. Importantly, all the neurons labeled by 23E10-LexA are part of the 23E10-GAL4
1324 expression pattern. Yellow arrows in C show the TPN1 neurons and gray arrows the
1325 VNC-SP neurons. Green, anti-GFP; magenta, anti-RFP.

1326 **F)** Box plots of total sleep change in % for vehicle-fed and retinal-fed *23E10-GAL4/+*
1327 and *UAS-CsChrimson/+* parental controls and *23E10-GAL4>UAS-CsChrimson* female
1328 flies stimulated by 627nm LEDs. The bottom and top of each box represents the first
1329 and third quartile, and the horizontal line dividing the box is the median. The whiskers
1330 represent the 10th and 90th percentiles. Two-way ANOVA followed by Sidak's multiple
1331 comparisons revealed that retinal-fed *23E10-GAL4>UAS-CsChrimson* flies significantly
1332 increase sleep when stimulated with 627nm LEDs. Both parental controls show no
1333 difference. ****P<0.0001, n.s= not significant. n=24-42 flies per genotype and condition.

1334 **G)** Box plots of total sleep change in % for vehicle-fed and retinal-fed *23E10-LexA/+*
1335 and *LexAop2-CsChrimson/+* parental controls and *23E10-LexA>LexAop2-CsChrimson*
1336 female flies stimulated by 627nm LEDs. The bottom and top of each box represents the
1337 first and third quartile, and the horizontal line dividing the box is the median. The
1338 whiskers represent the 10th and 90th percentiles. A two-way ANOVA followed by Sidak's
1339 multiple comparisons revealed that no differences in sleep following stimulation. n.s=
1340 not significant. n=23-31 flies per genotype and condition.

1341 **Figure 8: The 23E10-GAL4 contains two groups of sleep regulating neurons.**

1342 **A)** Representative confocal stacks of a female *23E10-GAL4>UAS-GFP* fly showing dFB
1343 neurons and VNC-SP neurons.

1344 **B)** Box plots of total sleep recovered in % during the first 24h following 12h of sleep
1345 deprivation at night for *23E10-GAL4/+* and *UAS-Kir2.1/+* parental controls and *23E10-*
1346 *GAL4>UAS-Kir2.1* female flies. A one-way ANOVA followed by Tukey's multiple
1347 comparisons demonstrate that both parental controls have a bigger homeostatic sleep
1348 rebound than *23E10-GAL4>UAS-Kir2.1* female flies. *P<0.05, n.s= not significant.
1349 n=47-62 flies per genotype.

1350 **C)** Box plots of total sleep recovered in % during the first 24h following 12h of sleep
1351 deprivation at night for *Empty-AD; 23E10-DBD>UAS-Kir2.1* and *VT013602-AD; 23E10-*
1352 *DBD>UAS-Kir2.1* female flies. A two-tailed unpaired t test revealed that there is no
1353 difference in homeostatic sleep rebound. n.s= not significant. n=24-29 flies per
1354 genotype.

1355 **D)** Box plots of total sleep recovered in % during the first 24h following 12h of sleep
1356 deprivation at night for *Empty-AD; 23E10-DBD>UAS-Kir2.1* and *FBS4>UAS-Kir2.1*
1357 female flies. A two-tailed unpaired t test revealed that *FBS4>UAS-Kir2.1* flies have a
1358 significantly reduced homeostatic sleep rebound compared to controls. **P<0.01. n=15-
1359 28 flies per genotype.

1360

1361 **Table Legends**

1362 **Table 1: Quantification of the number of cells labeled by the 23E10-Gal4 driver.**

1363 Average number ± SEM and range of dFB neurons, all brain neurons and VNC neurons
1364 labeled in *23E10-GAL4>UAS-GFP* female flies.

1365

1366 **Table 2: Description of FBS lines.**

1367 Identification of the AD construct combined with 23E10-DBD in each FBS line. Average
1368 number ± SEM and range of dFB neurons labeled by each line. Bowtie (Y/N) indicates
1369 whether “bowtie” processes are seen in the brain, Y= yes, N= no. Range of additional
1370 (non-dFB) neurons labeled in the brain of each line. Average number ± SEM of VNC
1371 metathoracic cells labeled by each FBS line. TPN1 (Y/N) indicates whether TPN1
1372 neurons are present in the expression pattern, Y= yes, N= no. Range of additional cells
1373 in the VNC include any VNC neurons that is not TPN1 or “bowtie” like (VNC-SP).

1374

1375 **Video Legends**

1376 **Video 1: Brain of a 23E10-GAL4>UAS-GFP female.**

1377 **Video 2: VNC of a 23E10-GAL4>UAS-GFP female.**

1378 **Video 3: Brain of a FBS5>UAS-GFP female.**

1379 **Video 4: VNC of a FBS5>UAS-GFP female.**

1380 **Video 5: Brain of a VT013602AD-23E10-DBD (VNC-SP)>UAS-GFP female.**

1381 **Video 6: VNC of a VT013602AD-23E10-DBD (VNC-SP)>UAS-GFP female.**

1382

1383 **Supplemental Figure Legends**

1384 **Figure 2-figure supplement 1: Additional sleep profiles and confocal images of**
1385 **FBS lines.**

1386 **A-R)** Sleep profile (left) and representative confocal stacks (right) for brain and VNC of
1387 female *FBS>UAS-TrpA1; UAS-GFP* for each FBS line not presented in Figure 2.

1388 **Figure 2-figure supplement 2: Additional sleep parameters for FBS female flies**
1389 **thermogenetically activated.**

1390 **A)** Box plots of daytime sleep bout duration in minutes for flies presented in Figure 2B.
1391 The bottom and top of each box represents the first and third quartile, and the horizontal

1392 line dividing the box is the median. The whiskers represent the 10th and 90th percentiles.
1393 Two-way repeated measures ANOVA followed by Sidak's multiple comparisons test
1394 revealed that 9 FBS line show a significant increase in daytime sleep bout duration
1395 between 22°C and 31°C. *P<0.05, **P<0.01, ***P<0.001, ****P<0.0001, n=30-51 flies
1396 per genotype.

1397 **B)** Box plots of nighttime sleep bout duration in minutes for flies presented in Figure 2B.
1398 The bottom and top of each box represents the first and third quartile, and the horizontal
1399 line dividing the box is the median. The whiskers represent the 10th and 90th percentiles.
1400 Two-way repeated measures ANOVA followed by Sidak's multiple comparisons test
1401 revealed that control and most FBS line show a significant decrease in nighttime sleep
1402 bout duration between 22°C and 31°C. Only 6 sleep-promoting FBS lines show no
1403 difference between 22°C and 31°C. Dunnett's multiple comparisons reveal that for 5 of
1404 them, nighttime sleep bout duration at 31°C is significantly increased compared with
1405 Empty control flies (# on figure). *P<0.05, **P<0.01, ***P<0.001, ****P<0.0001, n.s= not
1406 significant. n=30-51 flies per genotype.

1407

1408 **Figure 2-figure supplement 3: Thermogenetic activation in male flies.**

1409 **A)** Box plots of total sleep change in % ((total sleep on day3-total sleep on day2/total
1410 sleep on day2) X 100) for male control (Empty-AD; 23E10-DBD) and 22 FBS lines
1411 expressing UAS-TrpA1; UAS-GFP. The bottom and top of each box represents the first
1412 and third quartile, and the horizontal line dividing the box is the median. The whiskers
1413 represent the 10th and 90th percentiles. The gray rectangle spanning the horizontal axis
1414 indicates the interquartile range of the control. Kruskal-Wallis ANOVA followed by
1415 Dunn's multiple comparisons revealed that 9 FBS lines increase sleep significantly more
1416 than control flies when transferred to 31°C. *P<0.05, **P<0.01, ****P<0.0001, n=26-46
1417 flies per genotype.

1418 **B)** Box plots of locomotor activity counts per minute awake for flies presented in A. The
1419 bottom and top of each box represents the first and third quartile, and the horizontal line
1420 dividing the box is the median. The whiskers represent the 10th and 90th percentiles.

1421 Two-way repeated measures ANOVA followed by Sidak's multiple comparisons test
1422 found that for 4 sleep-promoting FBS lines (FBS5, FBS45, FBS53 and FBS68)
1423 locomotor activity per awake time is increased while no differences are seen for the
1424 other 5 sleep-promoting lines between 22°C and 31°C. *P<0.05, **P<0.01, ***P<0.001,
1425 ****P<0.0001, n=26-46 flies per genotype.

1426 **C)** Box plots of daytime sleep bout duration for flies presented in A. The bottom and top
1427 of each box represents the first and third quartile, and the horizontal line dividing the
1428 box is the median. The whiskers represent the 10th and 90th percentiles. Two-way
1429 repeated measures ANOVA followed by Sidak's multiple comparisons test found that for
1430 7 out of the 9 sleep-promoting FBS lines, daytime sleep bout duration is significantly
1431 increased at 31°C compared with 22°C. *P<0.05, **P<0.01, ***P<0.001, ****P<0.0001,
1432 n=26-46 flies per genotype.

1433 **D)** Box plots of nighttime sleep bout duration for flies presented in A. The bottom and
1434 top of each box represents the first and third quartile, and the horizontal line dividing the
1435 box is the median. The whiskers represent the 10th and 90th percentiles. Two-way
1436 repeated measures ANOVA followed by Sidak's multiple comparisons revealed that
1437 control and most FBS line show a significant decrease in nighttime sleep bout duration
1438 between 22°C and 31°C. 5 sleep-promoting FBS lines show no difference between
1439 22°C and 31°C (FBS5, FBS42, FBS53, FBS81 and FBS84) while FBS45 and FBS68
1440 show an increase in nighttime sleep bout duration at 31°C. Dunnett's multiple
1441 comparisons reveal that for FBS5, FBS42, FBS45, FBS53, FBS68,FBS81 and FBS84,
1442 nighttime sleep bout duration at 31°C is significantly increased compared with Empty
1443 control flies (# on figure). **P<0.01, ***P<0.001, ****P<0.0001, n=26-46 flies per
1444 genotype.

1445

1446 **Figure 3-figure supplement 1: Vehicle-fed sleep data for females in optogenetic**
1447 **experiments.**

1448 **A)** Box plots of locomotor activity counts per minute awake for vehicle-fed flies
1449 presented in Figure 3B. The bottom and top of each box represents the first and third

1450 quartile, and the horizontal line dividing the box is the median. The whiskers represent
1451 the 10th and 90th percentiles. Two-way repeated measures ANOVA followed by Sidak's
1452 multiple comparisons test found that all lines except FBS42 show no difference in
1453 locomotor activity per awake time when the flies are stimulated with 627nm LEDs.
1454 ***P<0.001. n=20-39 flies per genotype.

1455 **B)** Box plots of daytime sleep bout duration for vehicle-fed flies presented in Figure 3B.
1456 The bottom and top of each box represents the first and third quartile, and the horizontal
1457 line dividing the box is the median. The whiskers represent the 10th and 90th percentiles.
1458 Two-way repeated measures ANOVA followed by Sidak's multiple comparisons test
1459 found that most vehicle-fed sleep-promoting lines show no difference in daytime sleep
1460 bout duration when the flies are stimulated with 627nm LEDs. *P<0.05, **P<0.01,
1461 ***P<0.001. n=20-39 flies per genotype.

1462 **C)** Box plots of nighttime sleep bout duration for vehicle-fed flies presented in Figure 3B.
1463 The bottom and top of each box represents the first and third quartile, and the horizontal
1464 line dividing the box is the median. The whiskers represent the 10th and 90th percentiles.
1465 Two-way repeated measures ANOVA followed by Sidak's multiple comparisons test
1466 show no difference in nighttime sleep bout duration when vehicle-fed flies are stimulated
1467 with 627nm LEDs. n=20-39 flies per genotype.

1468

1469 **Figure 3-figure supplement 2: Optogenetic activation in males.**

1470 **A)** Box plots of total sleep change in % ((total sleep on day3-total sleep on day2/total
1471 sleep on day2) X 100) for control (Empty) and 22 experimental vehicle-fed and retinal-
1472 fed male flies expressing CsChrimson upon 627nm LED stimulation. The bottom and
1473 top of each box represents the first and third quartile, and the horizontal line dividing the
1474 box is the median. The whiskers represent the 10th and 90th percentiles. Two-way
1475 ANOVA followed by Sidak's multiple comparisons revealed that 9 retinal-fed FBS lines
1476 increase sleep significantly when stimulated with 627nm LEDs when compared with
1477 vehicle-fed flies. *P<0.05, **P<0.01, ****P<0.0001. n=20-44 flies per genotype and
1478 condition.

1479 **B)** Box plots of locomotor activity counts per minute awake for retinal-fed flies presented
1480 in A. The bottom and top of each box represents the first and third quartile, and the
1481 horizontal line dividing the box is the median. The whiskers represent the 10th and
1482 90th percentiles. Two-way repeated measures ANOVA followed by Sidak's multiple
1483 comparisons test found that for most sleep-promoting FBS lines, locomotor activity per
1484 awake time is not affected when the flies are stimulated with 627nm LEDs while it is
1485 increased in *FBS72>UAS-CsChrimson* flies. *P<0.05, n=24-44 flies per genotype.

1486 **C)** Box plots of daytime sleep bout duration (in minutes) for retinal-fed flies presented in
1487 A. The bottom and top of each box represents the first and third quartile, and the
1488 horizontal line dividing the box is the median. The whiskers represent the 10th and
1489 90th percentiles. Two-way repeated measures ANOVA followed by Sidak's multiple
1490 comparisons indicate that daytime sleep bout duration is increased in 12 FBS lines
1491 expressing CsChrimson when stimulated with 627nm LEDs. *P<0.05, ***P<0.001,
1492 ****P<0.0001, n=24-44 flies per genotype.

1493 **D)** Box plots of nighttime sleep bout duration (in minutes) for retinal-fed flies presented
1494 in A. The bottom and top of each box represents the first and third quartile, and the
1495 horizontal line dividing the box is the median. The whiskers represent the 10th and
1496 90th percentiles. Two-way repeated measures ANOVA followed by Sidak's multiple
1497 comparisons indicate that nighttime sleep bout duration is increased in 7 FBS lines
1498 expressing CsChrimson when stimulated with 627nm LEDs. *P<0.05, **P<0.01,
1499 ****P<0.0001, n=24-44 flies per genotype.

1500

1501 **Figure 3-figure supplement 3: Vehicle-fed sleep data for males in optogenetic**
1502 **experiments.**

1503 **A)** Box plots of locomotor activity counts per minute awake for vehicle-fed flies
1504 presented in Figure 3-figure supplement 2A. The bottom and top of each box represents
1505 the first and third quartile, and the horizontal line dividing the box is the median. The
1506 whiskers represent the 10th and 90th percentiles. Two-way repeated measures ANOVA
1507 followed by Sidak's multiple comparisons test found no difference in locomotor activity

per awake time when the flies are stimulated with 627nm LEDs. n=20-40 flies per genotype.

B) Box plots of daytime sleep bout duration for vehicle-fed flies presented in Figure 3-figure supplement 2A. The bottom and top of each box represents the first and third quartile, and the horizontal line dividing the box is the median. The whiskers represent the 10th and 90th percentiles. Two-way repeated measures ANOVA followed by Sidak's multiple comparisons test found that most vehicle-fed sleep-promoting lines show no difference in daytime sleep bout duration when the flies are stimulated with 627nm LEDs. *P<0.05, **P<0.01, ***P<0.001. n=20-40 flies per genotype.

C) Box plots of nighttime sleep bout duration for vehicle-fed flies presented in Figure 3-figure supplement 2A. The bottom and top of each box represents the first and third quartile, and the horizontal line dividing the box is the median. The whiskers represent the 10th and 90th percentiles. Two-way repeated measures ANOVA followed by Sidak's multiple comparisons test show no difference in nighttime sleep bout duration when vehicle-fed flies are stimulated with 627nm LEDs. n=20-40 flies per genotype.

Figure 4-figure supplement 1: Vehicle-fed sleep data for females in optogenetic activation of lines containing only VNC neurons.

A) Box plots of locomotor activity counts per minute awake for vehicle-fed flies presented in Figure 4K. The bottom and top of each box represents the first and third quartile, and the horizontal line dividing the box is the median. The whiskers represent the 10th and 90th percentiles. Two-way repeated measures ANOVA followed by Sidak's multiple comparisons test found that locomotor activity per awake time is reduced in vehicle-fed *VT020742-AD; 23E10-DBD>UAS-CsChrimson* and *VT013602-AD; 23E10-DBD>UAS-CsChrimson* flies that are stimulated with 627nm LEDs. **P<0.01, ***P<0.001. n.s.= not significant. n=13-32 flies per genotype.

B) Box plots of daytime sleep bout duration for vehicle-fed flies presented in Figure 4K. The bottom and top of each box represents the first and third quartile, and the horizontal line dividing the box is the median. The whiskers represent the 10th and 90th percentiles.

1537 Two-way repeated measures ANOVA followed by Sidak's multiple comparisons test
1538 found no difference in daytime sleep bout duration when the flies are stimulated with
1539 627nm LEDs. n.s= not significant. n=13-32 flies per genotype.

1540 **C)** Box plots of nighttime sleep bout duration for vehicle-fed flies presented in Figure 4K.
1541 The bottom and top of each box represents the first and third quartile, and the horizontal
1542 line dividing the box is the median. The whiskers represent the 10th and 90th percentiles.
1543 Two-way repeated measures ANOVA followed by Sidak's multiple comparisons test
1544 show that nighttime sleep bout duration is not different when vehicle-fed flies are
1545 stimulated with 627nm LEDs. n.s.= not significant. n=13-32 flies per genotype.

1546

1547 **Figure 4-figure supplement 2: Optogenetic activation of lines containing only VNC**
1548 **neurons. Male data.**

1549 **A)** Box plots of total sleep change in % for control (*Empty-AD; 23E10-DBD>UAS-*
1550 *CsChrimson*), *VT020742-AD; 23E10-DBD>UAS-CsChrimson*, *30A08-AD; 23E10-*
1551 *DBD>UAS-CsChrimson* and *VT013602-AD; 23E10-DBD>UAS-CsChrimson* vehicle-fed
1552 and retinal-fed male flies upon 627nm LED stimulation. The bottom and top of each box
1553 represents the first and third quartile, and the horizontal line dividing the box is the
1554 median. The whiskers represent the 10th and 90th percentiles. Two-way ANOVA
1555 followed by Sidak's multiple comparisons revealed that retinal-fed *VT020742-AD;*
1556 *23E10-DBD>UAS-CsChrimson* and *VT013602-AD; 23E10-DBD>UAS-CsChrimson* flies
1557 increase sleep significantly when stimulated with 627nm LEDs when compared with
1558 vehicle-fed flies. ****P<0.0001, n.s.= not significant. n=18-40 flies per genotype and
1559 condition.

1560 **B)** Box plots of locomotor activity counts per minute awake for retinal-fed flies presented
1561 in A. The bottom and top of each box represents the first and third quartile, and the
1562 horizontal line dividing the box is the median. The whiskers represent the 10th and
1563 90th percentiles. Two-way repeated measures ANOVA followed by Sidak's multiple
1564 comparisons test show that locomotor activity per awake time is increased in
1565 *VT020742-AD; 23E10-DBD>UAS-CsChrimson* flies and is not affected in the other

genotypes when the flies are stimulated with 627nm LEDs. **P<0.05, n.s.= not significant. n=21-40 flies per genotype.

C) Box plots of daytime sleep bout duration (in minutes) for retinal-fed flies presented in A. The bottom and top of each box represents the first and third quartile, and the horizontal line dividing the box is the median. The whiskers represent the 10th and 90th percentiles. Two-way repeated measures ANOVA followed by Sidak's multiple comparisons indicates that daytime sleep bout duration is increased in retinal-fed *VT020742-AD; 23E10-DBD>UAS-CsChrimson* and *VT013602-AD; 23E10-DBD>UAS-CsChrimson* flies when stimulated with 627nm LEDs. ****P<0.0001, n.s.= not significant. n=21-40 flies per genotype.

D) Box plots of nighttime sleep bout duration (in minutes) for retinal-fed flies presented in A. The bottom and top of each box represents the first and third quartile, and the horizontal line dividing the box is the median. The whiskers represent the 10th and 90th percentiles. Two-way repeated measures ANOVA followed by Sidak's multiple comparisons indicates that nighttime sleep bout duration is increased in retinal-fed *VT020742-AD; 23E10-DBD>UAS-CsChrimson* and *VT013602-AD; 23E10-DBD>UAS-CsChrimson* flies when stimulated with 627nm LEDs. ****P<0.0001, n.s.= not significant. n=21-40 flies per genotype.

Figure 4-figure supplement 3: Vehicle-fed sleep data for males in optogenetic activation of lines containing only VNC neurons.

A) Box plots of locomotor activity counts per minute awake for vehicle-fed flies presented in Figure 4-figure supplement 2A. The bottom and top of each box represents the first and third quartile, and the horizontal line dividing the box is the median. The whiskers represent the 10th and 90th percentiles. Two-way repeated measures ANOVA followed by Sidak's multiple comparisons test found that locomotor activity per awake time is reduced in vehicle-fed *VT020742-AD; 23E10-DBD>UAS-CsChrimson* and *VT013602-AD; 23E10-DBD>UAS-CsChrimson* flies that are stimulated with 627nm LEDs. **P<0.01, n.s.= not significant. n=18-32 flies per genotype.

1595 **B)** Box plots of daytime sleep bout duration for vehicle-fed flies presented in Figure 4-
1596 figure supplement 2A. The bottom and top of each box represents the first and third
1597 quartile, and the horizontal line dividing the box is the median. The whiskers represent
1598 the 10th and 90th percentiles. Two-way repeated measures ANOVA followed by Sidak's
1599 multiple comparisons test found no difference in daytime sleep bout duration when the
1600 flies are stimulated with 627nm LEDs. n.s= not significant. n=18-32 flies per genotype.

1601 **C)** Box plots of nighttime sleep bout duration for vehicle-fed flies presented in Figure 4-
1602 figure supplement 2A. The bottom and top of each box represents the first and third
1603 quartile, and the horizontal line dividing the box is the median. The whiskers represent
1604 the 10th and 90th percentiles. Two-way repeated measures ANOVA followed by Sidak's
1605 multiple comparisons test show that nighttime sleep bout duration is not increased when
1606 vehicle-fed flies are stimulated with 627nm LEDs. n.s= not significant. n=18-32 flies per
1607 genotype.

1608

1609 **Figure 4-figure supplement 4: Additional data for TPN1 and VNC-SP neurons.**

1610 **A)** Representative confocal stacks of a female *30A08-LexA>LexAop2-GFP; VT020742-*
1611 *AD; 23E10-DBD>UAS-RFP* fly showing the brain, the VNC and a magnified view of the
1612 cell bodies in the metathoracic ganglion. Yellow arrows show the TPN1 neurons and
1613 their processes in the VNC and in the brain and gray arrows the VNC-SP neurons and
1614 their processes. TPN1 neurons are labeled by 30A08-LexA and VT020742-AD; 23E10-
1615 DBD while VNC-SP neurons are only present in VT020742-AD; 23E10-DBD. Green,
1616 anti-GFP; magenta, anti-RFP.

1617 **B)** Representative confocal stacks of a female *30A08-LexA>LexAop2-KZip^{+}; VT020742-*
1618 *AD; 23E10-DBD>UAS-GFP* fly showing the brain and the VNC. The KZip^{+} repressor
1619 effectively remove expression in the TPN1 neurons leaving only the VNC-SP neurons.
1620 Green, anti-GFP; magenta, anti-nc82 (neuropile marker).

1621 **C)** Box plots of total sleep change in % for *Empty-AD; 23E10-DBD>UAS-CsChrimson*,
1622 *VT020742-AD; 23E10-DBD>UAS-CsChrimson*, *Empty-AD; 23E10-DBD>UAS-*
1623 *CsChrimson; 30A08-LexA> LexAop2-KZip^{+}* and *VT020742-AD; 23E10-DBD>UAS-*

1624 *CsChrimson; 30A08-LexA> LexAop2-KZip*$^{+}$ vehicle-fed and retinal-fed female flies upon
1625 627nm LED stimulation. The bottom and top of each box represents the first and third
1626 quartile, and the horizontal line dividing the box is the median. The whiskers represent
1627 the 10th and 90th percentiles. Two-way ANOVA followed by Sidak's multiple
1628 comparisons revealed that retinal-fed *VT020742-AD; 23E10-DBD>UAS-CsChrimson*
1629 and *VT020742-AD; 23E10-DBD>UAS-CsChrimson; 30A08-LexA> LexAop2-KZip*$^{+}$ flies
1630 increase sleep significantly when stimulated with 627nm LEDs when compared with
1631 vehicle-fed flies. Tukey's multiple comparisons demonstrate that there is no difference
1632 in total sleep change between retinal-fed *VT020742-AD; 23E10-DBD>UAS-CsChrimson*
1633 and *VT020742-AD; 23E10-DBD>UAS-CsChrimson; 30A08-LexA> LexAop2-KZip*$^{+}$ flies.
1634 **P<0.01, ****P<0.0001, n.s.= not significant. n=17-31 flies per genotype and condition.

1635 **D)** Representative confocal stacks of a female *VT020742-AD/ VT013602-AD; 23E10-*
1636 *DBD>UAS-GFP* fly showing the brain and the VNC. This line labels the two TPN1 cells
1637 and the two VNC-SP neurons. Green, anti-GFP; magenta, anti-nc82 (neuropile marker).

1638 **E)** Representative confocal stacks of a female *VT013602-AD; VT020742-DBD>UAS-*
1639 *GFP* fly showing the brain and the VNC. This line labels the two VNC-SP neurons and
1640 their processes in the brain (gray arrows). Green, anti-GFP; magenta, anti-nc82
1641 (neuropile marker).

1642 **F)** Sleep profile of control female (*Empty-AD; Empty-DBD>UAS-TrpA1)* at 22°C (blue
1643 line) and 31°C (red line).

1644 **G)** Sleep profile of *VT013602-AD; VT020742-DBD>UAS-TrpA1* female flies at 22°C
1645 (blue line) and 31°C (red line).

1646 **H)** Box plots of total sleep change in % for flies presented in F and G. The bottom and
1647 top of each box represents the first and third quartile, and the horizontal line dividing the
1648 box is the median. The whiskers represent the 10th and 90th percentiles. A two-tailed
1649 unpaired t test revealed that activating VT013602-AD; VT020742-DBD neurons
1650 significantly increases sleep compared with controls. ****P<0.0001. n=13-14 flies per
1651 genotype.

1652

1653 **Figure 4-figure supplement 5: Arousal threshold for VNC-SP>UAS-Cs Chrimson**
1654 **flies**

1655 Arousal threshold in vehicle-fed and retinal-fed *VT013602-AD; 23E10-DBD>UAS-*
1656 *CsChrimson* female flies. Percentage of flies awakened by a stimulus of increasing
1657 strength (1, 2 and 4 downward movements in the SNAP apparatus) with and without
1658 627nm LEDs stimulation. Two-way ANOVA followed by Sidak's multiple comparisons
1659 indicates that in retinal-fed flies activation of VT013602-AD; 23E10-DBD neurons
1660 reduce the responsiveness to the 1 and 2 stimulus strength when compared with non-
1661 activated flies. No difference in responsiveness is seen at the strongest stimulus (4).
1662 Two-way ANOVA followed by Sidak's multiple comparisons indicates that in vehicle-fed
1663 flies no difference in responsiveness is seen between LED stimulated and non-
1664 stimulated flies. ****P<0.0001, n.s.= not significant. n=16 flies per genotype and
1665 condition.

1666

1667 **Figure 6-figure supplement 1: Additional data demonstrating that VNC-SP**
1668 **neurons are cholinergic.**

1669 **A)** Representative confocal stacks of a female *ChAT-LexA>LexAop2-GFP; VT013602-*
1670 *AD; 23E10-DBD (VNC-SP)>UAS-RFP* focusing on the cell bodies in the metathoracic
1671 ganglion of the VNC. Gray arrows show the VNC-SP neurons that are co-labelled by the
1672 ChAT-LexA driver. Green, anti-GFP; magenta, anti-RFP.

1673 **B)** Representative confocal stacks of a female *ChAT-LexA>LexAop2-GFP; 23E10-*
1674 *GAL4>UAS-RFP.* Top panels, focusing on the cell bodies in the metathoracic ganglion
1675 of the VNC. Gray arrows show the VNC-SP neurons that are co-labelled by the ChAT-
1676 LexA driver. Bottom panels, focusing on dFB neurons. Red arrows show 23E10-GAL4
1677 dFB neurons that are also labeled by ChAT-LexA. Green, anti-GFP; magenta, anti-RFP.

1678 **C)** Quantification of ChAT knockdown efficiency by RNAi. qPCR was performed on the
1679 body and eyes of control flies (*GMR-GAL4>+*) and flies expressing ChAT RNAi (line
1680 60028) in the eyes driven by GMR-GAL4 (*GMR-GAL4>ChAT RNAi*). Expression levels
1681 were normalized to control levels. Two-way ANOVA followed by Sidak's multiple

1682 comparisons revealed that in *GMR-GAL4>ChAT RNAi* flies ChAT levels are significantly
1683 reduced in the eyes but not in the body. **P<0.01. n.s.= not significant. n=3-4 replicates
1684 per genotype.

1685 **D)** ChAT immunostaining in *VNC-SP>UAS-GFP* (top panels) and *VNC-SP>UAS-GFP;*
1686 *UAS-ChAT RNAi* flies (bottom panels). Gray arrows point to neurons positive for GFP
1687 and ChAT. Green, anti-GFP; magenta, anti-ChAT.

1688 **E)** Quantification of data presented in D. A one-tailed unpaired t test revealed that
1689 expressing ChAT RNAi in VNC-SP neurons significantly reduce ChAT levels as
1690 measured with ChAT antibody staining. *P<0.05. n=14-17 VNC analyzed per genotype.

1691 **F)** Box plots of total sleep time (in minutes) for control (*Empty-AD; 23E10-DBD>ChAT*
1692 *60028*) and *VNC-SP>ChAT 60028* male flies. The bottom and top of each box
1693 represents the first and third quartile, and the horizontal line dividing the box is the
1694 median. The whiskers represent the 10th and 90th percentiles. A two-tailed Mann-
1695 Whitney U test revealed that *VNC-SP> ChAT*^{RNAi} male flies sleep significantly less than
1696 controls. ****P<0.0001. n=24-30 flies per genotype.

1697 **G)** Box plots of daytime sleep bout duration (in minutes) for control (*Empty-AD; 23E10-*
1698 *DBD>ChAT 60028*) and *VNC-SP>ChAT 60028* male flies. The bottom and top of each
1699 box represents the first and third quartile, and the horizontal line dividing the box is the
1700 median. The whiskers represent the 10th and 90th percentiles. A two-tailed Mann-
1701 Whitney U test revealed that *VNC-SP> ChAT*^{RNAi} male flies daytime sleep bout duration
1702 is significantly reduced compared with controls. ***P<0.001. n=24-30 flies per genotype.

1703 **H)** Box plots of nighttime sleep bout duration (in minutes) for control (*Empty-AD; 23E10-*
1704 *DBD>ChAT 60028*) and *VNC-SP>ChAT 60028* male flies. The bottom and top of each
1705 box represents the first and third quartile, and the horizontal line dividing the box is the
1706 median. The whiskers represent the 10th and 90th percentiles. A two-tailed Mann-
1707 Whitney U test revealed that *VNC-SP> ChAT*^{RNAi} male flies nighttime sleep bout
1708 duration is significantly reduced compared with controls. ***P<0.001. n=24-30 flies per
1709 genotype.

1710 **I)** Box plots of locomotor activity counts per minute awake for control (*Empty-AD;*
1711 *23E10-DBD>ChAT 60028*) and *VNC-SP>ChAT 60028* male flies. The bottom and top of
1712 each box represents the first and third quartile, and the horizontal line dividing the box is
1713 the median. The whiskers represent the 10th and 90th percentiles. A two-tailed unpaired
1714 t test revealed that there is no difference in waking activity between *VNC-SP> ChAT^{RNAi}*
1715 male flies and controls. n.s= not significant. n=24-30 flies per genotype.

1716 **J)** Box plots of total sleep change in % for *VT013602-AD; 23E10-DBD>UAS-*
1717 *CsChrimson; 2x LexAop2KZip^{+}* (control, no LexA driver) and for *VT013602-AD; 23E10-*
1718 *DBD>UAS-CsChrimson; ChAT-LexA>2x LexAop2KZip^{+}* vehicle-fed and retinal-fed
1719 female flies upon 627nm LED stimulation. The bottom and top of each box represents
1720 the first and third quartile, and the horizontal line dividing the box is the median. The
1721 whiskers represent the 10th and 90th percentiles. Two-way ANOVA followed by Sidak's
1722 multiple comparisons revealed that retinal-fed *VT013602-AD; 23E10-DBD>UAS-*
1723 *CsChrimson; ChAT-LexA>2x LexAop2KZip^{+}* flies do not increase sleep compared with
1724 vehicle-fed flies when stimulated with 627nm LEDs. Control flies increase sleep
1725 significantly. ***P<0.001, n.s.= not significant. n=11-16 flies per genotype and condition.

1726 **K)** Representative confocal stacks of *VT013602-AD; 23E10-DBD>UAS-GFP* (left) and
1727 *VT013602-AD; 23E10-DBD>UAS-GFP; ChAT-LexA>LexAop2KZip^{+}* (right) female flies.
1728 Expression of GFP in VNC-SP neurons is greatly reduced by the expression of the
1729 KZip^{+} repressor. Gray arrows show VNC-SP neurons. Green, anti-GFP; magenta, anti-
1730 RFP.

1731 **L)** Box plots of total sleep change in % for *Empty-AD; 23E10-DBD>UAS-CsChrimson;*
1732 *ChAT-LexA> LexAop2KZip^{+}* and for *FBS45>UAS-CsChrimson; ChAT-LexA>*
1733 *LexAop2KZip^{+}* vehicle-fed and retinal-fed female flies upon 627nm LED stimulation. The
1734 bottom and top of each box represents the first and third quartile, and the horizontal line
1735 dividing the box is the median. The whiskers represent the 10th and 90th percentiles.
1736 Two-way ANOVA followed by Sidak's multiple comparisons revealed no differences in
1737 sleep when flies are stimulated with 627nm LEDs. n.s.= not significant. n=22-29 flies per
1738 genotype and condition.

1739 **M)** Representative confocal stacks of *FBS45>UAS-GFP* (left) and *FBS45>UAS-GFP;*
1740 *ChAT-LexA>LexAop2KZip*$^{+}$ (right) female flies. Expression of GFP in VNC-SP neurons
1741 is completely abolished by the expression of the KZip^{+} repressor. Gray arrows show
1742 VNC-SP neurons. In addition, the KZip^{+} repressor also consistently remove expression
1743 in 4-6 dFB neurons. On average 19.33 ± 0.62 dFB neurons are labeled in *FBS45>UAS-*
1744 *GFP; ChAT-LexA>LexAop2KZip*$^{+}$ while it is more than 25 without the KZip^{+} repressor
1745 (Table 2). Green, anti-GFP; magenta, anti-RFP.

1746

1747 **Figure 6-figure supplement 2: VNC-SP neurons are well positioned to integrate**
1748 **sensory inputs in the VNC and send this information to the brain.**

1749 Representative confocal stacks of a female *VT013602-AD; 23E10-DBD> UAS-*
1750 *5xDenMark-V5; UAS-syt.eGFP.* Top panels, focusing on the brain "bowtie" processes.
1751 Middle panels, the VNC and bottom panels, a magnified view of the cell bodies area.
1752 Green, anti-GFP; magenta, anti-V5.

1753

1754

1755

Figure 1

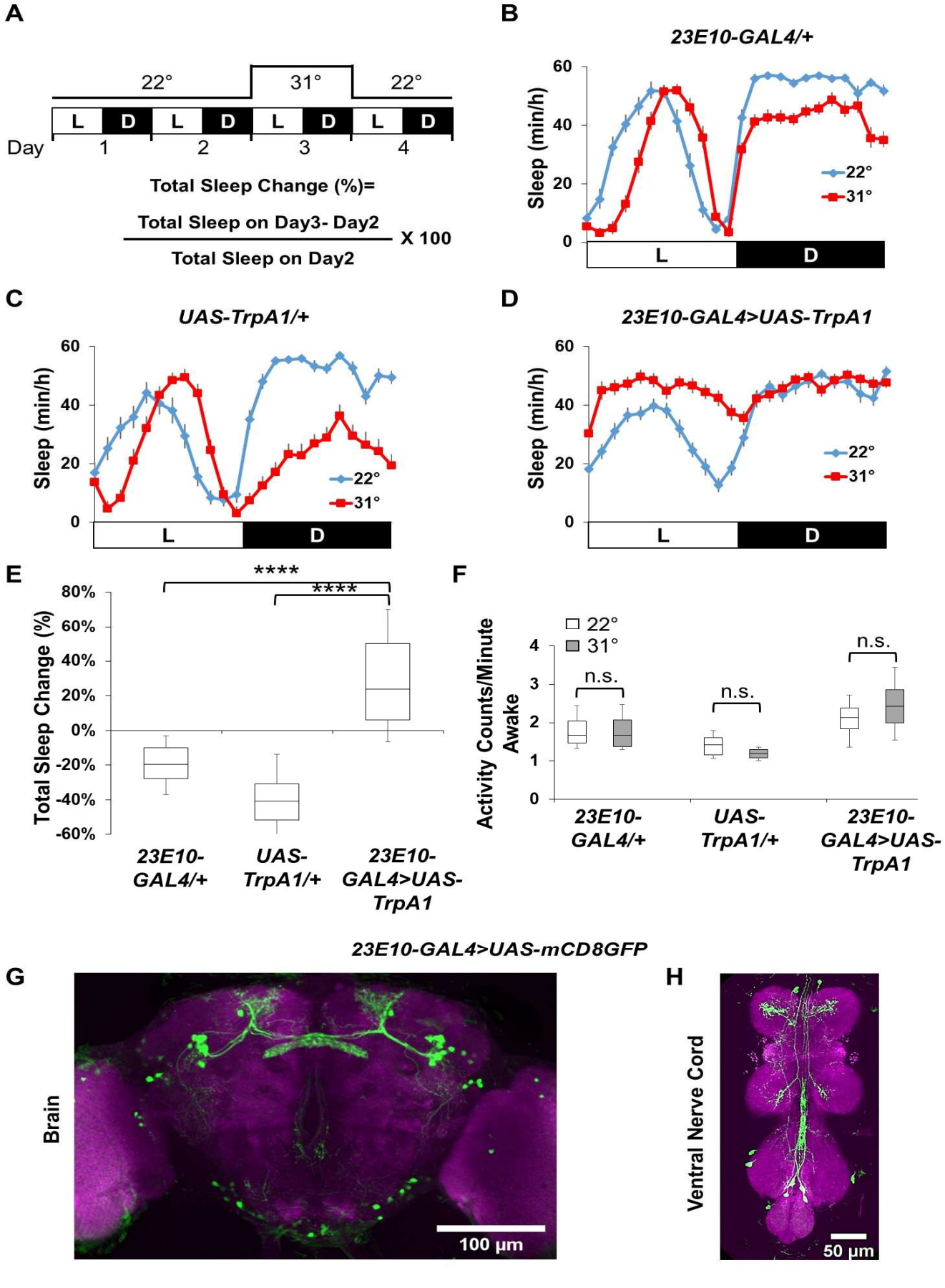
A
22°
31°
22°
L D L D L D L D
Day 1 2 3 4
Total Sleep Change (%)=
Total Sleep on Day3- Day2
Total Sleep on Day2
X 100
B
23E10-GAL4/+
Sleep (min/h)
22°
31°
L D
C
UAS-TrpA1/+
Sleep (min/h)
22°
31°
L D
D
23E10-GAL4>UAS-TrpA1
Sleep (min/h)
22°
31°
L D
E
****
****
Total Sleep Change (%)
23E10-GAL4/+
UAS-TrpA1/+
23E10-GAL4>UAS-TrpA1
F
22°
31°
n.s.
n.s.
n.s.
Activity Counts/Minute Awake
23E10-GAL4/+
UAS-TrpA1/+
23E10-GAL4>UAS-TrpA1
23E10-GAL4>UAS-mCD8GFP
G
Brain
100 µm
H
Ventral Nerve Cord
50 µm

Figure 2

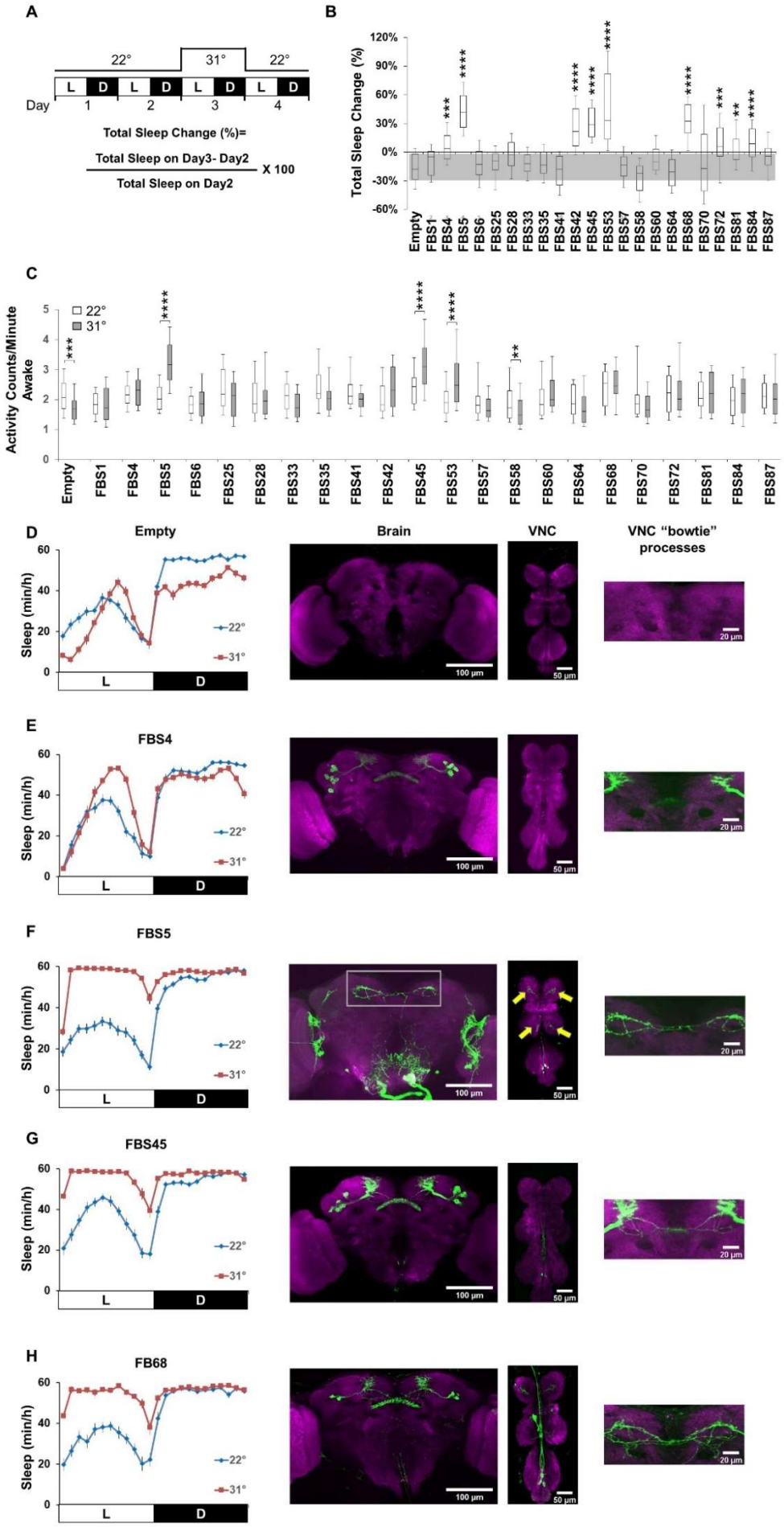
A
22°
31°
22°
L D L D L D L D
Day 1 2 3 4
Total Sleep Change (%)=
Total Sleep on Day3- Day2
Total Sleep on Day2
X 100
B
Total Sleep Change (%)
120%
90%
60%
30%
0%
-30%
-60%
Empty FBS1 FBS4 FBS5 FBS6 FBS25 FBS28 FBS33 FBS35 FBS41 FBS42 FBS45 FBS53 FBS57 FBS58 FBS60 FBS64 FBS68 FBS70 FBS72 FBS81 FBS84 FBS87
C
Activity Counts/Minute Awake
22°
31°
Empty FBS1 FBS4 FBS5 FBS6 FBS25 FBS28 FBS33 FBS35 FBS41 FBS42 FBS45 FBS53 FBS57 FBS58 FBS60 FBS64 FBS68 FBS70 FBS72 FBS81 FBS84 FBS87
D
Empty
Brain
VNC
VNC "bowtie" processes
Sleep (min/h)
22°
31°
L
D
100 µm
50 µm
20 µm
E
FBS4
F
FBS5
G
FBS45
H
FB68

Figure 3

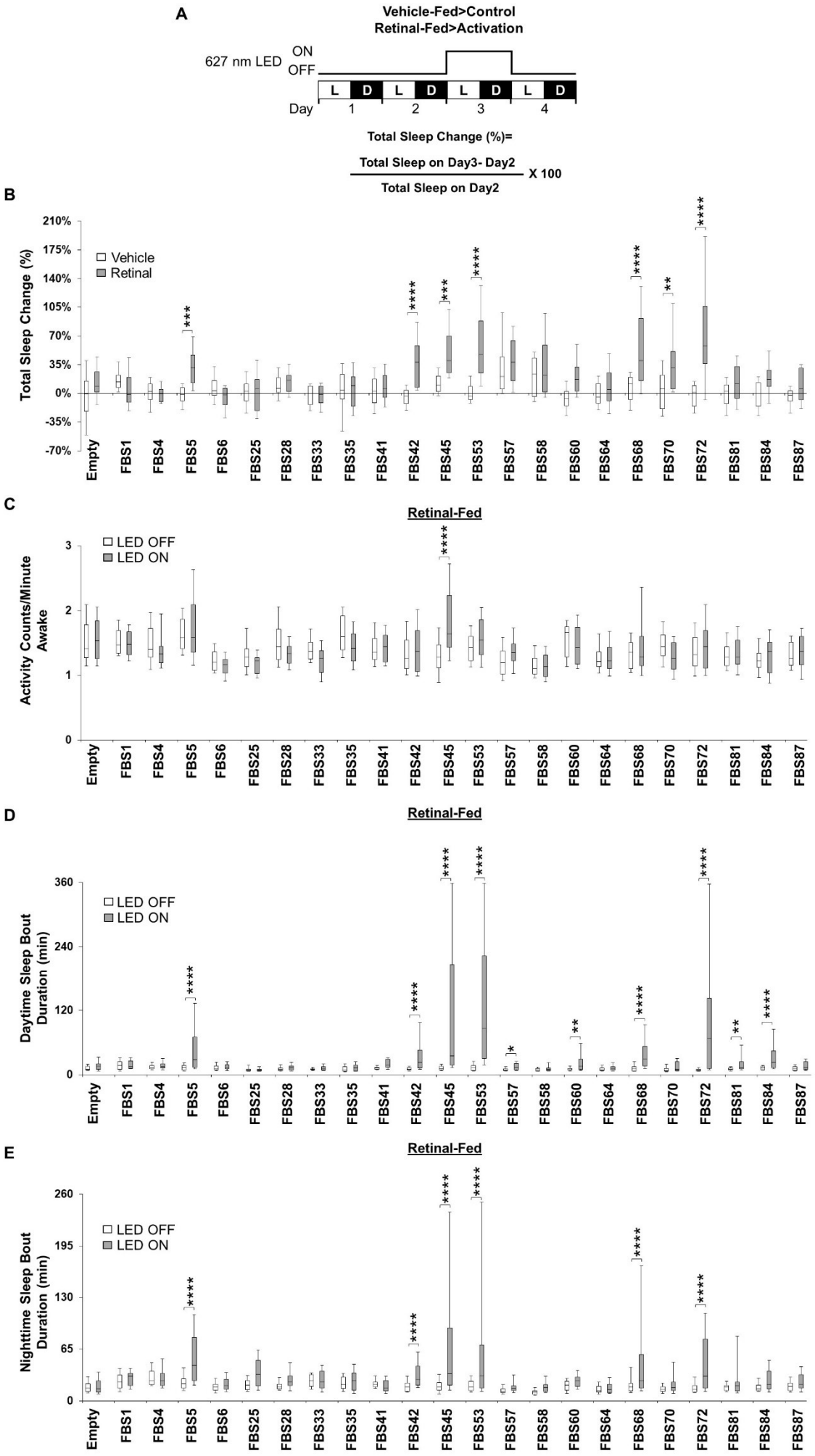
A
Vehicle-Fed>Control
Retinal-Fed>Activation
627 nm LED
ON
OFF
L D L D L D L D
Day 1 2 3 4
Total Sleep Change (%)=
Total Sleep on Day3- Day2
Total Sleep on Day2
X 100
B
Total Sleep Change (%)
Vehicle
Retinal
210%
175%
140%
105%
70%
35%
0%
-35%
-70%
Empty FBS1 FBS4 FBS5 FBS6 FBS25 FBS28 FBS33 FBS35 FBS41 FBS42 FBS45 FBS53 FBS57 FBS58 FBS60 FBS64 FBS68 FBS70 FBS72 FBS81 FBS84 FBS87
C
Retinal-Fed
Activity Counts/Minute Awake
LED OFF
LED ON
D
Retinal-Fed
Daytime Sleep Bout Duration (min)
LED OFF
LED ON
E
Retinal-Fed
Nighttime Sleep Bout Duration (min)
LED OFF
LED ON

Figure 4

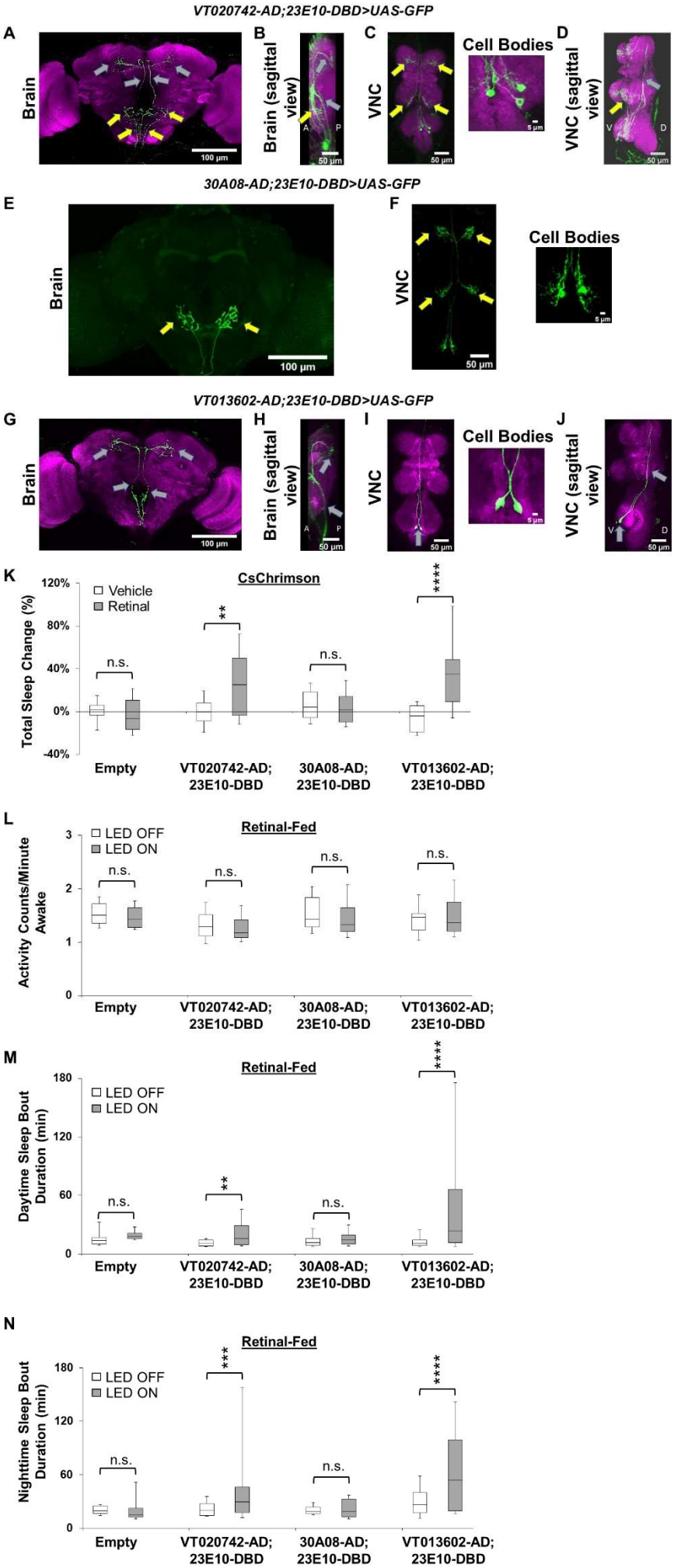
VT020742-AD;23E10-DBD>UAS-GFP
A
Brain
100 µm
B
Brain (sagittal view)
A
P
50 µm
C
VNC
50 µm
Cell Bodies
5 µm
D
VNC (sagittal view)
V
D
50 µm
30A08-AD;23E10-DBD>UAS-GFP
E
Brain
100 µm
F
VNC
50 µm
Cell Bodies
5 µm
VT013602-AD;23E10-DBD>UAS-GFP
G
Brain
100 µm
H
Brain (sagittal view)
A
P
50 µm
I
VNC
50 µm
Cell Bodies
5 µm
J
VNC (sagittal view)
V
D
50 µm
K
CsChrimson
Vehicle
Retinal
Total Sleep Change (%)
120%
80%
40%
0%
-40%
n.s.
**
n.s.
****
Empty
VT020742-AD; 23E10-DBD
30A08-AD; 23E10-DBD
VT013602-AD; 23E10-DBD
L
Retinal-Fed
LED OFF
LED ON
Activity Counts/Minute Awake
3
2
1
0
n.s.
n.s.
n.s.
n.s.
Empty
VT020742-AD; 23E10-DBD
30A08-AD; 23E10-DBD
VT013602-AD; 23E10-DBD
M
Retinal-Fed
LED OFF
LED ON
Daytime Sleep Bout Duration (min)
180
120
60
0
n.s.
**
n.s.
****
Empty
VT020742-AD; 23E10-DBD
30A08-AD; 23E10-DBD
VT013602-AD; 23E10-DBD
N
Retinal-Fed
LED OFF
LED ON
Nighttime Sleep Bout Duration (min)
180
120
60
0
n.s.
***
n.s.
****
Empty
VT020742-AD; 23E10-DBD
30A08-AD; 23E10-DBD
VT013602-AD; 23E10-DBD

Figure 5

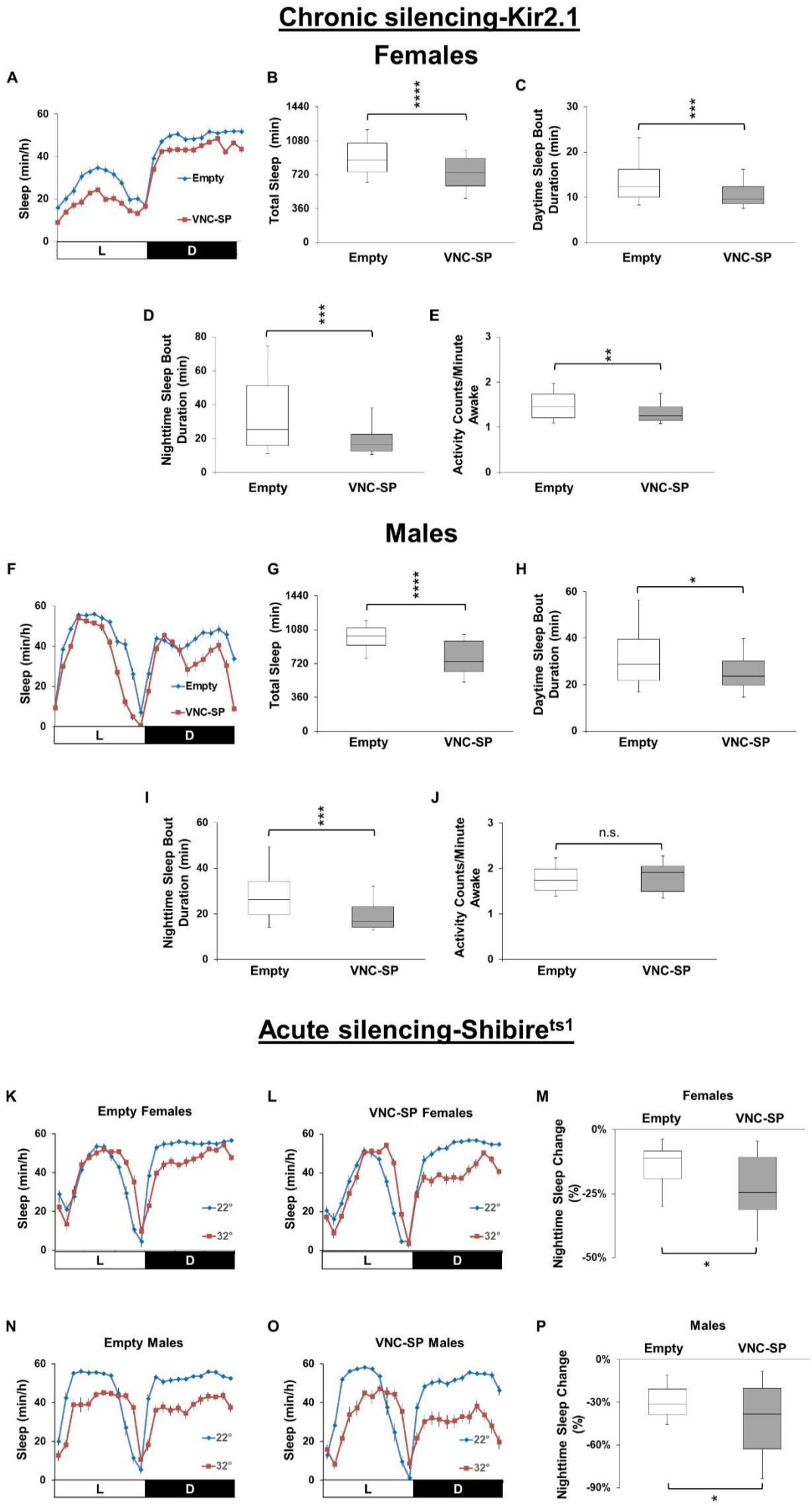
Chronic silencing-Kir2.1
Females
A
Sleep (min/h)
Empty
VNC-SP
L
D
B
Total Sleep (min)
****
Empty
VNC-SP
C
Daytime Sleep Bout Duration (min)
***
D
Nighttime Sleep Bout Duration (min)
***
E
Activity Counts/Minute Awake
**
Males
F
G
H
*
I
J
n.s.
Acute silencing-Shibire^{ts1}
K
Empty Females
L
VNC-SP Females
M
Females
Nighttime Sleep Change (%)
22°
32°
N
Empty Males
O
VNC-SP Males
P
Males

Figure 6

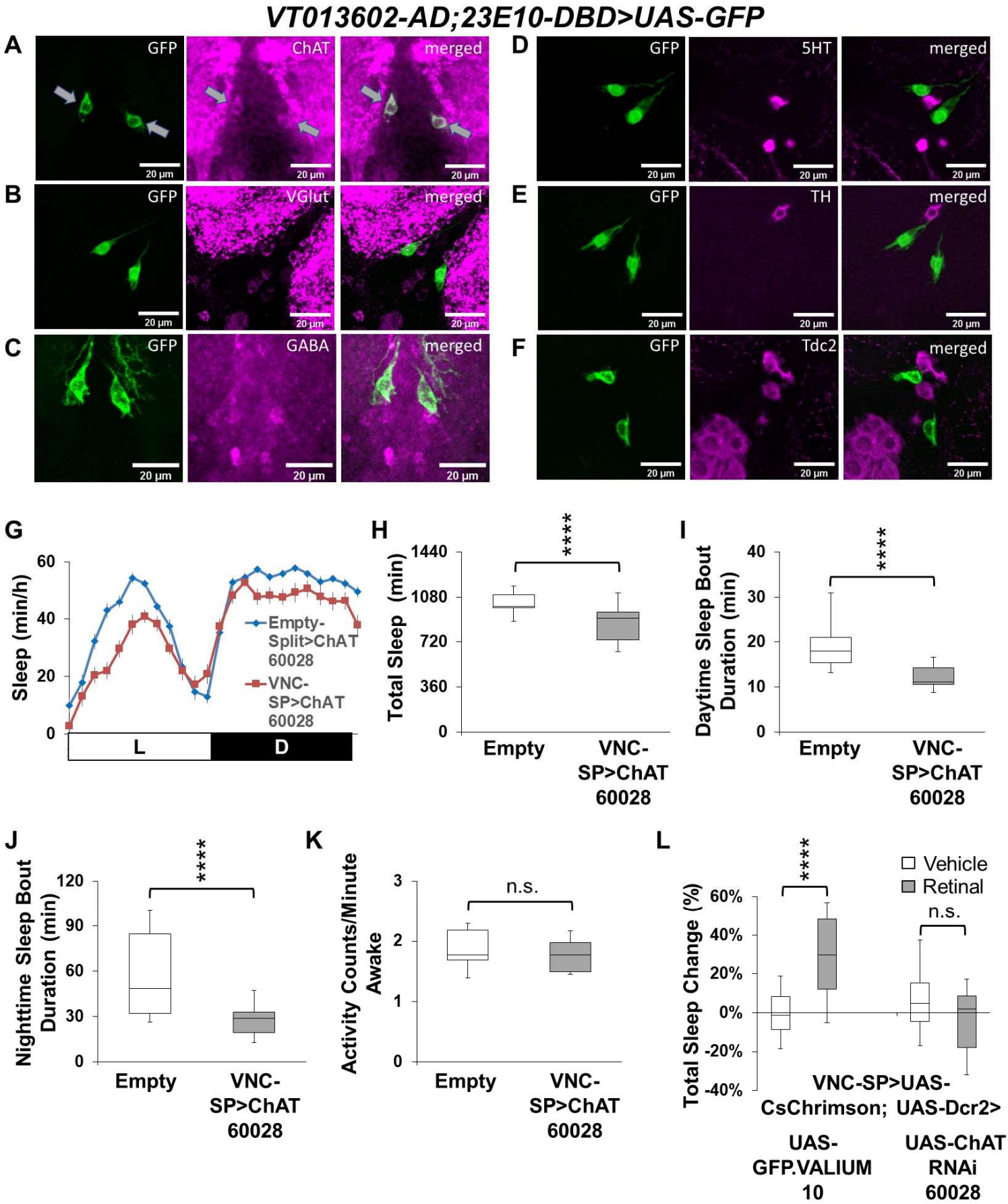
VT013602-AD;23E10-DBD>UAS-GFP
A
GFP
ChAT
merged
B
GFP
VGlut
merged
C
GFP
GABA
merged
D
GFP
5HT
merged
E
GFP
TH
merged
F
GFP
Tdc2
merged
20 µm
G
Sleep (min/h)
Empty-Split>ChAT 60028
VNC-SP>ChAT 60028
L
D
H
Total Sleep (min)
****
Empty
VNC-SP>ChAT 60028
I
Daytime Sleep Bout Duration (min)
****
Empty
VNC-SP>ChAT 60028
J
Nighttime Sleep Bout Duration (min)
****
Empty
VNC-SP>ChAT 60028
K
Activity Counts/Minute Awake
n.s.
Empty
VNC-SP>ChAT 60028
L
Total Sleep Change (%)
Vehicle
Retinal
****
n.s.
VNC-SP>UAS-CsChrimson; UAS-Dcr2>
UAS-GFP.VALIUM 10
UAS-ChAT RNAi 60028

Figure 7

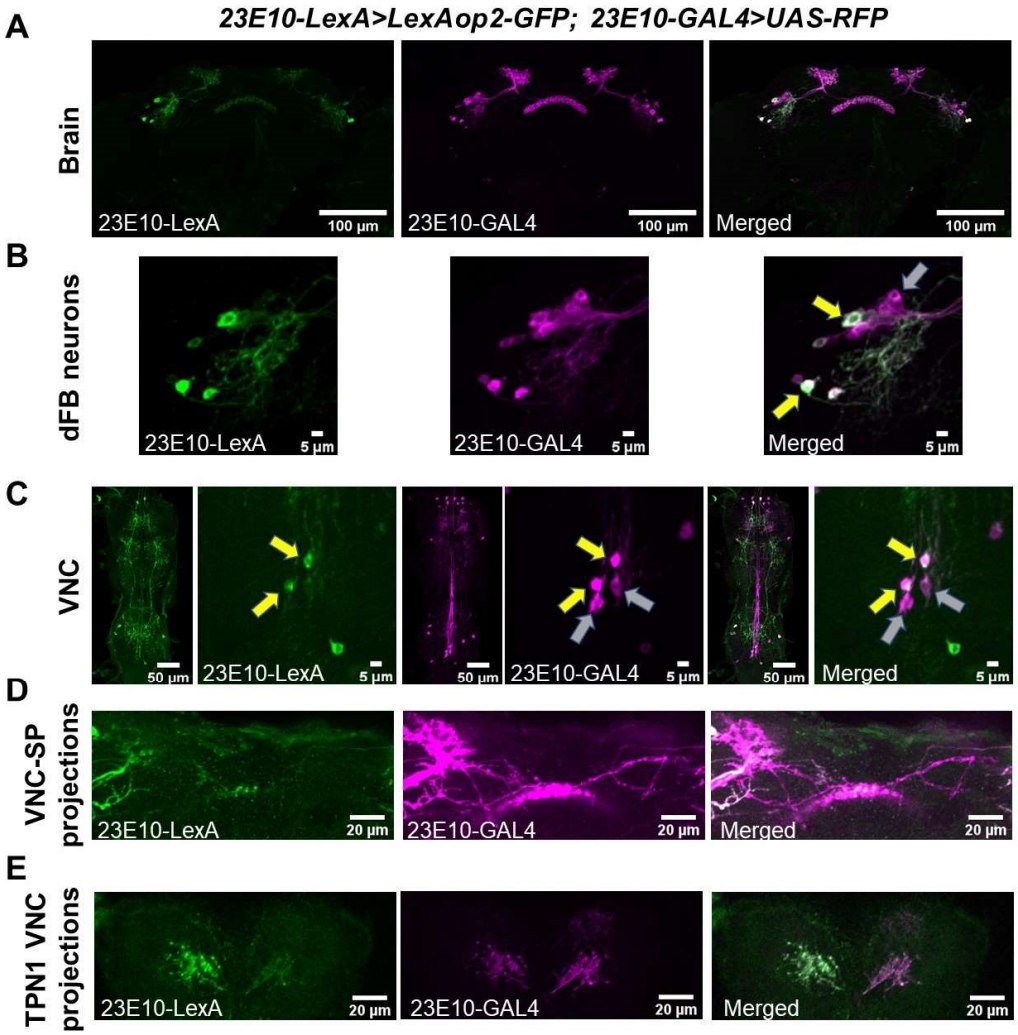
A
23E10-LexA>LexAop2-GFP; 23E10-GAL4>UAS-RFP
Brain
23E10-LexA
100 µm
23E10-GAL4
100 µm
Merged
100 µm
B
dFB neurons
23E10-LexA
5 µm
23E10-GAL4
5 µm
Merged
5 µm
C
VNC
50 µm
23E10-LexA
5 µm
50 µm
23E10-GAL4
5 µm
50 µm
Merged
5 µm
D
VNC-SP projections
23E10-LexA
20 µm
23E10-GAL4
20 µm
Merged
20 µm
E
TPN1 VNC projections
23E10-LexA
20 µm
23E10-GAL4
20 µm
Merged
20 µm

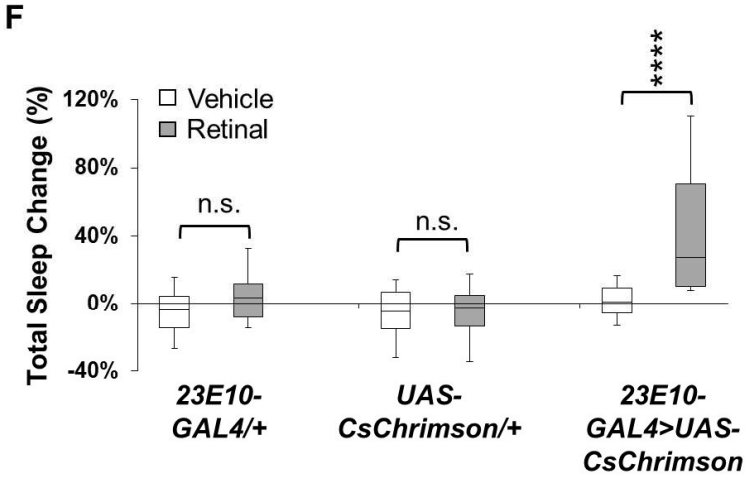
F
Total Sleep Change (%)
120%
80%
40%
0%
-40%
Vehicle
Retinal
n.s.
n.s.
****
23E10-GAL4/+
UAS-CsChrimson/+
23E10-GAL4>UAS-CsChrimson

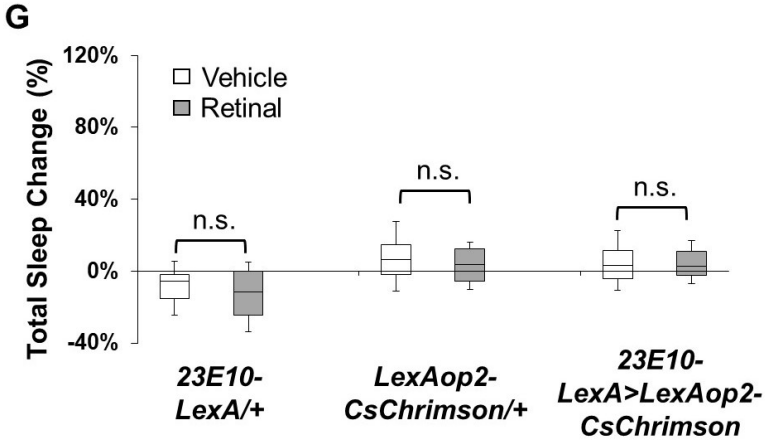
G
Total Sleep Change (%)
120%
80%
40%
0%
-40%
Vehicle
Retinal
n.s.
n.s.
n.s.
23E10-LexA/+
LexAop2-CsChrimson/+
23E10-LexA>LexAop2-CsChrimson

Figure 8

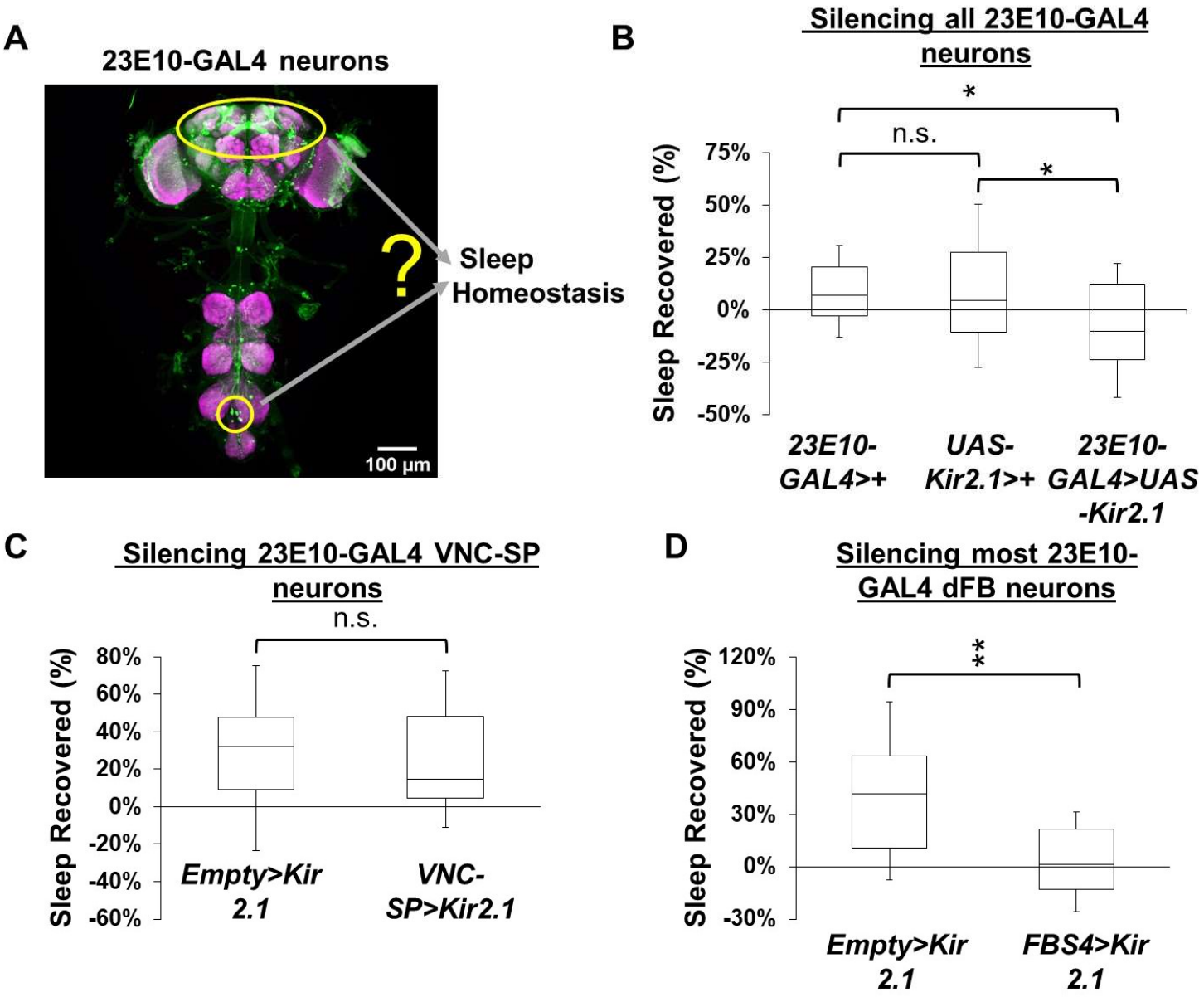
A
23E10-GAL4 neurons
?
Sleep
Homeostasis
100 µm
B
Silencing all 23E10-GAL4 neurons
Sleep Recovered (%)
75%
50%
25%
0%
-25%
-50%
n.s.
*
*
23E10-GAL4>+
UAS-Kir2.1>+
23E10-GAL4>UAS-Kir2.1
C
Silencing 23E10-GAL4 VNC-SP neurons
Sleep Recovered (%)
80%
60%
40%
20%
0%
-20%
-40%
-60%
n.s.
Empty>Kir 2.1
VNC-SP>Kir2.1
D
Silencing most 23E10-GAL4 dFB neurons
Sleep Recovered (%)
120%
90%
60%
30%
0%
-30%
**
Empty>Kir 2.1
FBS4>Kir 2.1

Table 1

	Average (n)	Range
dFB neurons	25.68 ± 0.50 (19)	23-30
All brain neurons	51.79 ± 1.05 (19)	44-62
VNC neurons	17.56 ± 0.99 (9)	12-22

Table 2

FBS line	AD component	Average whole brain dFB neurons ± SEM (n)	Range dFB neurons	Bowtie (Y/N)	Range of additional cells in brain	Average VNC cells in metathoracic ganglion ± SEM (n)	TPN1 (Y/N)	Range of additional cells in VNC
FBS 1	12D12-AD	4.64 ± 0.40 (n=14)	2-7	Y	0	2.00 ± 0.32 (n=11)	N	0
FBS 4	84C10-AD	20.80 ± 0.35 (n=15)	18-23	N	0	0.00 ± 0.50 (n=15)	N	0
FBS 5	23E12-AD	0 ± 0 (n=26)	0	Y	5-10	3.89 ± 0.11 (n=26)	Y	0
FBS 6	42H01-AD	3.85 ± 0.52 (n=13)	1-4	N	0	0.00 ± 0.00 (n=8)	N	0
FBS 25	22A12-AD	0 ± 0 (n=5)	0	N	0	0.00 ± 0.00 (n=5)	N	0
FBS 28	54G07-AD	13.08 ± 0.63 (n=12)	10-18	Y	0-1	3.09 ± 0.17 (n=22)	N	0
FBS 33	49C04-AD	26.50 ± 1.15 (n=10)	23-31	Y	0	3.17 ± 0.32 (n=12)	Y	0
FBS 35	65C03-AD	5.00 ± 1.06 (n=6)	2-8	Y	1-2	3.60 ± 0.24 (n=5)	Y	0
FBS 41	VT058545-AD	11.50 ± 0.43 (n=10)	10-14	N	0-2	3.00 ± 0.41 (n=4)	Y	0
FBS 42	12G09-AD	21.56 ± 0.80 (=10)	18-25	Y	2-4	3.00 ± 0.37 (n=6)	Y	0-2
FBS 45	VT050238-AD	25.11 ± 1.41 (n=9)	21-32	Y	0	2.40 ± 0.16 (n=15)	N	0
FBS 53	VT043400-AD	23.86 ± 0.51 (n=7)	22-26	Y	0	2.91 ± 0.31 (n=11)	N	0-1
FBS 57	VT025720-AD	7.40 ± 0.68 (n=5)	5-9	Y	0	3.00 ± 0.31 (n=7)	Y	0
FBS 58	VT064566-AD	21.50 ± 1.28 (n=6)	18-27	Y	0-2	3.10 ± 0.28 (n=10)	Y	0-1
FBS 60	VT023818-AD	24.56 ± 0.50 (n=9)	22-27	Y	0	3.27 ± 0.38 (n=11)	Y	0-2
FBS 64	VT027956-AD	15.00 ± 2.12 (n=7)	11-19	Y	0	3.40 ± 0.49 (n=10)	Y	0
FBS 68	VT023823-AD	4.45 ± 0.34 (n=11)	3-6	Y	0	4.08 ± 0.49 (n=13)	Y	0-4
FBS 70	VT034811-AD	4.86 ± 0.40 (n=7)	3-6	Y	0-7	3.90 ± 0.38 (n=10)	Y	0-4
FBS 72	VT026953-AD	24.40 ± 1.50 (n=7)	20-28	Y	0-1	3.27 ± 0.25 (n= 10)	Y	0
FBS 81	74G10-AD	22.17 ± 0.70 (n=6)	19-24	Y	0	2.80 ± 0.58 (n=5)	N	0-2
FBS 84	VT007754-AD	23.80 ± 0.58 (n=8)	22-25	Y	0-2	3.36 ± 0.31 (n=12)	Y	0-4
FBS 87	VT045793-AD	18.55 ± 0.53 (n=13)	17-22	Y	0-2	3.62 ± 0.29 (n=13)	Y	0-6

Figure 2-S1

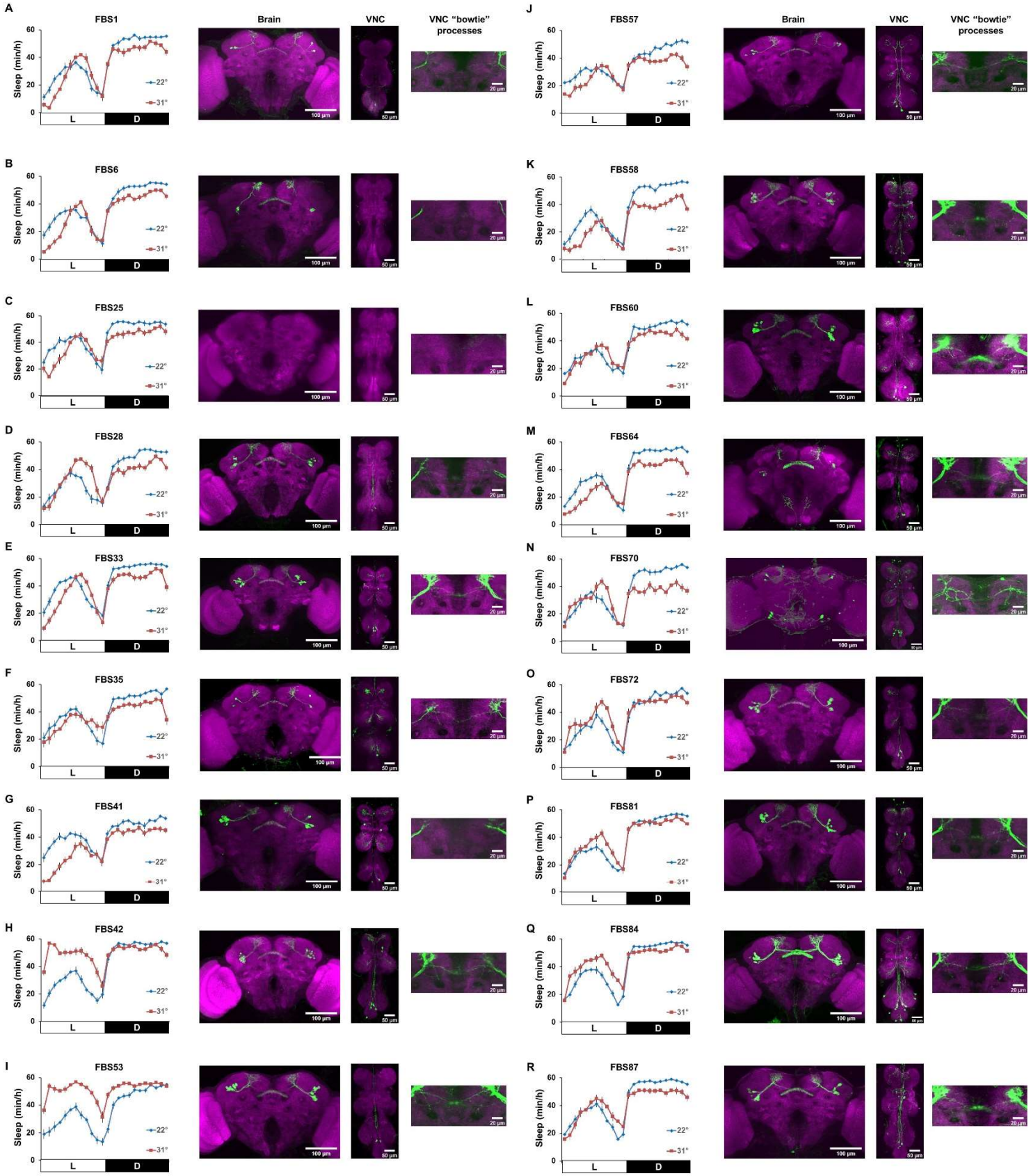
A
FBS1
Brain
VNC
VNC "bowtie" processes
B
FBS6
C
FBS25
D
FBS28
E
FBS33
F
FBS35
G
FBS41
H
FBS42
I
FBS53
J
FBS57
K
FBS58
L
FBS60
M
FBS64
N
FBS70
O
FBS72
P
FBS81
Q
FBS84
R
FBS87
Sleep (min/h)
60
40
20
0
22°
31°
L
D
100 µm
50 µm
20 µm

Figure 2-S2

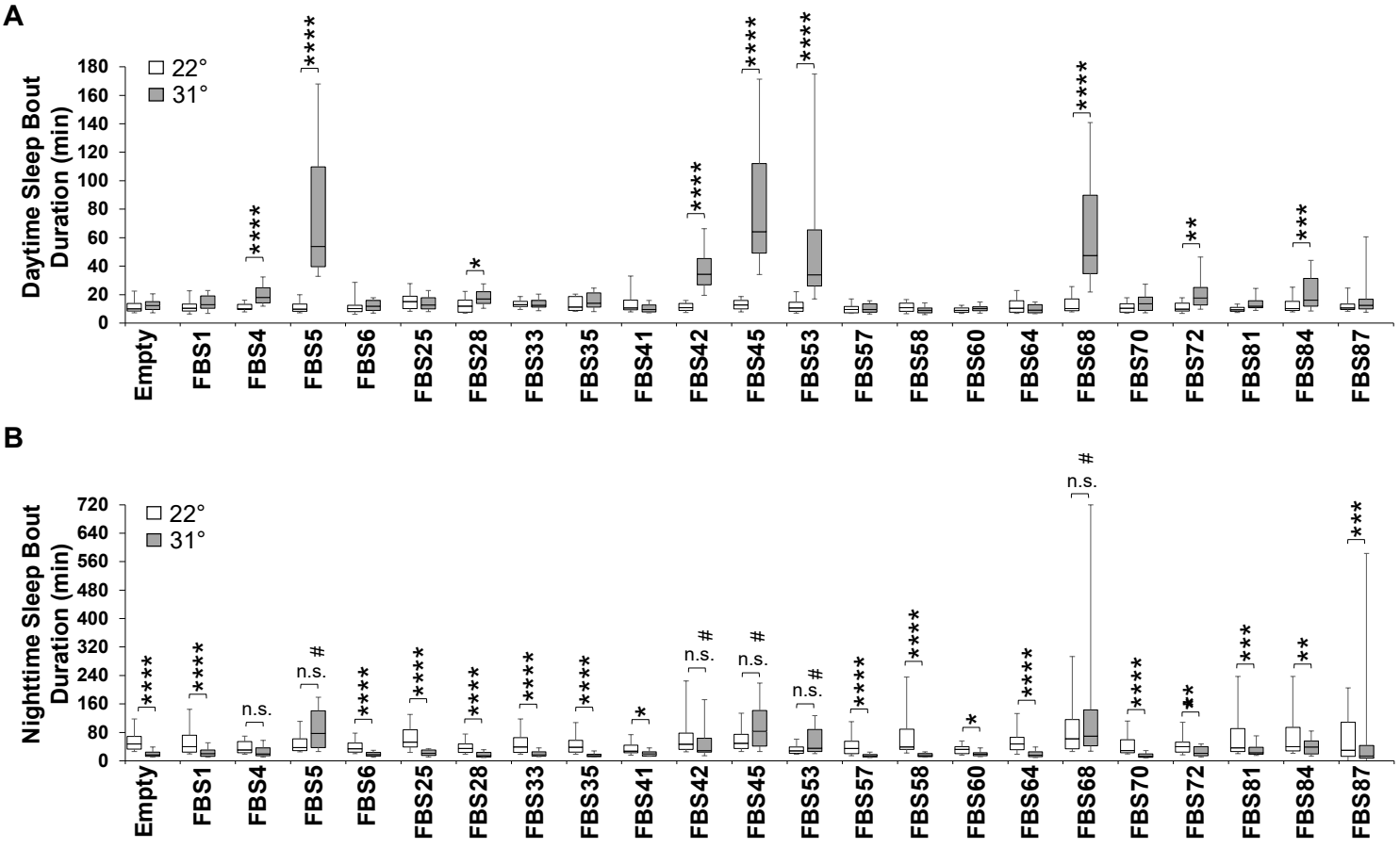
A
Daytime Sleep Bout Duration (min)
22°
31°
180
160
140
120
100
80
60
40
20
0
****
*
Empty
FBS1
FBS4
FBS5
FBS6
FBS25
FBS28
FBS33
FBS35
FBS41
FBS42
FBS45
FBS53
FBS57
FBS58
FBS60
FBS64
FBS68
FBS70
FBS72
FBS81
FBS84
FBS87
B
Nighttime Sleep Bout Duration (min)
22°
31°
720
640
560
480
400
320
240
160
80
0
n.s.
#
*
**
***
****

Figure 2-S3

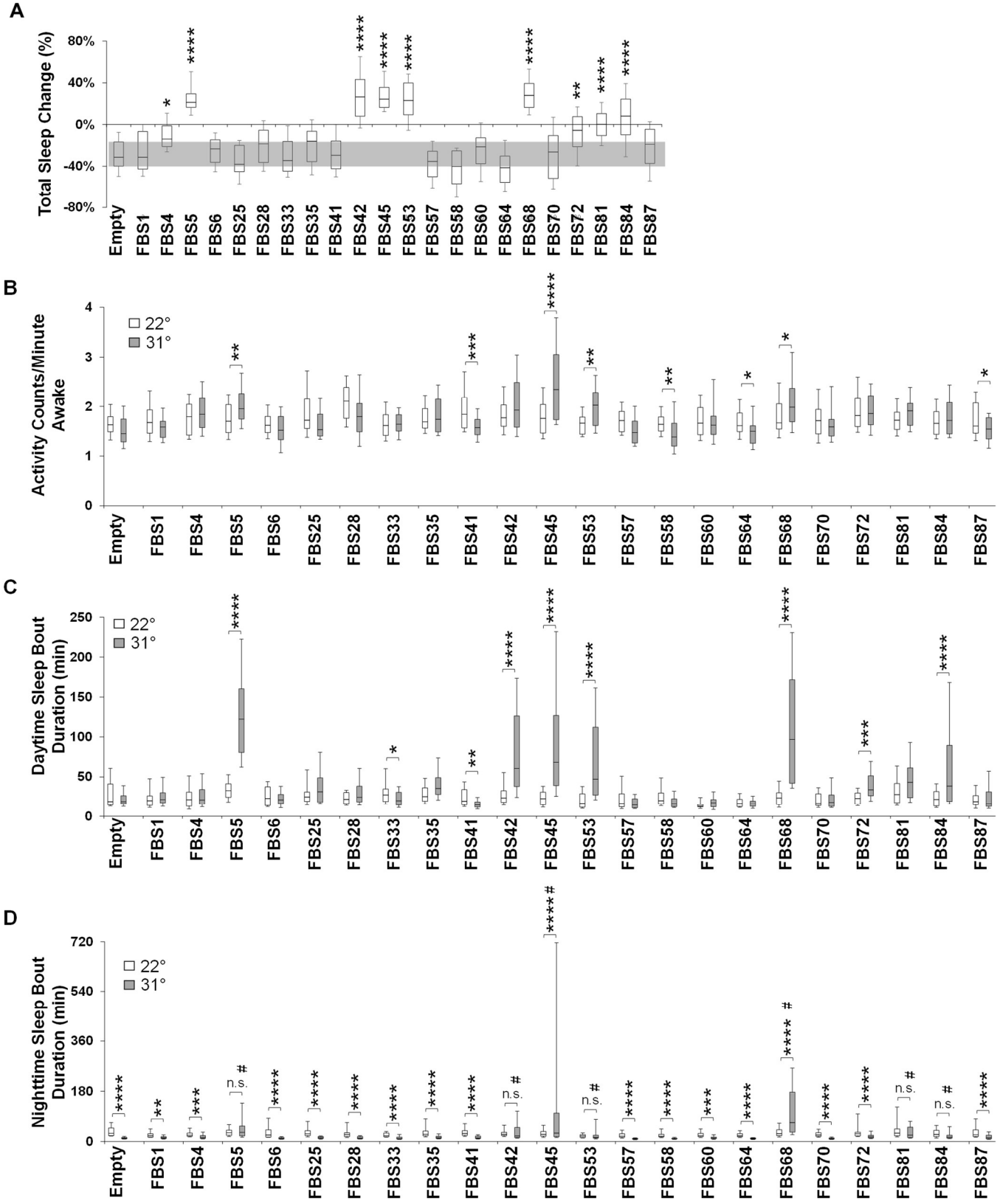
A
Total Sleep Change (%)
80%
40%
0%
-40%
-80%
B
Activity Counts/Minute Awake
22°
31°
C
Daytime Sleep Bout Duration (min)
D
Nighttime Sleep Bout Duration (min)
Empty
FBS1
FBS4
FBS5
FBS6
FBS25
FBS28
FBS33
FBS35
FBS41
FBS42
FBS45
FBS53
FBS57
FBS58
FBS60
FBS64
FBS68
FBS70
FBS72
FBS81
FBS84
FBS87

Figure 3-S1

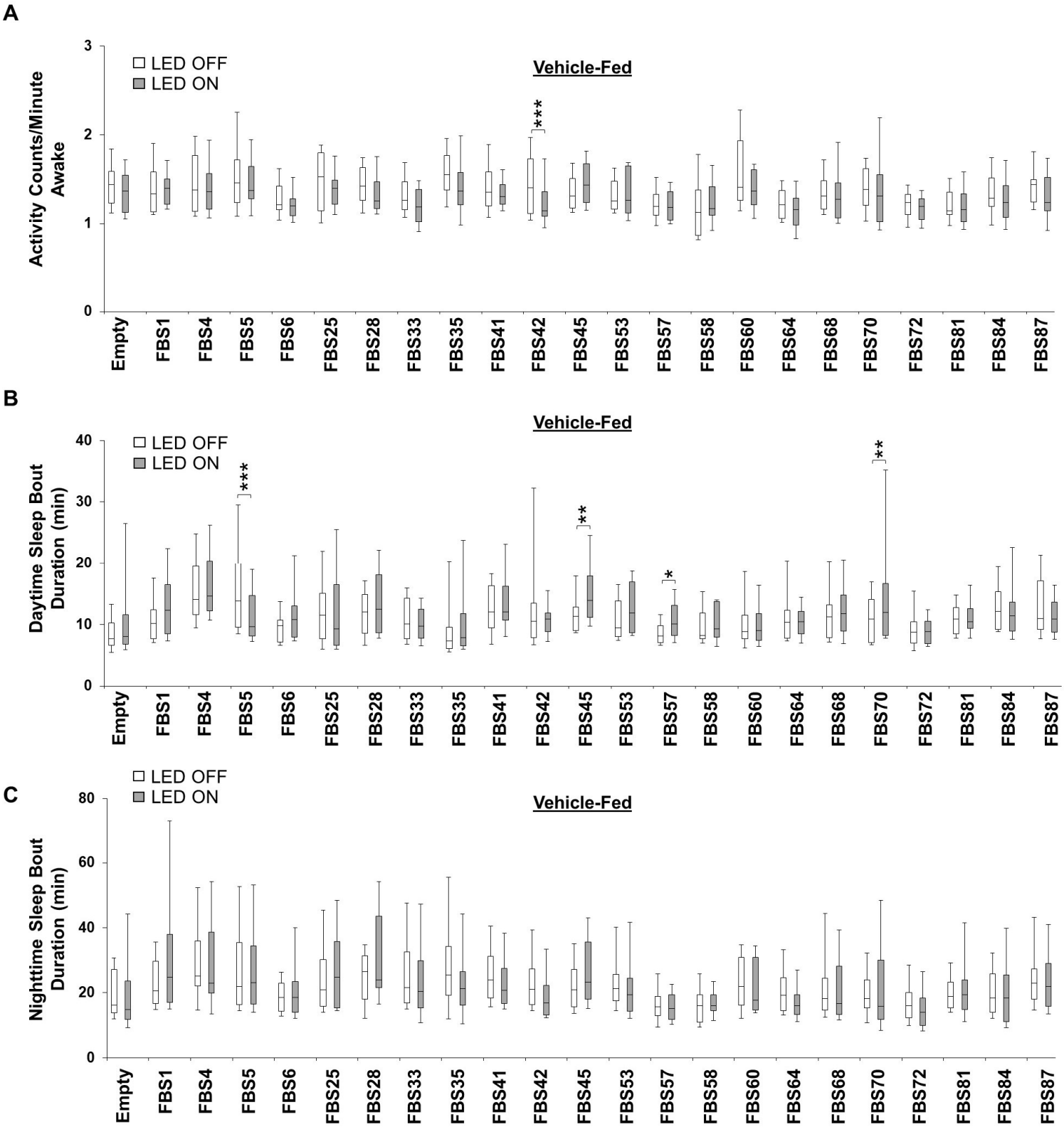
A
LED OFF
LED ON
Vehicle-Fed
Activity Counts/Minute Awake
***
B
Vehicle-Fed
LED OFF
LED ON
Daytime Sleep Bout Duration (min)
***
**
*
**
C
LED OFF
LED ON
Vehicle-Fed
Nighttime Sleep Bout Duration (min)
Empty
FBS1
FBS4
FBS5
FBS6
FBS25
FBS28
FBS33
FBS35
FBS41
FBS42
FBS45
FBS53
FBS57
FBS58
FBS60
FBS64
FBS68
FBS70
FBS72
FBS81
FBS84
FBS87

Figure 3-S2

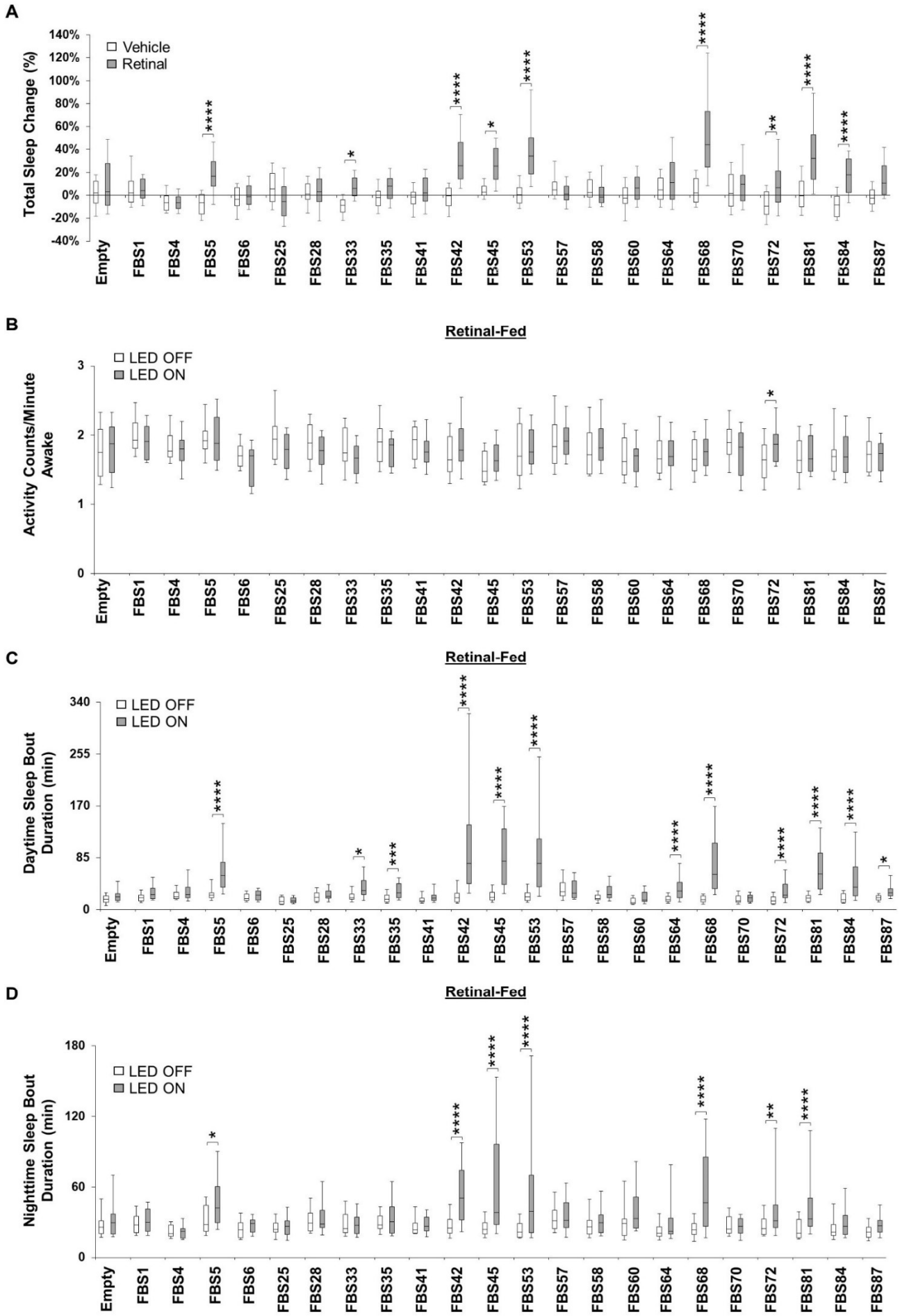
A
Total Sleep Change (%)
Vehicle
Retinal
140%
120%
100%
80%
60%
40%
20%
0%
-20%
-40%
Empty
FBS1
FBS4
FBS5
FBS6
FBS25
FBS28
FBS33
FBS35
FBS41
FBS42
FBS45
FBS53
FBS57
FBS58
FBS60
FBS64
FBS68
FBS70
FBS72
FBS81
FBS84
FBS87
B
Retinal-Fed
Activity Counts/Minute Awake
LED OFF
LED ON
C
Retinal-Fed
Daytime Sleep Bout Duration (min)
LED OFF
LED ON
D
Retinal-Fed
Nighttime Sleep Bout Duration (min)
LED OFF
LED ON

Figure 3-S3

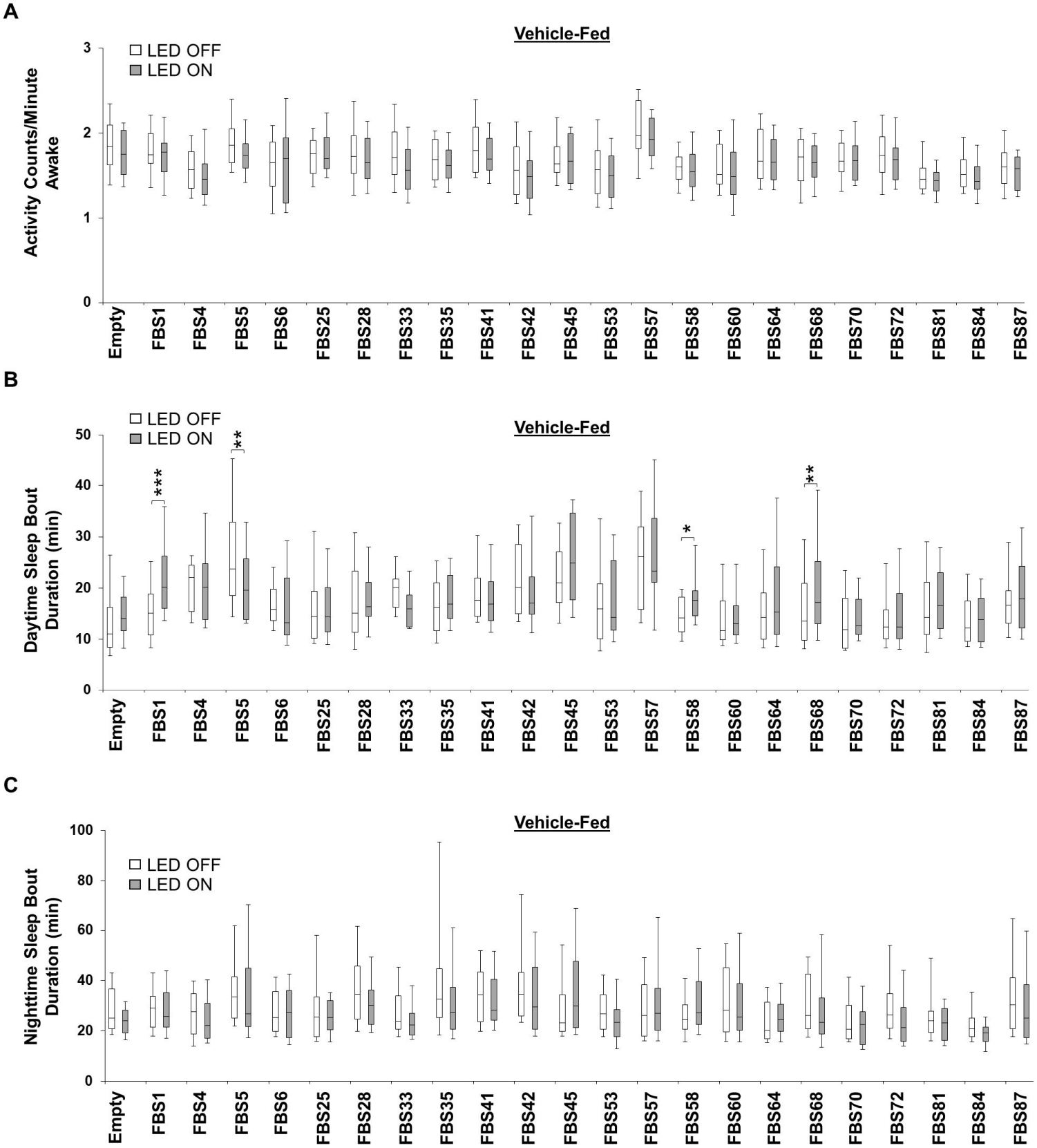
A
Vehicle-Fed
LED OFF
LED ON
Activity Counts/Minute Awake
0
1
2
3
Empty
FBS1
FBS4
FBS5
FBS6
FBS25
FBS28
FBS33
FBS35
FBS41
FBS42
FBS45
FBS53
FBS57
FBS58
FBS60
FBS64
FBS68
FBS70
FBS72
FBS81
FBS84
FBS87
B
Vehicle-Fed
LED OFF
LED ON
Daytime Sleep Bout Duration (min)
0
10
20
30
40
50
***
**
*
**
C
Vehicle-Fed
LED OFF
LED ON
Nighttime Sleep Bout Duration (min)
0
20
40
60
80
100

Figure 4-S1

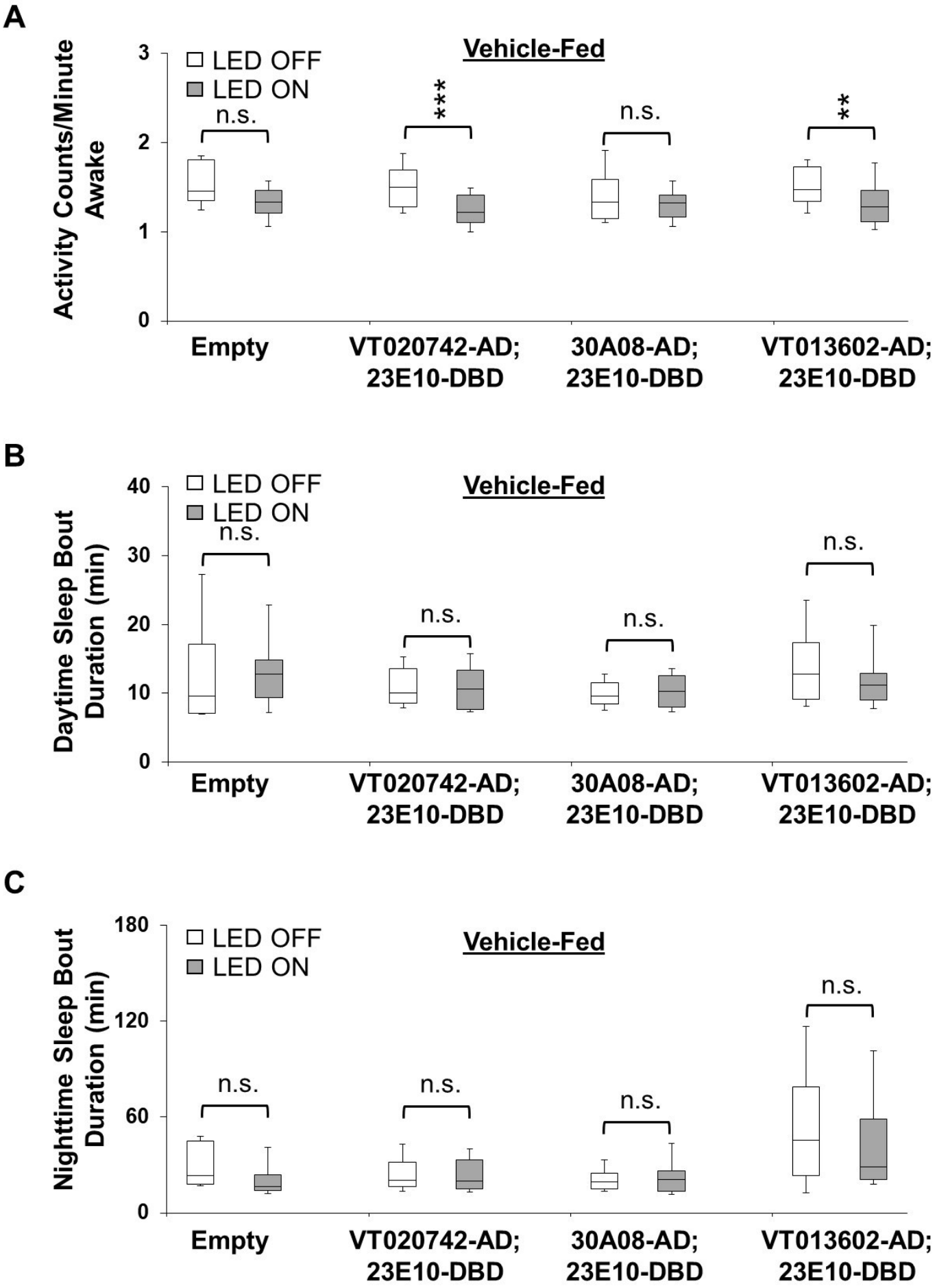
A
Vehicle-Fed
LED OFF
LED ON
Activity Counts/Minute Awake
3
2
1
0
n.s.
***
n.s.
**
Empty
VT020742-AD; 23E10-DBD
30A08-AD; 23E10-DBD
VT013602-AD; 23E10-DBD
B
Vehicle-Fed
LED OFF
LED ON
Daytime Sleep Bout Duration (min)
40
30
20
10
0
n.s.
n.s.
n.s.
n.s.
Empty
VT020742-AD; 23E10-DBD
30A08-AD; 23E10-DBD
VT013602-AD; 23E10-DBD
C
Vehicle-Fed
LED OFF
LED ON
Nighttime Sleep Bout Duration (min)
180
120
60
0
n.s.
n.s.
n.s.
n.s.
Empty
VT020742-AD; 23E10-DBD
30A08-AD; 23E10-DBD
VT013602-AD; 23E10-DBD

Figure 4-S2

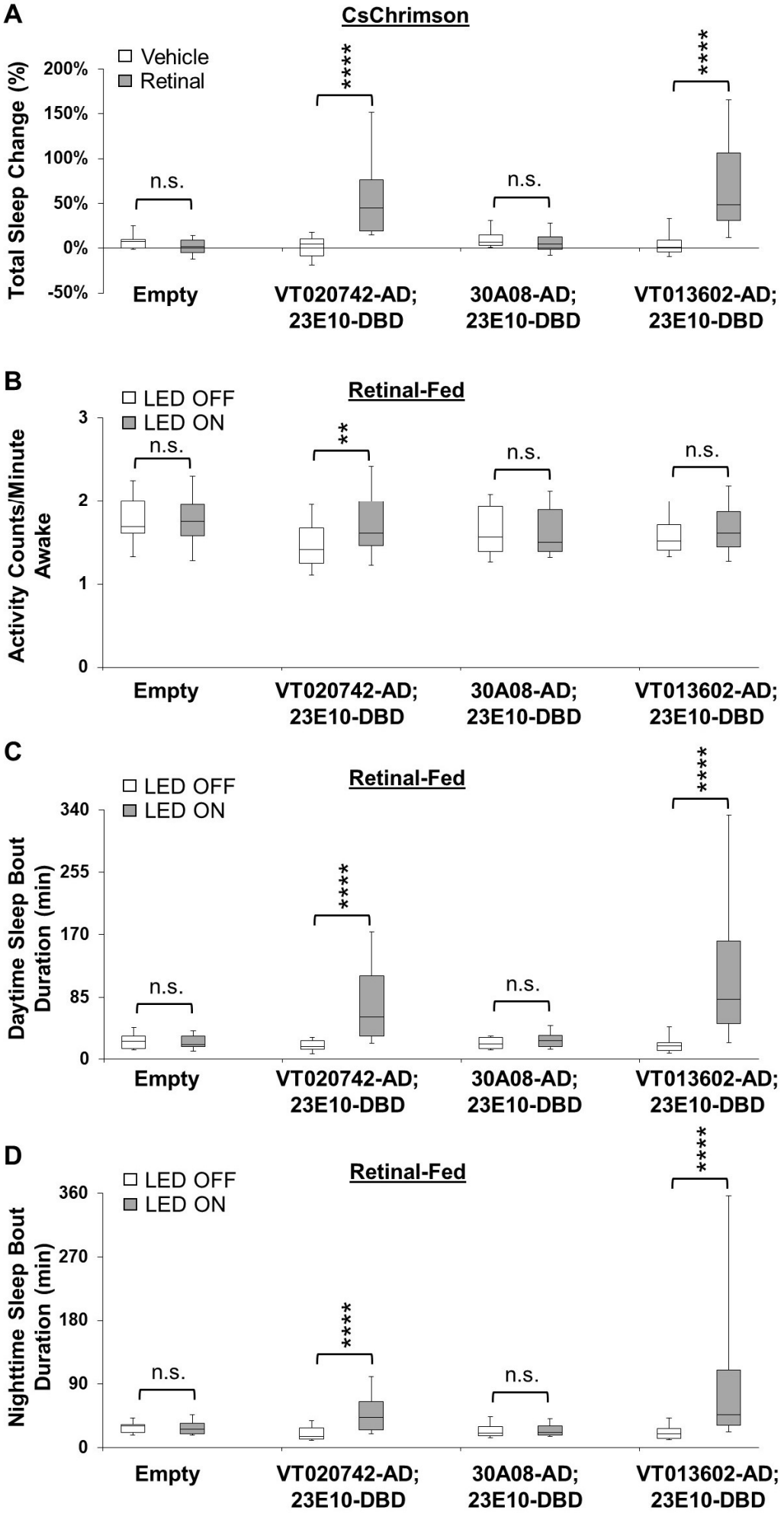
A
CsChrimson
Vehicle
Retinal
Total Sleep Change (%)
200%
150%
100%
50%
0%
-50%
n.s.
****
n.s.
****
Empty
VT020742-AD; 23E10-DBD
30A08-AD; 23E10-DBD
VT013602-AD; 23E10-DBD
B
Retinal-Fed
LED OFF
LED ON
Activity Counts/Minute Awake
3
2
1
0
n.s.
**
n.s.
n.s.
Empty
VT020742-AD; 23E10-DBD
30A08-AD; 23E10-DBD
VT013602-AD; 23E10-DBD
C
Retinal-Fed
LED OFF
LED ON
Daytime Sleep Bout Duration (min)
340
255
170
85
0
n.s.
****
n.s.
****
Empty
VT020742-AD; 23E10-DBD
30A08-AD; 23E10-DBD
VT013602-AD; 23E10-DBD
D
Retinal-Fed
LED OFF
LED ON
Nighttime Sleep Bout Duration (min)
360
270
180
90
0
n.s.
****
n.s.
****
Empty
VT020742-AD; 23E10-DBD
30A08-AD; 23E10-DBD
VT013602-AD; 23E10-DBD

Figure 4-S3

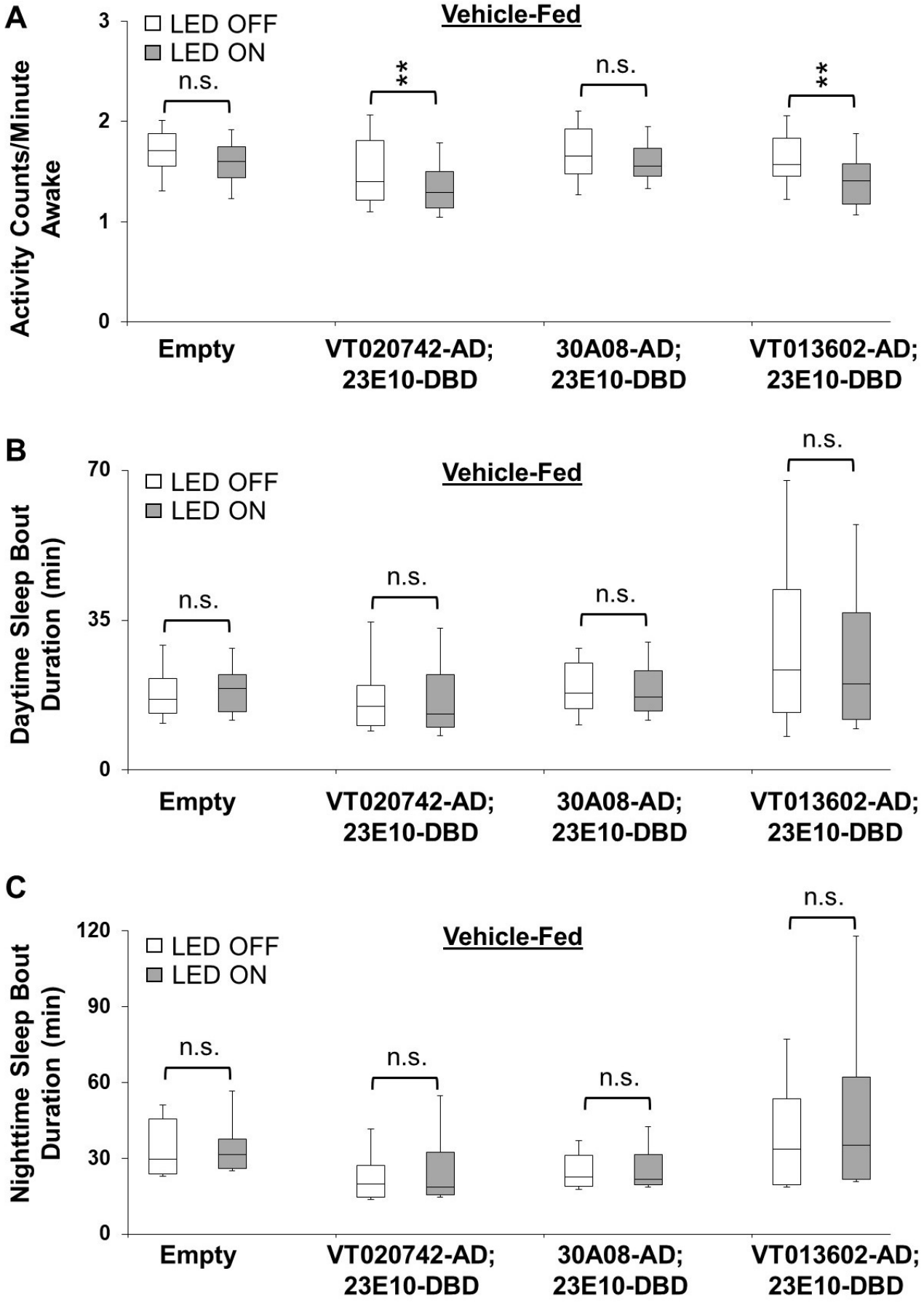
A
Vehicle-Fed
LED OFF
LED ON
Activity Counts/Minute Awake
3
2
1
0
n.s.
**
n.s.
**
Empty
VT020742-AD; 23E10-DBD
30A08-AD; 23E10-DBD
VT013602-AD; 23E10-DBD
B
Vehicle-Fed
LED OFF
LED ON
Daytime Sleep Bout Duration (min)
70
35
0
n.s.
n.s.
n.s.
n.s.
Empty
VT020742-AD; 23E10-DBD
30A08-AD; 23E10-DBD
VT013602-AD; 23E10-DBD
C
Vehicle-Fed
LED OFF
LED ON
Nighttime Sleep Bout Duration (min)
120
90
60
30
0
n.s.
n.s.
n.s.
n.s.
Empty
VT020742-AD; 23E10-DBD
30A08-AD; 23E10-DBD
VT013602-AD; 23E10-DBD

Figure 4-S4

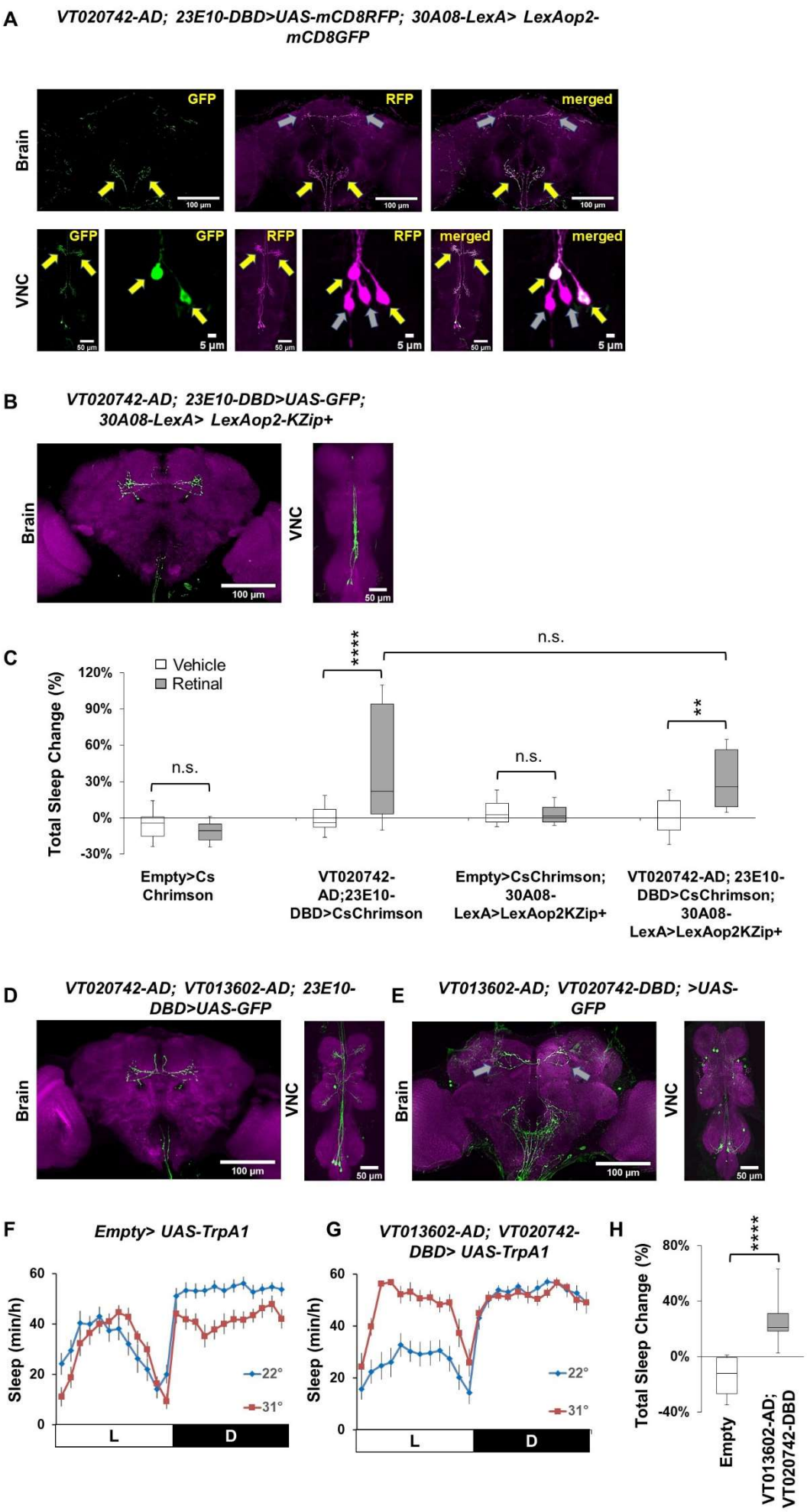
A
VT020742-AD; 23E10-DBD>UAS-mCD8RFP; 30A08-LexA> LexAop2-mCD8GFP
Brain
VNC
GFP
RFP
merged
100 µm
50 µm
5 µm
B
VT020742-AD; 23E10-DBD>UAS-GFP; 30A08-LexA> LexAop2-KZip+
Brain
VNC
100 µm
50 µm
C
Vehicle
Retinal
Total Sleep Change (%)
120%
90%
60%
30%
0%
-30%
n.s.
****
n.s.
**
Empty>Cs Chrimson
VT020742-AD;23E10-DBD>CsChrimson
Empty>CsChrimson; 30A08-LexA>LexAop2KZip+
VT020742-AD; 23E10-DBD>CsChrimson; 30A08-LexA>LexAop2KZip+
D
VT020742-AD; VT013602-AD; 23E10-DBD>UAS-GFP
Brain
VNC
100 µm
50 µm
E
VT013602-AD; VT020742-DBD; >UAS-GFP
Brain
VNC
100 µm
50 µm
F
Empty> UAS-TrpA1
Sleep (min/h)
60
40
20
0
22°
31°
L
D
G
VT013602-AD; VT020742-DBD> UAS-TrpA1
Sleep (min/h)
60
40
20
0
22°
31°
L
D
H
Total Sleep Change (%)
80%
40%
0%
-40%
****
Empty
VT013602-AD; VT020742-DBD

Figure 4-S5

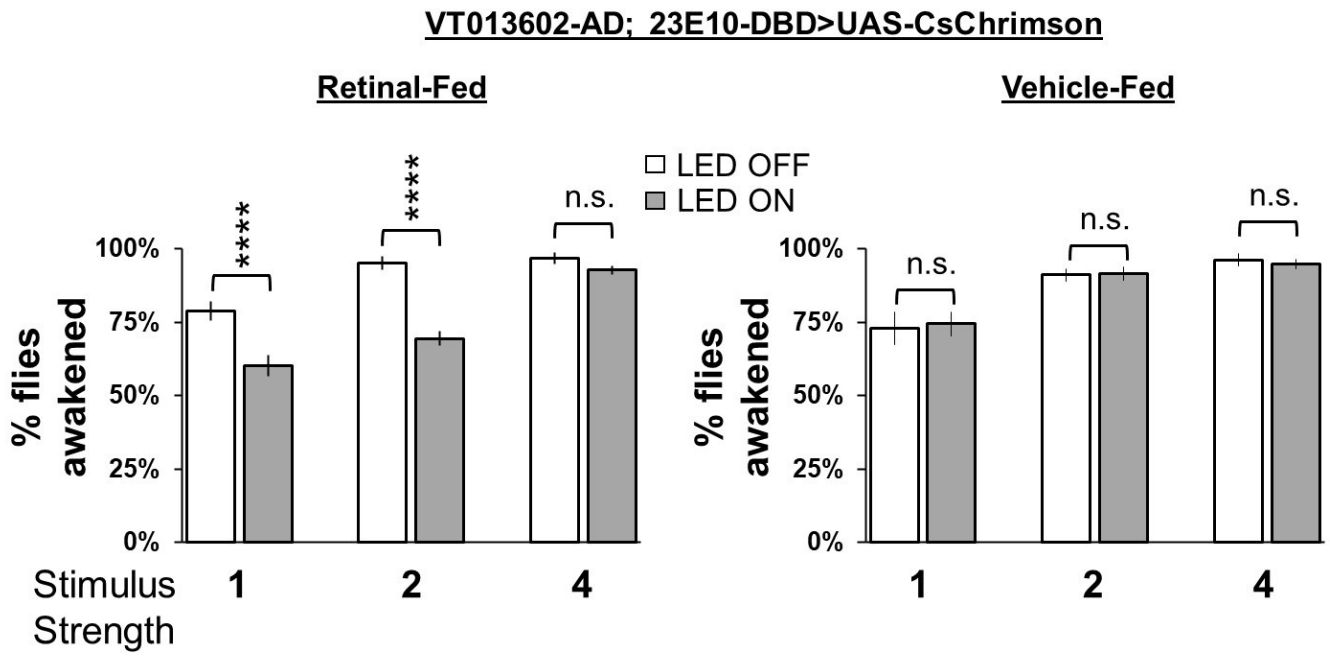
VT013602-AD; 23E10-DBD>UAS-CsChrimson
Retinal-Fed
Vehicle-Fed
LED OFF
LED ON
****
****
n.s.
n.s.
n.s.
n.s.
100%
75%
50%
25%
0%
% flies awakened
Stimulus Strength
1
2
4

Figure 6-S1

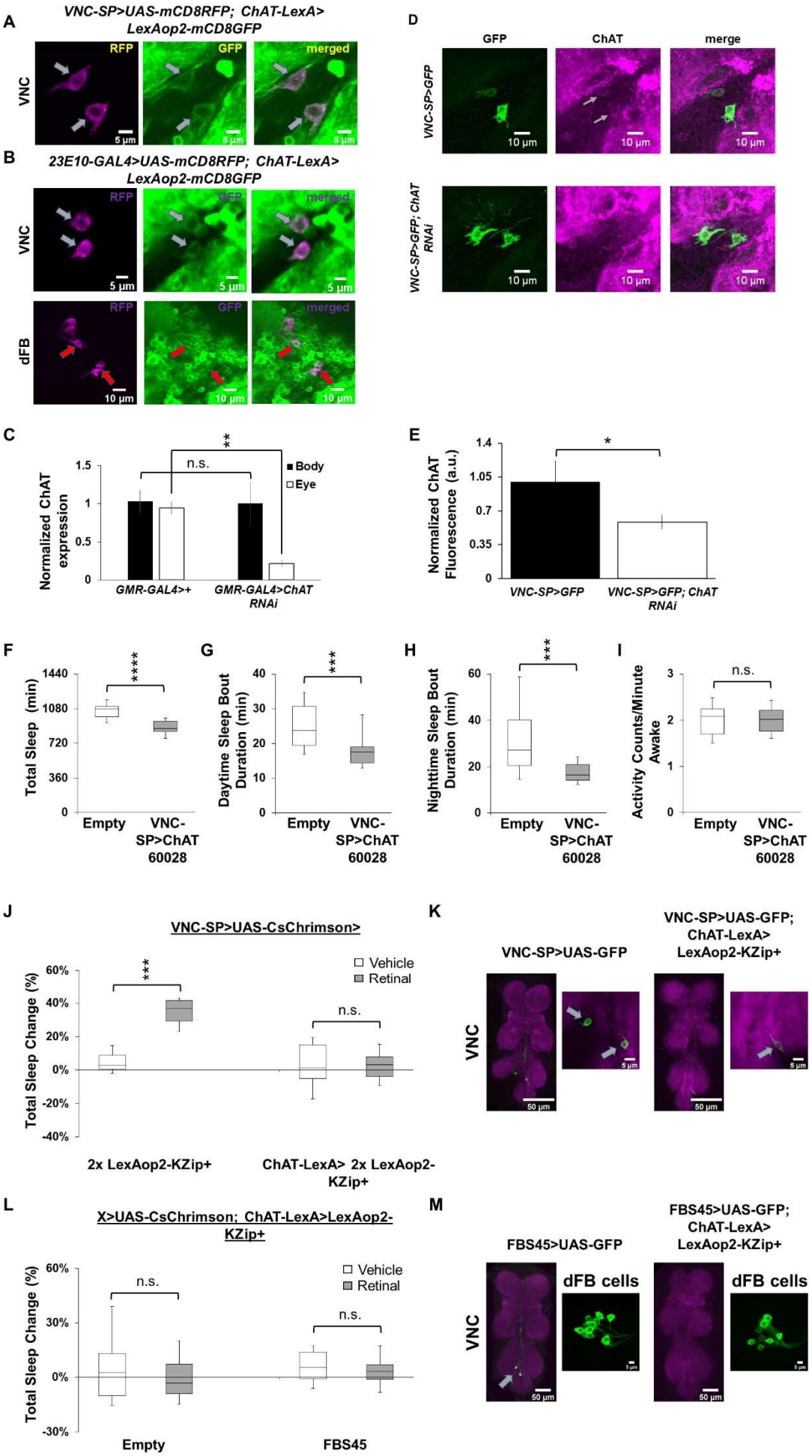
A
VNC-SP>UAS-mCD8RFP; ChAT-LexA>
LexAop2-mCD8GFP
VNC
RFP
GFP
merged
5 µm
B
23E10-GAL4>UAS-mCD8RFP; ChAT-LexA>
LexAop2-mCD8GFP
VNC
dFB
10 µm
C
Normalized ChAT expression
Body
Eye
n.s.
**
GMR-GAL4>+
GMR-GAL4>ChAT RNAi
D
GFP
ChAT
merge
VNC-SP>GFP
VNC-SP>GFP; ChAT RNAi
E
Normalized ChAT Fluorescence (a.u.)
*
VNC-SP>GFP
VNC-SP>GFP; ChAT RNAi
F
Total Sleep (min)
****
Empty
VNC-SP>ChAT 60028
G
Daytime Sleep Bout Duration (min)
***
H
Nighttime Sleep Bout Duration (min)
***
I
Activity Counts/Minute Awake
n.s.
J
VNC-SP>UAS-CsChrimson>
Total Sleep Change (%)
Vehicle
Retinal
***
n.s.
2x LexAop2-KZip+
ChAT-LexA> 2x LexAop2-KZip+
K
VNC-SP>UAS-GFP
VNC-SP>UAS-GFP; ChAT-LexA> LexAop2-KZip+
VNC
50 µm
L
X>UAS-CsChrimson; ChAT-LexA>LexAop2-KZip+
Total Sleep Change (%)
Vehicle
Retinal
n.s.
n.s.
Empty
FBS45
M
FBS45>UAS-GFP
FBS45>UAS-GFP; ChAT-LexA> LexAop2-KZip+
VNC
dFB cells
dFB cells

Figure 6-S2

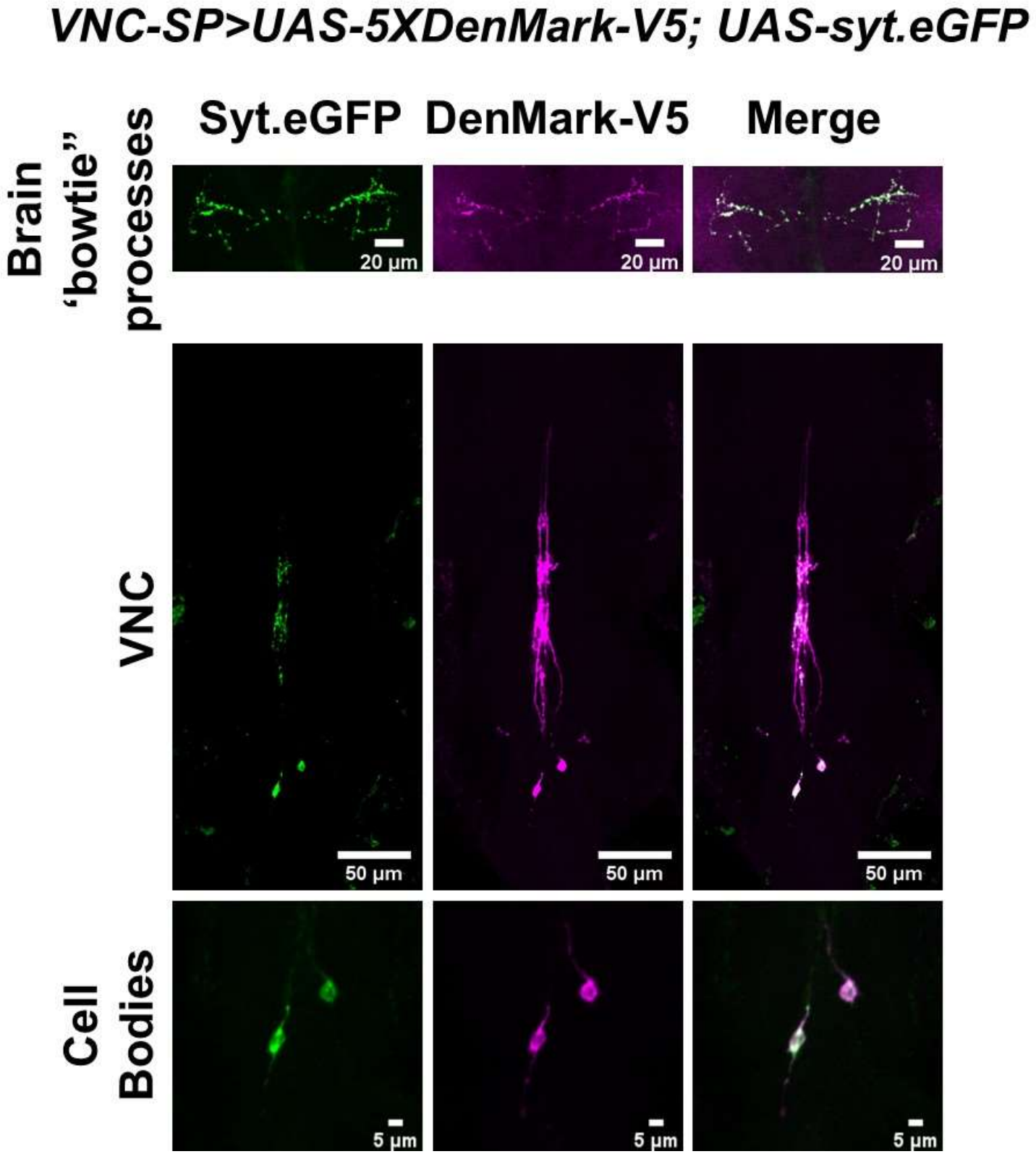
VNC-SP>UAS-5XDenMark-V5; UAS-syt.eGFP
Syt.eGFP
DenMark-V5
Merge
Brain 'bowtie" processes
20 µm
20 µm
20 µm
VNC
50 µm
50 µm
50 µm
Cell Bodies
5 µm
5 µm
5 µm